Thermal behaviour of Li-ion cells

TIMOFEY MALTSEV

KTH Industrial Engineering
and Management

Master of Science Thesis
Stockholm, Sweden 2012

Thermal behaviour of Li-ion cells

Master Thesis project at Volvo GTT ATR

Timofey Maltsev

Master of Science Thesis MMK 2012:72 IDE 092
KTH Industrial Engineering and Management
Machine Design
SE-100 44 STOCKHOLM

KTH Industriell teknik och management

Examensarbete MMK 2012:72 IDE 092

Termiskt beteende av Li-jon celler

Timofey Maltsev

Godkänt	Examinator	Handledare
2012-10-10	Conrad Luttropp	Conrad Luttropp
	Uppdragsgivare	Kontaktperson
	Volvo GTT ATR	Magnus Larsson

Sammanfattning

Examensarbetet gjordes på Volvo Group Trucks Technology. Målet med arbetet var att studera värmeutveckling i Li-jon cell för hybrid- och elbilar, HEV och EV. Battericeller undersöktes under sina normala arbetsförhållanden och vid förstörande prov. Undersökningen baserades på cellernas yttemperatur. Arbetet beskrev cellernas beteende och syftade att vara ett underlag för konstruktörer av batterisystem.

En litteraturstudie gjordes för att studera faktorer som påverkar värmeutvecklingen. Sedan analyserades källor till samtliga faktorer. En moduleringsmetod för analys av cellens värmeeffektivitet togs fram. Miljöpåverkan och ekonomiska aspekter av batterier undersöktes.

Tre tester togs fram för att undersöka värmeutvecklingsfaktorer på fem celler. De flesta faktorerna var externa såsom laddning och urladdning, puls och kontinuerlig ström och omgivningstemperatur. En infraröd kamera användes vid experimenten.

Testerna visade hur olika faktorer påverkade cellernas temperatur. Vidare analys av källor visade kritiska områden i cellernas konstruktion.

Förstörande värmeprov gjordes på tre par av celler. Dessa värmdes upp till 300°C vilket orsakade ”thermal runaway”. I vissa fall gick temperaturen över 600°C och celler fattade eld. Olika kemiska sammansättningar och uppbyggnad av cellerna gjorde att de betedde sig olika vid genomförda tester.

Testerna visade att olika celler presterade olika vid liknande testförhållanden. Därför är det viktigt att ta fram specifikationer för användningsförhållanden för att välja ut en cell för ett batterisystem. Sedan kan prestandan av olika celler jämföras och effektivitet kan utvärderas för samma belastningscyklar.

Thermal Management System kan förhöja batteriets effektivitet och måste designas med användningsförhållanden i åtanke. Batteriernas säkerhet är väldigt viktig och människor får inte skadas av batterier. Därför måste säkerheten finnas i åtanke i alla steg av batteridesign.

Arbetets resultat blev en sammanfattning av viktiga faktorer och specifikationer för batteridesign som baserades på värmeutvecklingen. Samtliga riktlinjer sammanfattades i Appendix 5.

Nyckelord: Litium-jon batteri, HEV, EV, temperatur, värme, thermal runaway, förstörande prov

KTH Industrial Engineering and Management

Master of Science Thesis MMK 2012:72 IDE 092

Thermal behaviour of Li-ion cells

Timofey Maltsev

Approved	Examiner	Supervisor
2012-10-10	Conrad Luttropp	Conrad Luttropp
	Commissioner	Contact person
	Volvo GTT ATR	Magnus Larsson

Abstract

Master thesis work was done at Volvo Group Trucks Technology. Aim of the project was to study thermal behaviour of Li-ion battery for hybrid and electric vehicles, HEVs and EVs. Battery cells were tested in regular working conditions and abuse conditions. Surface temperature of cells was chosen for studying heat evolution.

A literature study was conducted to research factors that influence cell temperature. Analysis of sources of these factors was then performed. A modelling method for analyzing cell thermal efficiency was designed. Sustainability and economics aspects of batteries were also studied.

When factors were established three tests were designed to study their effects. Five cells were studied. Tests mainly examined external factors such as charge and discharge, pulse and continuous current, ambient temperature to name a few. An infrared camera was used.

Study showed how different factors influenced cell temperature. Further analysis of sources pointed out some hot spots of cell designs.

Thermal abuse test were performed on three pairs of cells. Cells were heated up to 300°C and went through thermal runaway which in some cases increased temperatures up to 660°C in less than a second and caused fire. Different cell chemistries and cell designs reacted differently to the abuse conditions.

A conclusion was reached that cells performed differently in similar test conditions. When designing a battery system a set of specifications for usage conditions is crucial for choosing a cell. When conditions and load cycles are known cells can be tested and their thermal and electrical efficiency evaluated.

Thermal Management System TMS can largely enhance cell efficiency and lifecycle. Such system must also be designed according to usage conditions and particular cell's performance.

Battery safety showed to be a very important factor of designing a battery system. Humans shall not be injured by systems with batteries which must be kept in mind during design.

Work resulted in summary of important factors and specifications for designing a battery system based on cell thermal behaviour. These guidelines are presented in Appendix 5.

Index terms: Lithium-ion battery, HEV, EV, heat, temperature, thermal runaway, abuse test

FOREWORD

This Master thesis was done at KTH (The Royal School of Technology, Stockholm, Sweden) and Volvo Group Trucks Technology (GTT) (Gothenburg, Sweden). The work was possible with help from both sides.

I would like to thank my professors and supervisors at KTH, Conrad Luttropp and Carl Michael Johannesson for helpful insights and making this work possible. Everyone I was in contact with at KTH and my fellow students helped me broaden my view of this work.

At Volvo I would like to thank my supervisors Magnus Larsson and Sophie Tintignac for being my mentors during thesis work. You have helped me navigate through the sea of batteries.

I have received great help and support from the battery team at Volvo and everyone I have been in contact with throughout the work which I am very grateful for. Particularly I would like to thank Ricard Blanc for mentoring on the practical issues.

I wish you pleasant reading.

Timofey Maltsev

Stockholm, Sweden

September 2012

NOMENCLATURE

Symbols and abbreviations used in this report are described here

Notations

Symbol	*Description*
Ah	Ampere-hour
C	C-rate
CO_2	Carbon dioxide
E	Energy (J)
I	Current (A)
Q	Heat (J)
ΔQ	Power (W)
R	Resistance (Ω)
ΔS	Entropy (J/K)
U	Voltage (V)

Abbreviations

ANOVA	Analysis of Variance
BMU	Battery Management Unit
EV	Electric Vehicle
ESS	Energy Storage System
HEV	Hybrid Electric Vehicle
LCA	Lifecycle Assessment
LIB	Lithium-ion Battery
OCV	Open Circuit Voltage
SEI	Solid Electrolyte Interface
SOC	State of Charge
SOH	State of Health
TMS	Thermal Management System

Abbreviations for cell chemistries and materials are presented in 2.2.1 Chemical design

TABLE OF CONTENTS

1 INTRODUCTION

This chapter describes the background, the purpose, the limitations and the methods used in the project.

1.1 Background

Hybrid electric vehicles HEV and electric vehicles EV are being researched, prototyped and built now more than ever before. Operation of such vehicles is less expensive compared to regular internal combustion engine powered ones and emission levels are reduced drastically. City buses and delivery trucks that produce much less emissions contribute to cleaner air in cities and lower energy cost for operative companies as an example.

The above-mentioned technologies rely on energy storage systems in order to prolong operation times. In the past few years Li-ion based batteries have taken the pole-position as an effective energy storage unit. These batteries have both high power and energy that EV and HEV systems require. Li-ion is a young technology and its performance and safety is constantly improving. However Li-ion has more potential to offer and extensive studies will help the technology to mature.

1.2 Problem definition

There are a number of different Li-ion based chemistries as well as cell designs on the market today. As a consequence all cells will operate differently one from another. To develop an electric drivetrain designer needs to know how batteries operate in different conditions and where safety limit lies. Therefore batteries require a study and evaluation of battery heat, efficiency and safety.

Li-ion batteries present inherent risks and some cases where batteries caught fire or exploded have been reported. These consequences can often happen during a *thermal runaway* which is a condition when internal chemical reactions get out of hand at a high temperature. Thermal runaway will cause heat and fire and will destroy the battery. Also it can potentially harm humans. Thermal runaway effects therefore need to be known and obvious for battery designers.

1.3 Target

- Conduct a literature study to investigate thermal behaviour of Li-ion battery cells and safety aspects of thermal runaway
- Determine factors that affect the heat evolution. Conduct experimental study on Li-ion cells provided by Volvo to evaluate the influence. Experiments shall be based on a study of cell surface temperature
- Conduct thermal runaway experiments on Li-ion cells
- Evaluate theoretical and practical results and discuss thermal behaviour and safety issues of batteries. Discuss how thermal and safety factors should be addressed when designing a battery system

1.3 Delimitations

- Only cells provided by Volvo were used for testing
- Tests were limited to a study of surface temperature
- Tests of some few internal factors were impossible to perform accurately because they required cells that were identical in all characteristics but one. Thus a particular factor for example two different electrolyte contents could have been studied. Such factors were omitted from the test procedure
- Project time was 20 weeks. Due to resource limitations this project could not result in specific solutions for every particular application

1.4 Method

Thesis work started with a short study of cell design, thermal behaviour and safety. Thesis target was set throughout the study and a work schedule was created. Risks of interruption of working process were analysed and solutions to the anticipated problems were produced.

Further literature study concentrated on details of thermal behaviour and heat evolution, battery safety and thermal runaway. Books, scientific articles and internet were used for information search as well as interviews with drivetrain and battery experts at Volvo.

In parallel a test layout was designed for the experiments and the tests were carried out. A particular experiment design was chosen to make experiments structured and time-efficient. Thermal behaviour tests were carried out on all cells available during the work. Test results were used to draw conclusions on which factors influence cell temperature and how.
Thermal runaway abuse tests were performed on three types of cells. Test data was then analyzed and compared to theoretical results.

Results of test analysis and literature study were reviewed and recommendations for battery design were developed. Consequences of cell performance were analyzed from a sustainable and economic point of view.

Thesis report was updated continuously during the work.

2 FRAME OF REFERENCE

This chapter presents the theoretical reference frame that is necessary for the performed research and modeling.

2.1 Batteries and cells

What are batteries?

A battery is a device that can store chemical energy and convert it to electrical energy.

The first battery was made in 1800 by Alessandro Volta which was called voltaic pile. It operated based on a potential difference between the metal plates that were connected to each other through a conductive liquid called electrolyte. The principle of operation was discovered by Volta's colleague Luigi Galvani in his experiment with frog's legs. Metal that was more noble (had higher potential) went through a reduction reaction and absorbed electrons from a less noble metal that underwent oxidation, copper and zinc respectively in the voltaic pile, *Figure 1*.

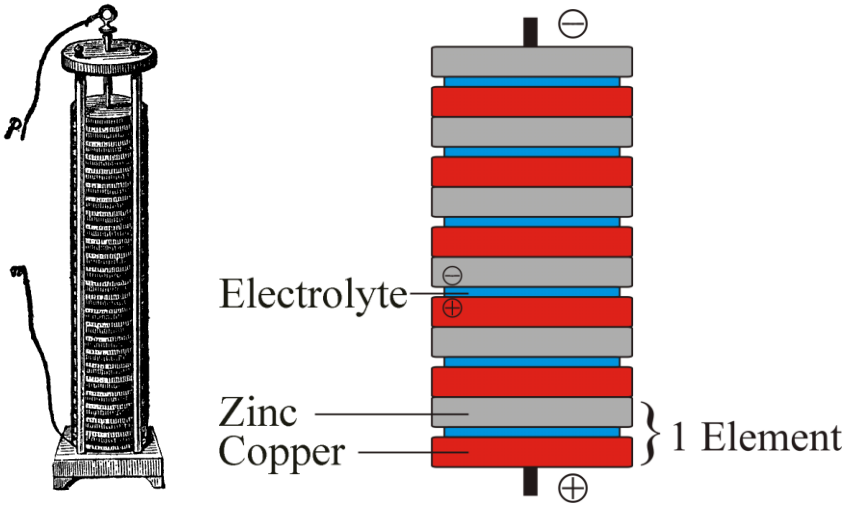

Figure 1. Voltaic pile and its structure

A difference in potentials of the electrodes of the cells is referred to as cell voltage and represents cell's ability to force current through a circuit. Capacity is the amount of electric charge that a cell stores and is often expressed in Ampere-hours or Ah.

Battery market is very large and we encounter batteries daily in all sorts of appliances that are not connected to the power grid by a cable. Primary batteries such as those we use in remote controls and clocks are made to be used only once while secondary batteries like mobile phone or typical car batteries are made for both discharging and charging cycles.

What are cells?

The name *battery* refers to a device that consists of a number of single units – *cells*, see *Figure 2*. These are examples of Li-ion cells which on average have voltage of 3.6V and capacity typically ranging from 2 to 20 Ah in automotive applications.

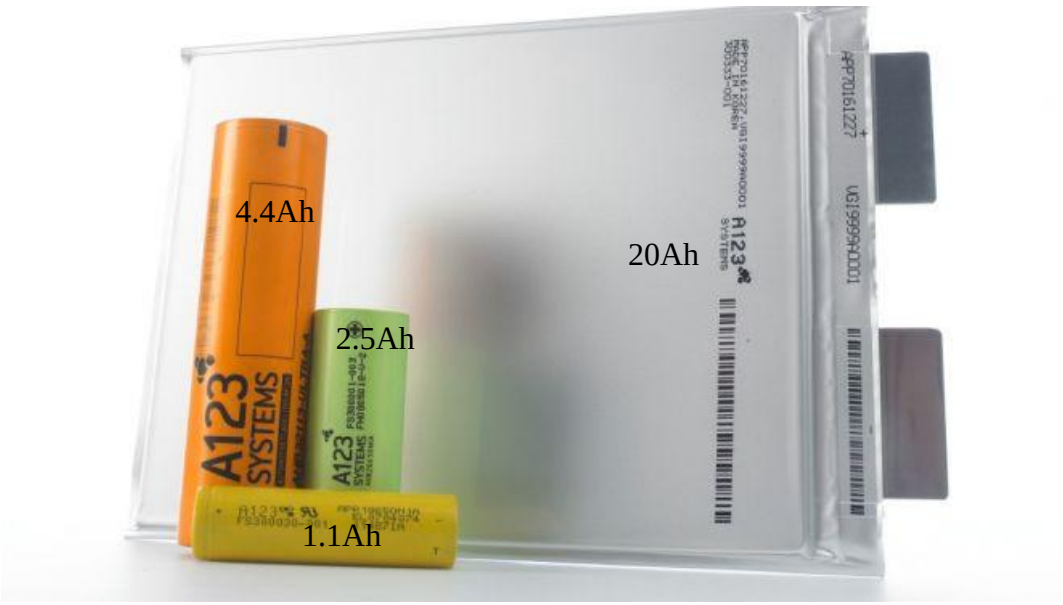

Figure 2. A variety of cells from manufacturer A123 System including three cylindrical cells and one pouch. Picture is courtesy of http://www.a123systems.com

When cells are connected to each other in series their voltage is added together and a parallel connection adds the capacity. Therefore by connecting a number of cells both in parallel and series a battery pack is built. Packs are also called Energy Storage System, ESS and are often assembled out of modules. Modules are a number of cells connected together with heat conductors for the cooling system and some sensors for battery management equipment. Such modules are made to be put together and enclosed in an ESS.

A typical ESS for a HEV or EV is a closed system that is air-tight, has built-in safety devices, cooling and Battery Management Unit, BMU. It is usually designed with a hard shell to protect the cells from mechanical impact from outside as well as protect humans and the environment in case of a cell malfunction, see *Figure 3*.

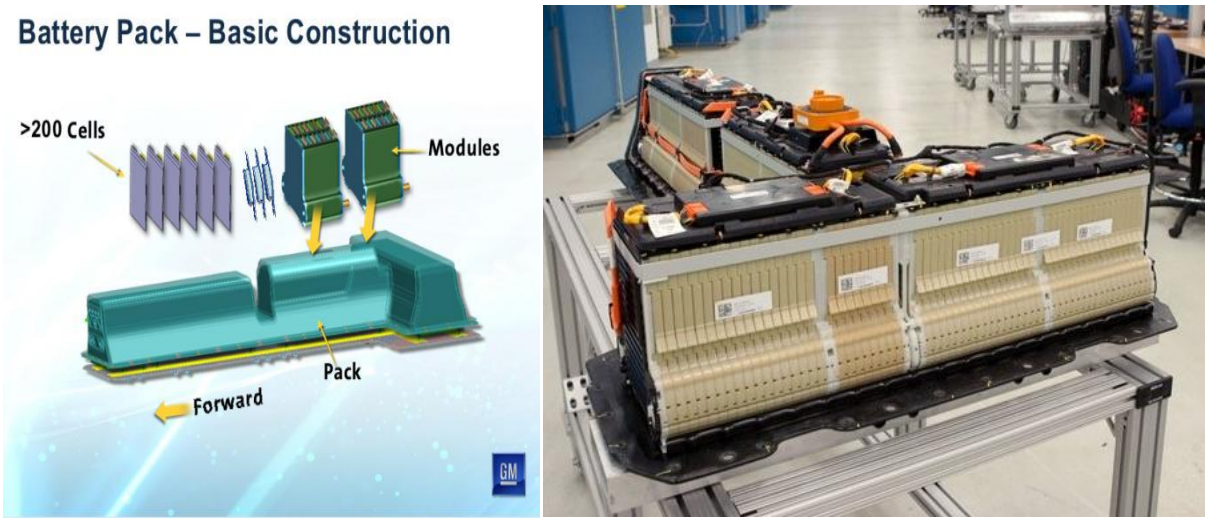

Figure 3. ESS that is used in Chevrolet Volt from General Motors is built up from cells arranged in modules. Picture courtesy of www.gm.com and www.gm-volt.com

A cell being a basic unit of an ESS has the largest influence on the ESS performance. Requirements are often set by the type of vehicle or system where ESS is used. For example hybrid heavy machinery requires high power to run its demanding applications while an electric city car needs high energy for longer drives without charging. Cells that are on the market today

are quantified by their Energy Density and Power Density. Cells are generally designed to satisfy one type of application and therefore are either tailored to give a lot of power fast or store a lot of energy. Cells are built with different electrode materials and different current collector thicknesses to achieve the desired properties.

A search for alternative energy sources to fossil fuels has caused a new market to grow for the past 10-15 years. Systems with electric motors were being implemented to aid and even replace combustion engines which meant that a powerful energy supply was required. A demand for cells that would hold a large amount of energy which could be used in various vehicle applications was addressed by both major players on the battery market and small companies with know-how. The usage of the new breed of automotive cells is not only confined to vehicles and the cells are used for:

- Hybrid and electric cars
- Buses and trucks
- Construction equipment
- Bicycles and motorbikes
- Racing cars, bikes, boats and other vehicles
- Airplanes and helicopters
- Telecommunication industry
- Stand-alone energy sources

Batteries are being used to both drive vehicles as well as to power their internal systems. So far hybrid systems have been implemented with most success. Such systems include both an electric system and a combustion engine in a vehicle. Many hybrid systems are also used to utilize excessive energy that is produced under different stages in vehicle operation. Particularly braking energy is often used by the electric motor working as a generator to recover some energy. An example of a hybrid system is shown below with a short explanation of benefits, *Figure 4*.

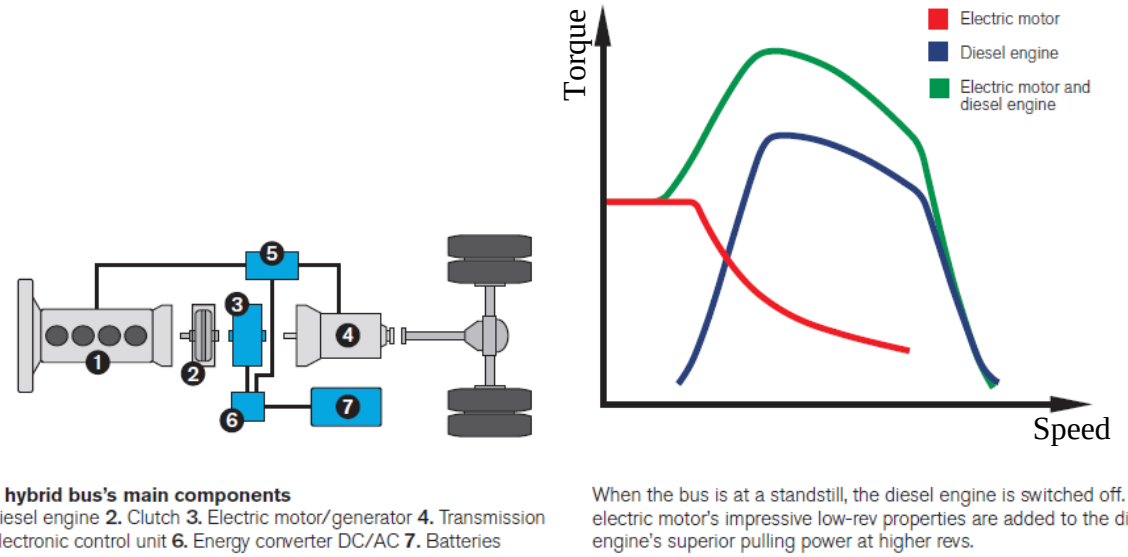

The hybrid bus's main components
1. Diesel engine **2.** Clutch **3.** Electric motor/generator **4.** Transmission **5.** Electronic control unit **6.** Energy converter DC/AC **7.** Batteries

When the bus is at a standstill, the diesel engine is switched off. The electric motor's impressive low-rev properties are added to the diesel engine's superior pulling power at higher revs.

Figure 4. A schematic of a hybrid system of a Volvo 7700 bus and a diagram of torque versus speed. Green curve represents how both engines together produce a higher torque. Picture courtesy of Volvo Bus Corporation www.volvobuses.com

Hybrid vehicles use less fuel and produce less exhaust gases and particles than vehicles powered only by combustion engines. Electric vehicles produce no emissions at all and electricity which is needed to power them is considerably cheaper than fossil fuel. *Figure 4* shows also how an

electric motor accelerates a bus with less emissions and part of that energy is regained while braking.

Electric systems have higher overall efficiency than systems with combustion engines. These energy savings mean that more electric motors will be used in future products and their performance relies on efficient batteries. At the same time the need for longer operational times and lower weight and volume for small cordless devices like mobile phones and laptops is constantly increasing. Success of both big and large electric systems is based on batteries with high energy and power and a lot of research and development is conducted in this area. Better Li-ion batteries are already in big demand and it is likely to only increase in the future.

2.2 Cell design

Li-ion cells have different *chemistries* – or in other words material compositions. The basic principle is however the same for all cells and is based on a transfer of ions of lithium. Lithium Cobalt Oxide (LCO) is an example of a chemistry and it will be used to explain the operational principle.

All cells have a *positive electrode (cathode)* and a *negative electrode (anode)*. Positive electrode is usually a lithium-based material like Lithium Cobalt Oxide and negative electrode is some form of carbon, usually graphite. See *Figure 5*.

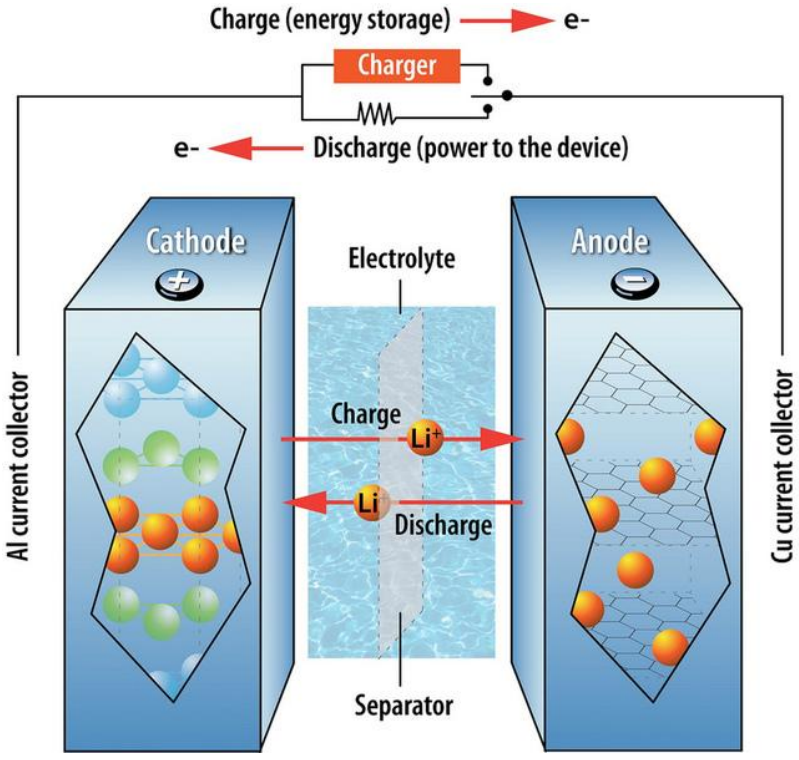

Figure 5. An example of Lithium Cobalt Oxide (LCO) chemistry

When a cell is discharging, ions of Li leave graphite electrode and travel through *electrolyte* and separator to the Lithium Cobalt Oxide where they are intercalated in the material. As ions leave graphite electrons are also released. They cannot travel through the insulating *separator* so they travel through the external circuit and create electric current. During charge the process is reversed and ions leave the Lithium Cobalt Oxide and are intercalated in graphite structure.

Electrode materials have different inherent electric potentials. Ions will always flow in the direction of a lower potential. Thus when the external circuit is closed reduction and oxidation

reactions start because of the potential difference and electrons are released through the external circuit while ions travel between electrodes through electrolyte.

Cell operates through a redox reaction, or reduction and oxidation [1]. Each electrode or half-cell is either reduced which means it absorbs ion and electron or oxidized which means it releases an ion-electron pair. The direction of redox reaction is ruled by whether the cell is charging or discharging. During discharge an electrode that undergoes reduction and absorbs is called cathode and electrode that oxidizes and releases is called anode. The reaction in LCO chemistry is illustrated in *Figure 6* A discharging cell is also known as galvanic because it generates current. A charging cell is called electrolytic because it absorbs current to drive the reaction.

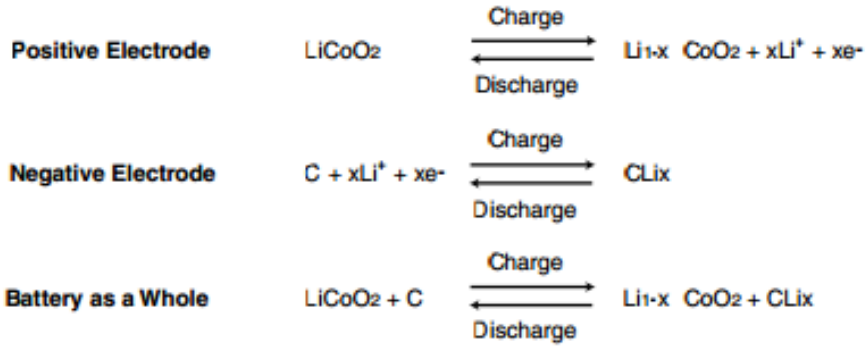

Figure 6. Reduction and oxidation reactions in an LCO cell

Redox reaction only operates based on difference in potentials of the electrodes. A correct potential of material can only be measured together with another material by forming an electrode pair.

The cell voltage is difference in electrode potentials and it reflects cell's ability to force current through a circuit. The capacity is the amount of electric charge that a cell is able to store and is generally expressed in Ampere-hours or Ah.

When a cell is fully charged its State Of Charge, SOC is considered 100% and cell capacity is full. During discharge SOC and capacity decreases when ions leave graphite. Typically cell voltage decreases with SOC, *Figure 7.* One of the Li-ion characteristics is a flat voltage curve – stable voltage throughout a wide SOC range which is practical for electric systems. Top curve symbolizes charge and bottom curve represents discharge respectively. The difference between charge and discharge voltage is due to internal resistance of a cell which is in a range of milliohms or mΩ.

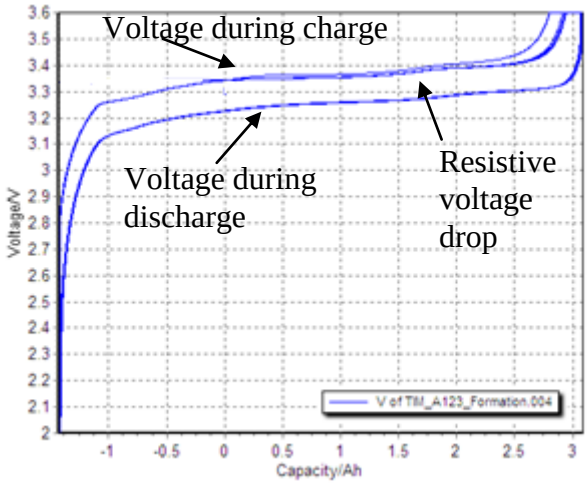

Figure 7. Cell voltage throughout the SOC range(Capacity range)

Cell voltage is typically different for when the cell is operating or resting. The Open-Circuit Voltage or OCV is a difference between electrode potentials, measured when there is no current flow and the cell has reached electrochemical equilibrium (rest). OCV is typically different if a cell was charging or discharging prior to the measurement.

Charging and discharging current is often expressed through a C-rate. C is a full capacity of a cell and current is a multiple of C. For example a rate of 1C for a 4.4Ah cell would be drawing 4.4A current under 1hour or $4.4Ah \times 1C = 4.4A$

2.2.1 Chemical design

Lithium is a very light metal that has a specific capacity of 3.86Ah/g and a reduction potential of 3.045V [1]. This study is concentrated on cells where at least one Li-based electrode is used together with Li-ions that facilitate transfer of charge. These properties of metal give Li-based batteries high specific energy and specific power compared to other commercially available battery chemistries. Choosing particular material for each component of a cell will give it specific properties.

Positive and negative electrodes

Electrode materials show different potentials and capacities. Cell voltage is the difference between positive and negative electrode potentials, *Figure 8*. Capacity illustrates the amount of charge in Ampere-hours or Coulombs the material can store. A desirable design would be a combination of two materials which results in a high capacity and high voltage. The electrode materials must also show sufficient electronic and ionic conductivities in order to ensure good kinetics in absorbing or releasing the Li ions.

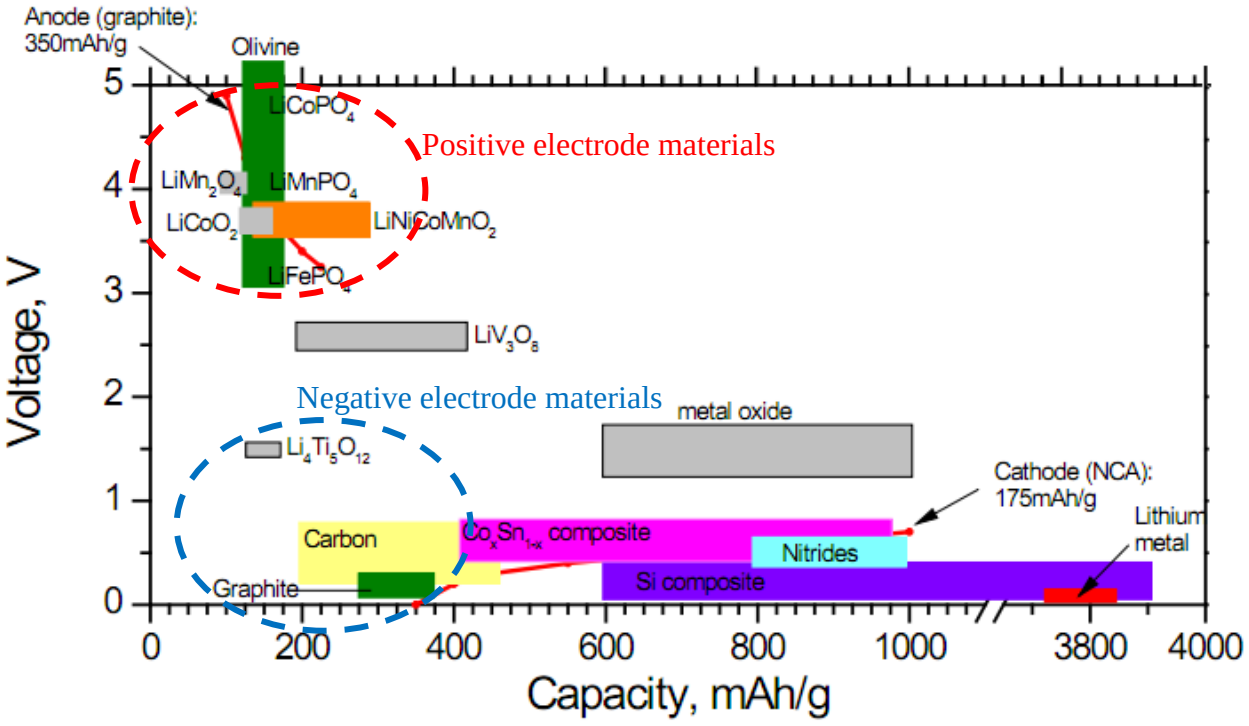

Figure 8. Positive and negative materials on a Voltage-Capacity scale

Positive electrodes are generally based on materials that contain lithium ions. The active material is coated onto an aluminium current collector with a polymer PVdF binder. Some of the common cathode materials are Lithium Cobalt Oxide (LCO), Lithium Manganese Oxide (LMO), Lithium Iron Phosphate (LFP) and Lithium Cobalt Nickel Manganese Oxide (NMC). Some materials are listed in *Table 1*

Table 1. Positive electrode materials [2]

Material	Abbreviation	Density [g/cm3]	Average potential [V]	Reversible specific capacity [Ah/g]	Volumetric energy density [Wh/cm3]
$LiCoO_2$	LCO	5.05	3.9	0.15 (to 4.2V)	2.95
$Li[Ni_{1/3}Mn_{1/3}Co_{1/3}]O_2$	NMC	4.77	3.7	0.163 (to 4.3V)	2.87
$Li_{1.1}Mn_{1.9}O_4$	LMO	4.18	4.1	0.12	2.06
$LiFePO_4$	LFP	3.6	3.44	0.16	1.98

Many cell designs employ carbon-based negative electrodes. Most often it is a form of graphite, sometimes with coke additives that is coated onto a copper current collector with PVdF as a binder. Graphite has a low potential compared to Li-based electrodes and a high capacity which makes it a desirable choice in building cells with high voltage and capacity. Another material is Lithium Titanate Oxide (LTO). LTO is said to have a particular structure that has a large surface area which facilitates fast ion intercalation/ejection [3]. Drawback however is the higher material potential and thus lower cell voltage. Materials are summarized in *Table 2*.

Table 2. Negative electrode materials [4]

Material	Abbreviation	Average potential [V]	Reversible specific capacity [Ah/g]
Graphite		0.1	0.37
$\boldsymbol{Li_4Ti_5O_{12}}$	LTO	1.5	0.16

When a cell with graphite electrode is first charged lithium reacts with graphite and forms a thin *Solid Electrolyte Interface* (SEI) layer. SEI mainly consists of Li_2CO_3, alkyl-carbonates and polymers. Lithium is irreversibly lost during this process. The layer is sufficiently thin to allow transfer of ions but thick enough to passivate the surface and not to involve more lithium into further formation [5].

Electrolyte

Electrolytes in Li-ion cells usually consist of [6]:

- lithium salt such as $LiPF_6$, $LiBF_4$ or $LiB(C_2O_4)_2$,
- organic solvent such as *EC*(Ethylene Carbonate), *PC*(Propylene Carbonate), *DMC*(Dimethyl Carbonate), *DEC*(Diethyl Carbonate), *EMC*(Ethylmethyl Carbonate) or a mixture of the above
- additives for optimization of performance and safety

Aqueous electrolytes are not used in cells because of unstable performance. SEI layer protects electrolyte from reacting with anode and decomposing.

Separator

Separator properties are a balance between high electric resistance acting as a barrier to the electrons and high porosity[%] and sufficient pore sizes(gurley,[s]) for ion transfer. Separators must be light to bring down the weight but have enough strength to withstand mechanical impact. Typical materials that are used in separators are PP and PE polymers in different

combinations, *Figure 9*. If temperature rises above roughly 130°C materials tend to start melting and closing up pores effectively shutting down ion transfer and securing the battery. [7] Some examples of separators are shown in *Table 3* below

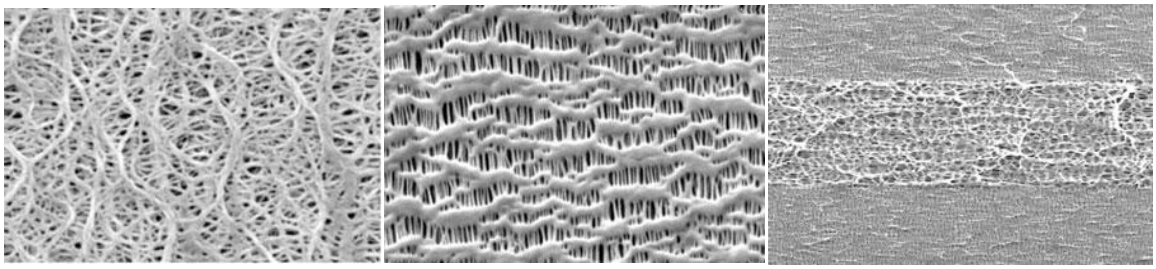

Figure 9. Celgard separators. From the left Monolayer PE, Monolayer PP, Trilayer PP/PE/PP Pictures courtesy of www.celgard.com

Table 3. Examples of commercial separators [7]

Table Typical Properties of Some Commercial Microporous Membranes

separator/properties	Celgard 2730	Celgard 2400	Celgard 2320	Celgard 2325	Asahi Hipore	Tonen Setela
structure	single layer	single layer	trilayer	trilayer	single layer	single layer
composition	PE	PP	PP/PE/PP	PP/PE/PP	PE	PE
thickness (um)	20	25	20	25	25	25
gurley (s)	22	24	20	23	21	26
ionic resistivity[a] (Ω cm^2)	2.23	2.55	1.36	1.85	2.66	2.56
porosity (%)	43	40	42	42	40	41
melt temp (°C)	135	165	135/165	135/165	138	137

[a] In 1 *M* $LiPF_6$ EC:EMC (30:70 by volume).

Cell performance

Cells are designed for high Power or high Energy Density. High Power cells should be able to charge and discharge at high currents but the cycles are generally short. High energy density cells are focused on absorbing and releasing more energy than being able to withstand high currents.

Energy depends on amount of active material in the cell. Electrodes are made with a thick layer of active material to intercalate more ions. Current collectors are usually made thinner. Electrode/collector ratio is high and such cells are heavier than power-optimized ones.

Higher power is achieved with lower resistivity. Active electrode material is made with large contact area for faster ion intercalation and release. Usually it is made thinner while current collectors slightly thicker for faster currents. As a result electrode/collector ratio is low and power-optimized cells weigh less.

2.2.2 Mechanical design

When cells are manufactured the electrodes are either long and rolled into a “jelly-roll” together with separator or cut in rectangles and stacked on top of each other, see *Figure 10*. For rolled cells the capacity is increased with electrode length while stacked cells use larger amount of electrodes.

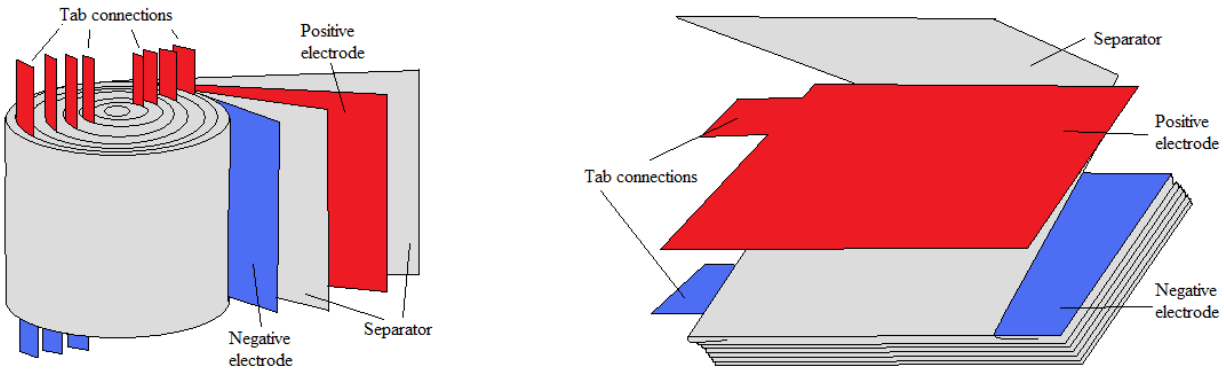

Figure10. A rolled and a stacked cell

Cells have two poles, or *tabs*. Tabs are connected to all current collectors inside the cell and are usually made of the same material. Typically one tab is in contact with the outside shell and the other tab is insulated with a polymer. Tabs are often placed with a space in between or even on the opposite sides of the cell to simplify connections or adjust flow of current. Separator is soaked with electrolyte and placed in between the electrodes.

The cells can be packaged in three ways:

- Cylindrical – thick aluminium shell with a cylindrical form, hard casing
- Prismatic – thick aluminium shell which makes a hard, box-like casing
- Pouch – thin aluminium shell covered with a thin polymer layer which makes a ”soft” prismatic cell

Typically cylindrical and prismatic cells are rolled while pouch cells are stacked.

Figure 11. Examples of Cylindrical (http://www.gaia-akku.com), Prismatic (www.gs-yuasa.com) and Pouch (www.eigbattery.com) cells

Cells are made air-tight by manufacturing in air-free conditions and therefore all cells are pressured. Opened cells are damaged and cannot function because electrolyte is venting out as well as moisture coming in and destroying cell materials. Packaging must be tight to push electrodes close to each other to eliminate gaps and also protect cell from mechanical impact.

2.2.3 Safety features

Cells have built-in mechanisms to deal with some of the problems that can come up during operation. Some major failure causes are listed below:

- Mechanical impact
- Vibrations
- Thermal abuse, ambient temperature rise/fall
- Overcharging
- Short-circuit, external/internal

Most of failures are due to malfunctions in battery system while some are due to contamination or material damage or malfunction inside the cell. In order to protect cells from such failures some safety devices are built into the cells. Safety devices include [8]:

- Safety vents. These are mechanical valves that open when cell pressure builds up from development of gases. This can happen due to a fault in usage for example if cell gets too hot. Pouch cell do not have vents and soft packaging opens on the side which makes it hard to predict where cell will rupture
- PTC (positive temperature coefficient devices) are usually used in small cells. These thermistors limit current when they are heated up
- Separators start to melt after around 130°C which shuts down ion transfer
- Electrolyte additives are aimed at decreasing flammability
- Redox Shuttle mechanisms absorb overcharge. Helpful only for a slight overcharge
- Ionic liquids are a different kind of electrolyte which eliminates flammability

As mentioned above cell casing is often in aluminium and connected to one of the poles. The casing is isolated with a thin polymer layer for it not to act as a third pole. If the layer is damaged current will leak through the casing to any conductor material in contact with the cell. In case of cell building up pressure due to overheating one or more safety vents open to release gases which will vent out most of electrolyte and by that neutralize the cell. Moreover it is important that all the gases that are vented out of the cell and all liquid electrolyte that comes out are not flammable. For that special additives are used in electrolyte which minimize flammability but at the same time lower cell performance.

2.3 Heat evolution in cells

2.3.1 Internal factors that influence cell temperature

Electric current in a cell is facilitated through ion flow between the electrodes and electron flow through the external circuit. Electric and thermal efficiency depends on how well energy is used in these processes. Factors that affect ion transfer are therefore:

- Withdrawal from anode (chemical)
- Transfer resistance
- Intercalation in cathode (chemical)
- Ion concentration

Electron flow is dependent on:

- Electron concentration (finite amount)
- Impurities in metal (alloys or contaminations, corrosion), obstruct electron flow
- Metal lattice imperfections (substituted atoms, shifted grains, etc. dislocations, vacancies, interstitial defects and impurity atoms) , obstruct electron flow
- Vibration of atoms in lattice due to higher temperature

As the reduction and oxidation sets in cell temperature starts to rise. Redox flows better when there is more thermal energy available. As cell temperature rises the movement of metal lattice increases which obstructs electron flow. Electrolyte and separator resistance also increases. A good balance between heat from these sources is essential for an efficient usage.

2.3.2 Heat sources and calculation

Sources that contribute to heat production on a cell level are [9]:

- Q_{joule} Joule heat (Ohmic heat)
- Q_P Potential deviation heat
- Q_S Entropy change heat

Ohmic heat is developed by resistance to current flowing through the cell and potential deviation heat describes cell resistance to potential deviation. Both can be expressed through *resistance losses*: $Q_P = I(V - V_0) = I^2R$ [43]

Entropic heat is developed by reduction and oxidation reactions in the cell and is expressed through a change of *entropy ΔS*: $Q_S = I\Delta S = IT\frac{\partial E_{emf}}{\partial T}$ [9], E_{emf} is electromotive force, or voltage during charge or discharge.

Measuring the overall heat produced by the cell for a specific cycle without analyzing the sources can be done through a calorimetric study or temperature study. Calorimetric studies have high accuracy but examining cell temperatures has on the other hand its benefits. Temperature measurement requires less time, equipment and delivers satisfactory accuracy as well as additional information about cell design like temperature spread and problematic areas.

In order to conduct a temperature study specific heat capacity *C* must be determined for a cell. An average value for Li-ion cells can be about 800 J/kg/°C [10]. Heat can be calculated through $Q = C \cdot m \cdot T$ where *m* is cell mass in kg and *T* is difference in average cell temperature throughout the studied cycle in degrees C.

Some heat losses will not be recorded by solely measuring cell temperature and must be accounted for. Such losses could for example be heat transferred through cell tabs and connecting wires. These losses can on average account for 22% of total heat [11].
Thus $Q_{tot} = 1.28 \cdot Q$

Thermal efficiency of a cell can then be calculated by dividing overall heat by the sum of energy that was put in and taken out of the cell during the studied cycle:
$Efficiency = 1 - (Q_{tot}/E_{in/out})$ [10]

Dividing total heat by cycle time gives heat generation rate *ΔQ* which is measured in W and is important for dimensioning thermal management system. $\Delta Q = Q/t$

An example for a cell that weighs 0.4 kg and changes its temperature by 14 °C during 120 seconds while drawing a 100A current at 3.6V would show that:

$$Q = 800J/kg°C \cdot 0.4kg \cdot 14°C = 4480J$$
$$Q_{tot} = 1.28 \cdot 4480J = 5750J$$
$$E_{in/out} = U \cdot I \cdot t = 3.6V \cdot 100A \cdot 120s = 432000J$$
$$Efficiency = 1 - (5750J/432000J) = 98\%$$
$$\Delta Q = 5100/120 = 42.5W$$

Knowing the specifics of internal factors, the I^2R and $I\Delta S$ losses can be used for creating a cell model that can simulate all usage conditions.

2.3.3 Thermal patterns

Current always takes the shortest way through the cell. Some areas in the cell therefore have higher current density then the others. More intense current means that redox reaction rate is higher and resistance losses are higher and subsequently such areas will become hotter than the rest of the cell. Cells are difficult to study from the inside physically because they need to be intact for proper operation. A lot of research in current distribution is therefore based on modelling.

Cylindrical cells exhibit highest current density close to the core [12], see *Figure 12*. Temperature on the inside will therefore also be higher. Prismatic cells follow a similar trend because they are manufactured in a very similar manner. Positioning tabs on the opposite sides will give highest temperature in the centre of the cell core while for cells with tabs on the same side highest temperature is likely to shift slightly closer to the tabs [13].

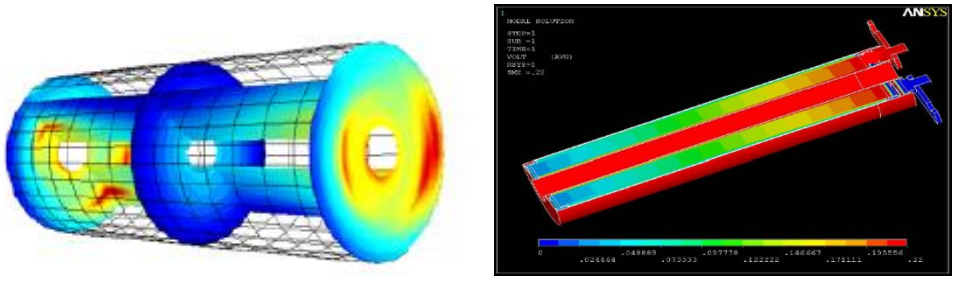

Figure 12. Current density distribution in a cylindrical cell with tabs on opposite and same sides

Pouch cells with tabs on the same side will have highest current density in area close to the tabs [14]. The further away the lower the current density will be and the colder the cell will be. Tabs on the opposite sides will give a very even current distribution throughout the cell but density right around the tabs will be higher. Results are shown in *Figure 13*.

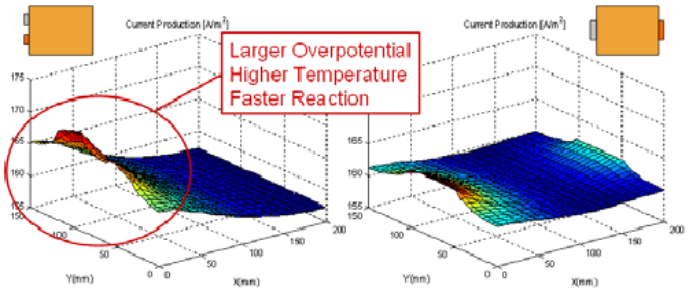

Figure 13. Current density distribution in a pouch cell with tabs on same and opposite sides

2.4 Thermal runaway

Thermal runaway occurs when exothermic reactions in the cell go out of control. The heat that is produced by the cell rises beyond the heat dissipation boundary where the reaction can be sustained. Thermal runaway does not stop without external influence and heat destroys the cell in the process, see *Figure 14*. Thermal runaway is a complex reaction that involves electrochemistry, cell materials and cell design which is why it is not fully studied and understood. Several thermal runaway explanations exist and show a similar general pattern but differ extensively on detail level.

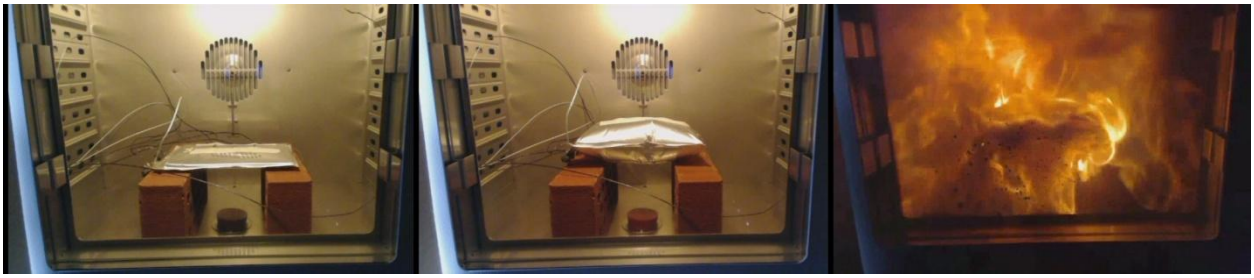

Figure 14. Progress of thermal runaway

Thermal runaway involves a number of exothermic reactions inside the cell that power each other in a sequence, *Figure 15*. Heat is therefore both a reaction starter and a catalyser. Thermal runaway can start if a cells temperature rises above roughly 80 °C.

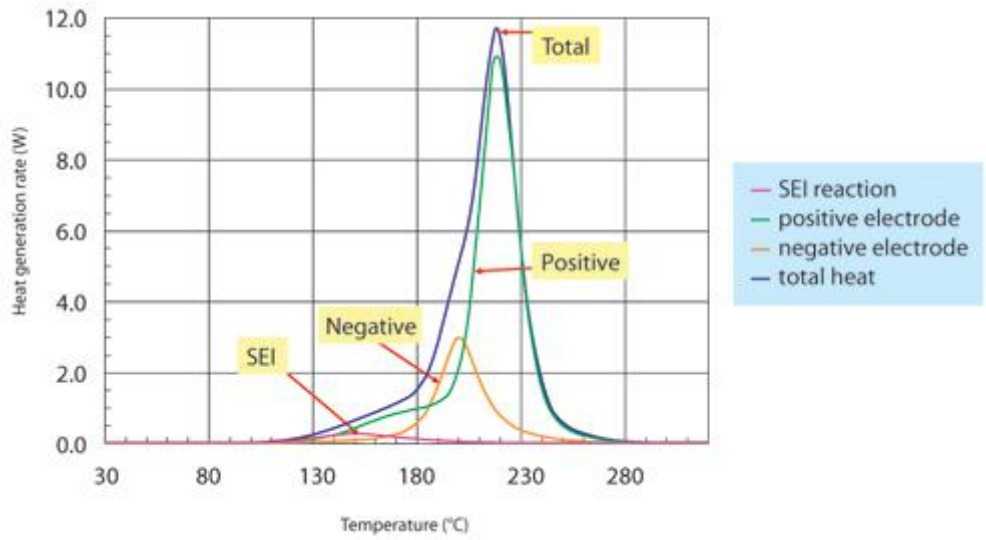

Figure 15. Cell before and after a thermal runaway, temperature evolution and peak

Thermal runaway can start from one of the following causes:

- Short circuit of the cell, external or internal. Cell temperature will rise
- Heat absorption from the environment, for example a fire or a neighbouring cell in a pack having thermal runaway
- Puncture or mechanical damage, which could also cause short circuit
- Overcharging
- High currents causing cell temperature to rise

Thermal runaway process progression is largely influenced by cell chemistry but also by particular materials and additives in a cell. Even a generalized description for a chemistry will likely differ from a result for a particular cell.

Thermal runaway stages

Process described below is a general summary for a LCO chemistry cell [15].

1. At around 69°C SEI layer on the negative electrode starts to decompose which leads to electrolyte reacting directly with graphite. The SEI decomposition is an exothermic reaction in itself and it contributes to the temperature rise. Reaction of electrolyte and graphite has even higher heat rate which keeps increasing the temperature.
2. As SEI decomposes the heat powers a reaction between organic solvents and intercalated lithium which starts at about 100°C. As a result flammable hydrocarbon gases are

released but no oxygen is yet present. Therefore the gases don't burn and just get accumulated and raze the cell pressure.

3. Separator melts at around 130°C and electrodes touch each other which short circuits the cell.
4. Heat from electrolyte breakdown causes positive electrode decomposition which releases oxygen due to material being lithium oxide. Electrolyte and gases start to burn. Reaction starts at around 130°C and temperature rises to 230°C.
5. Anode continues to release heat after SEI decomposition and reaches a second peak at 210°C. High amounts of energy are released at this point and cell gets extremely hot.
6. Metallic lithium goes in a reaction with EC in electrolyte which produces CO_2 (228°C)and POF3 at 200 - 240°C. Electrolyte decomposes in parallel with these reactions at temperatures between 200 and 300°C. Gases are vented and will likely catch fire.
7. After 260°C fluorinated binder material in electrodes reacts with electrode materials which results in heat emission. Hydrofluoric acid HF is released.

Many accidents has happened involving Li-ion cells catching fire or exploding because of thermal runaway. Cell problems in all kinds of vehicles and appliances can have high costs, and even human health can be damaged which is why thermal runaway must be studied thoroughly and prevented or passed safely.

2.5 Analysis of sustainability and economy

2.5.1 Sustainability of Li-ion batteries

Sustainable energy for the future is a challenge of today. Energy is produced and then shared with consumers through the network, or a grid. Quite many devices are not connected to the grid during operation. In stand-alone mode they need an energy source. Batteries are a solution. They provide a simple way of storing electric energy.

Li-ion batteries today provide the most efficient and convenient way to store energy, both for portable and stationary applications. Stationary battery systems have the power to accumulate electric energy from the grid and return it back in when demand arises. Portable devices only consume electricity from the grid. They however can use it under a long period of time. Energy transfer between producers and consumers within the grid can lower amount of consumed energy and thus the impact on the environment it makes to produce it. A lifecycle of a battery however has an impact on environment as well. Sustainability of battery technology can be studied with a Lifecycle Assessment, LCA.

LCA is a tool that helps study environmental impact of each step of a product from raw material production to manufacturing and assembly, usage and end of life. Since the LCA was not the primary objective of this thesis two existing reports were analyzed [16][17]. Goal of the analysis was to determine how environmental impact is distributed between components in Li-ion cells.

Studies were performed on EV and HEV respectively. Both studies included 100 Wh/kg batteries however EV study [16] assumed an LMO 30 kWh (300 kg) battery for the vehicle while HEV study [17] had an LFP 10kWh (100 kg). Battery sizes varied due to difference in drivetrain requirements. Usage phase was in both cases 150 000 km.

Positive electrodes caused 52% of CO_2 emissions of all cell materials where aluminium production was roughly half and active material was another half. Environmental influence was calculated with EI99 indicator. EI99 is a methodology that calculates weight of environmental

aspects of a product's lifecycle [18]. Highest environmental impact calculated with EI99 eco indicator was due to negative electrode (60%) of which copper production was roughly 55% [16]. Results are reported in *Figure 17*.

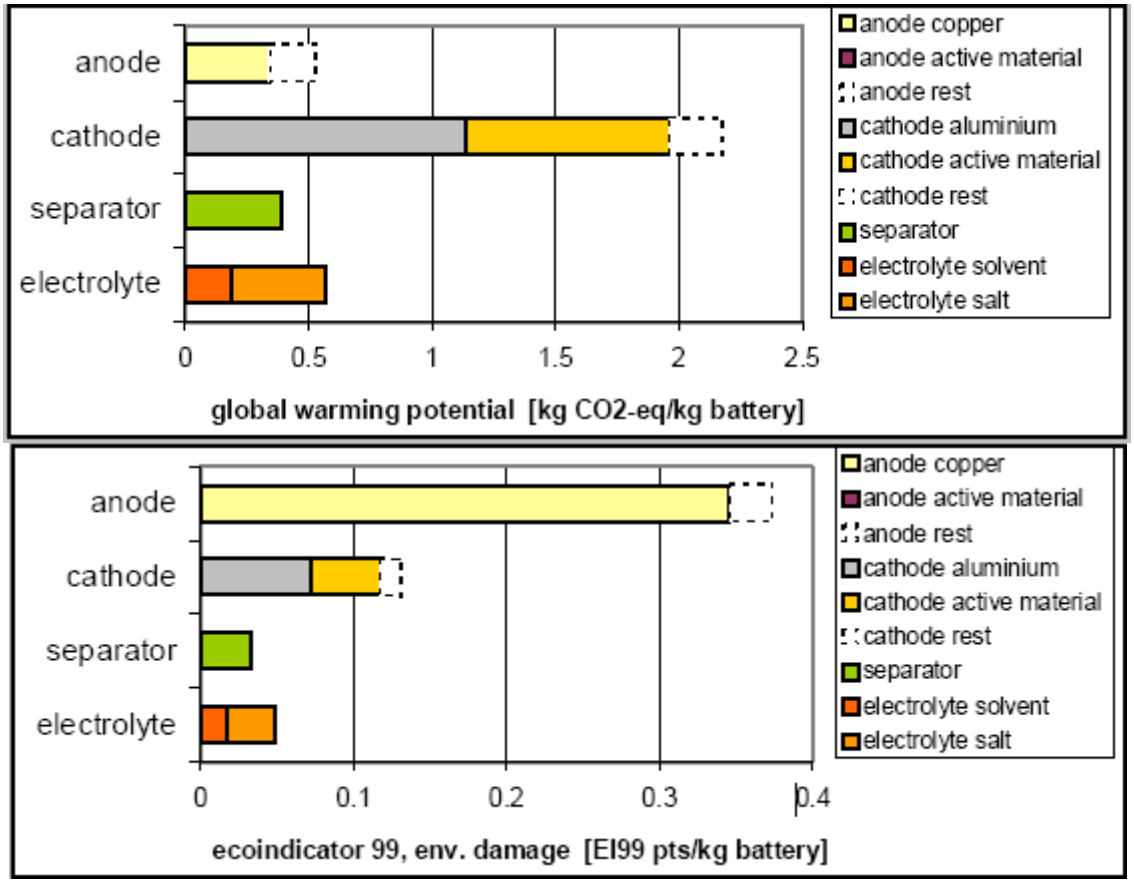

Figure 17. Eco-analysis of a li-ion cell [51]

Metals showed the highest influence of all cell materials. Aluminium caused highest CO_2 emissions while copper highest environmental damage. Both materials are downcycled in the end of life which recovers part of manufacturing losses. Recycled materials however cannot be used in battery cells because contaminants will cause performance losses or even malfunction.

How batteries are used has a large impact on the environment. Electricity comes from different sources in different areas of the world. Cars driven in Western Europe or particularly Scandinavia will be powered by electricity produced with fewer emissions (water and wind powered, also nuclear which however is not environment-friendly) than China where most electricity comes from fossil fuels. Battery usage in electric cars in China will produce more emissions than during cell manufacturing while in Europe the manufacturing is dominating by far [17].

Sustainability also depends on cell efficiency [17]. Optimizing usage conditions for best cell performance will cut the losses and less electricity would be needed for charging. Also inverter efficiency can be added to these losses. These losses were found to be dominating throughout battery usage (roughly 75%) and not the weight that it adds to a car.
Simpler and more efficient design of battery packs will have a positive influence on sustainability. Easy connections between the cells can save material. Pack electronic equipment can also be designed more efficiently material-wise and in terms of performance. Battery Thermal Management System TMS is large and energy consuming unit. Further development of a TMS will contribute to both production and usage sustainability. Re-using the thermal energy

is a potential approach to dealing with this problem. More advanced insulating and heat transfer materials can also be used for that matter.

Length of battery's life is a limitation of battery technology. Battery health decreases throughout the cycles which is one of the reasons why battery systems cannot be designed to employ full cell capacity. Better understanding of cell health is crucial for designing a system that will utilize cell power to the maximum within reasonable limits. A support for battery service or upgrade will prolong the life of the vehicle which will have a positive influence on sustainability.
A trend is visible that more advanced electrode materials and electrolyte greatly improve cell performance and Li-ion market is moving towards those materials. There is a risk that manufacturing of such materials will be more pollutant and energy-consuming than today until manufacturing technology advances towards sustainability. The gain however lies in usage phase of the cells making them last longer and work more efficiently.

2.5.2 Economical analysis

Cost of components of a cell is distributed in the following way [19]:

- Anode: 5% to 15%
- Cathode: 5% to 11%
- Electrolyte: 10% to 14%
- Separator: 40% to 60%

Battery cells are always put together into a battery pack which includes cell connections, electronics and sometimes cooling. Cell cost is therefore only a part of total cost.

Reduction of components prices can potentially lower cell cost by 25%. Manufacturing improvements stand for another 30% reduction. Improvement of capacity of cell materials has a 40-45% price reduction opportunity [20]. More advanced materials however will likely raise the manufacturing cost until a better manufacturing method is developed or scale of manufacturing is increased.

Latest McKinsey & Company analysis suggests that Li-ion prices will fall from today's 500-600$/kWh to 160$/kWh in 2025. Research suggested that prices below 250$ will make HEV and EV cars competitive with combustion engine powered on the cost-of-ownership basis [20].

Manufacturing of cells is confined to geographical areas where cells are being manufactured and developed now and where local businesses serve as a base for manufacturing of materials that are included in cells. These clusters are located in places where the market for batteries lies. Li-ion batteries are in big demand by companies that incorporate them in hand-held and cordless devices. Sufficient income allows battery manufacturers to drive internal research and development.

Analysis shows that Japan holds largest amount of patents in Li-ion technology as of 2009, *Figure 18*. Largest amount of Li-ion batteries is also manufactured there.

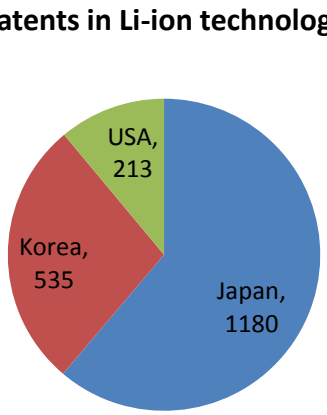

Figure 18. Amount of patents in Li-ion technology in different countries [21]

Large Li-ion cells are produced not only for HEV and EV purposes. These kinds of cells are used in power supply systems and aircrafts and helicopters. Development of big cells is driven by the companies that are sensitive to battery performance enhancement. HEV and EV batteries has only a small share on the battery market but many big manufacturers and small technological companies and startups see potential in this market and develop solutions for it. So far the demand for pure HEV/EV cells is low compared to small cells for appliances and consequently development process is slow.

3 THE PROCESS

This chapter describes methodology that was employed in the four experiments that were carried out.

In order to get a broad view of cell thermal behaviour the study included tests in conditions that were similar to cell usage conditions and in environment that simulated extreme cases that a cell can be exposed to.

3.1 Cells used in experiments

An overview of cells that were tested during the study is presented below in *Figure 19*. A more detailed description of cell specifications follows in *Table 4*. All cells are suitable for both EV and HEV applications. Apart from battery cells a supercapacitor was studied. Following items were tested:

Pouch

1. LG Chem 5.3 Ah LMO
2. EiG 7 Ah LFP
3. EiG 20 Ah NMC

Cylindrical

4. A123 4.4 Ah LFP

Prismatic

5. Cell 1 3.1 Ah LMO/LTO

Supercapacitor

6. JSR 2000F

Figure 19. Tested cells

Table 4. Test cells specifications from manufacturers [22]

	Cylindrical	Pouch			Prismatic	Supercapacitor
	A123 4.4Ah	EiG 7Ah	EiG 20Ah	LG Chem 5.3Ah	Cell 1	JSR 2000F
Capacity [Ah]	4.4	7	20	5.3	3	0.98
Cathode chemistry	LFP	LFP	NMC	LMO	LMO	Activated carbon
Anode chemistry	Graphite	Graphite	Graphite	Graphite	LTO	Li-doped carbon
Tab position (side)	Opposite	Same	Same	Opposite	Same	Opposite
Max Voltage [V]	3.6	3.65	4.15	4.2	2.8/2.9	3.8
Min Voltage [V]	2.19	2	3/2.5	2.5/2	1.8/1.5	
Nominal Voltage [V]	3.3	3.2	3.65		2.4	2.2
Max Discharge current (Cont/pulse)	130/260 A	20/30 C	5/10 C	120 A	31/200 A	
Max Charge current (Cont/pulse)	44/183 A	0.5 C	0.5 C	150 C	31/200 A	
Size [mm]	32x113	221x130x4.5	216x129x7.2			280x126x9
Weight [g]	205	237	410			208
Specific Energy [Wh/kg]	71	95	180			14

3.2 Thermal behaviour experiments

Available equipment for the test included:

- Infrared camera
- Thermocouples
- Cycler and logger
- Climate chamber

Cells were mounted in fixtures and connected to a cell tester (cycler) with cables. Cycler could be programmed to do charge and discharge cycles. Pulses were created by making a series of charges or discharges and adding breaks. *Figure 20* below shows current in red and actual voltage in blue in an example of pulse and continuous cycles.

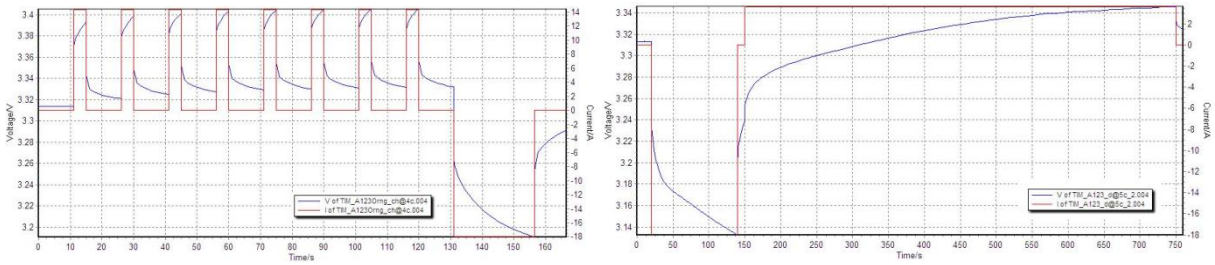

Figure 20. Current and Voltage through pulse charge and continuous discharge cycles. Current is in red and cell voltage in blue

In order to save test and data analysis time a limit on the length of test run was chosen to be two minutes. Therefore each run was two minutes whether it was pulse or continuous cycle. Pulses however were designed to draw the same amount of energy as corresponding continuous runs to facilitate a fair comparison. An energy counter in software was used for programming.

Cells were placed in a climate chamber on top of a polymer shelf. Climate chamber kept ambient temperature stable and shielded against temperature fluctuations from air-conditioning unit and pulses from other equipment in the lab. A sketch of the test setup is shown in *Figure 21*.

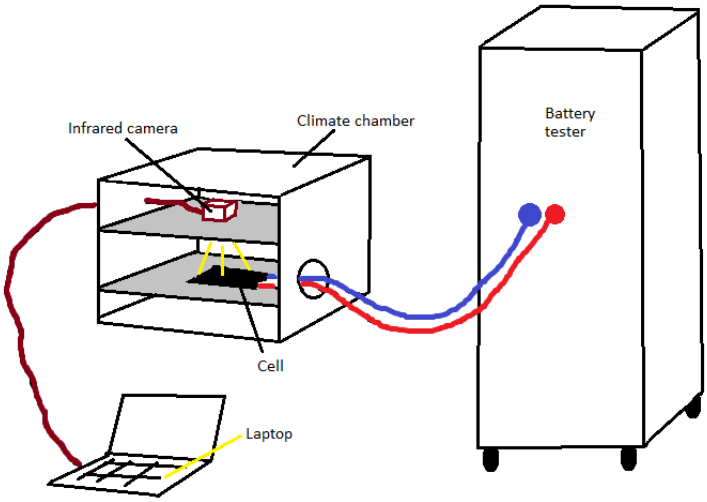

Figure 21. Setup during thermal behaviour testing

An infrared camera was positioned above the cell. Distance between the camera and the cells was different in order to get the cell as close as possible to the camera to get a good resolution of images. A sampling rate of 1 second was chosen for the images. Cells were painted matt black to improve emissivity and thus data reliability. Test results were obtained by comparing an image from the beginning of the test and one from the end of the two minutes.

An example of infrared camera image is shown in *Figure 22* below. White rectangle covered area of the image that was battery cell. Data was analysed only from the cell surface. Hot and cold areas on the cell were visible in accordance with the temperature scale. Hot areas were coloured in blue and white tones.

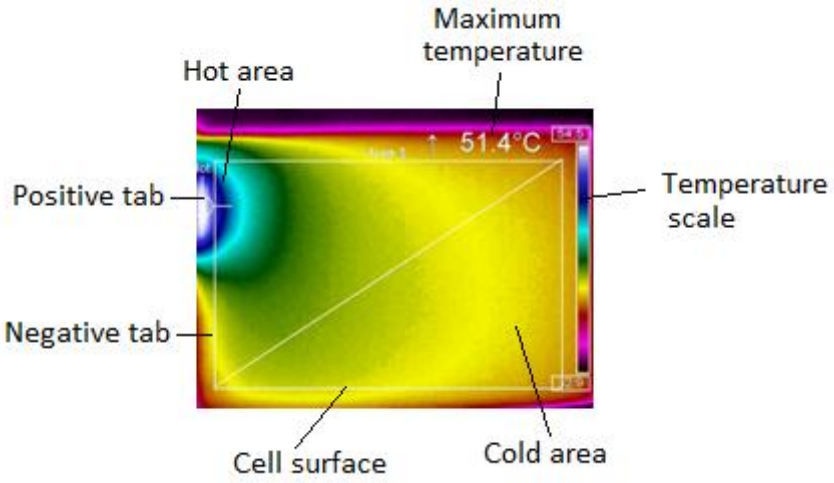

Figure 22. Thermal image. Different areas explained

Images that were obtained with the camera were saved as a 160 by 120 matrix with temperatures. Data was transferred to Matlab [23] and analyzed to retrieve responses.

To illustrate how cell surface temperature varied the following responses were noted:

- Δ Max T, a difference in maximum temperature in the beginning and end of test run. Maximum temperature was defined as an average of top five percent of measured cell area in order to eliminate spikes due to equipment faults

- Δ Mean T, a difference in mean temperature of the cell surface in the beginning and end of test run
- Std Dev, standard deviation or spread in the end of test run to show how evenly temperature was distributed on the area. No comparison was used for spread because cell at starting conditions was meant to have as even as possible surface temperature

These experiments were divided into three tests to bring down level of complexity of experiment design. Tests 1 and 2 were based on a 2^3 factorial design. Such test procedure was chosen to reduce number of runs and have a built-in way to evaluate factor influence by means of response comparison by calculating factor effects. Effect calculation was chosen over Analysis of Variance, ANOVA to make analysis simpler and more efficient without a significant interference with quality. Both effect calculation and ANOVA are statistical analyses that compare mean values of groups of data. A significant difference in mean values indicates factors that have influence and direction of the effect. Test 3 was a slightly simpler design that compared only 2 factors at a time.

Practical issues using the equipment and nature of cells facilitated studies of temperature solely on cell surface. Tests 1, 2 and 3 were performed on all Li-ion cells. Test 1 also included a supercapacitor cell.

All cells were lying on a surface during all tests which effectively induced two zones for heat transfer: largest cell area was in air while the rest of the cell was in contact with a surface. Cylindrical A123 cell had quite a small contact are due to its form. Also the prismatic 3.1Ah cell was standing on its small side having a small contact area as well.

Test 1

This test was designed to compare influence on cell temperature from three following factors:

- Charge/discharge
- High/low current
- Continuous/pulse

A test procedure was the set up to obtain results. Firstly responses were defined. To illustrate how cell surface temperature varied the following responses were noted:

- Δ Max T
- Δ Mean T
- Std Dev

Thermal camera was used for response logging. A screenshot at the beginning of the test and in the end of test was taken with the camera. Cell surface could be analyzed as a matrix with temperature values which made it possible to perform necessary calculations to compare responses.

Secondly high and low levels of study factors were defined which are shown in *Table 5*.

Table 5. High and low levels of study factors in test 1

	+	-
(A) Charge/Discharge	Charge	Discharge
(B) Current rate	High	Low
(C) Continuous/pulse current	Continuous	Pulse

Thirdly a test procedure including all the test runs was designed. As a 2^3 design was chosen all factors A, B and C were compared to each other and their interactions AB, AC, BC and ABC were studied. Interactions however tend to give faulty results when many factors are at play therefore no special attention was paid to the results of interaction influence unless it was particularly significant. The test runs are presented in *Table 6* below.

Table 6. Test runs in test 1

		Factors and interactions							
		A	B	C	AB	AC	BC	ABC	
		Ch/disch	Hi/low	Cont/pulse					
Test runs	1	-	-	-	+	+	+	-	Discharge Low Pulse
	a	+	-	-	-	-	+	+	Charge Low Pulse
	b	-	+	-	-	+	-	+	Discharge High Pulse
	c	+	+	-	+	-	-	-	Charge High Pulse
	ab	-	-	+	+	-	-	+	Discharge Low Continuous
	ac	+	-	+	-	+	-	-	Charge Low Continuous
	bc	-	+	+	-	-	+	-	Discharge High Continuous
	abc	+	+	+	+	+	+	+	Charge High Continuous

All cells had different capacity, size and charge and discharge current limits therefore different currents were used for all cells. Manufacturer specifications were followed and currents were chosen as close to cell limits as possible to strive for a larger influence.

In order to save test and data analysis time the test runs were two minutes long. Therefore both pulse and continuous runs were two minutes. Pulses however were designed to draw the same amount of energy as corresponding continuous runs to facilitate a fair comparison.

Next step was carrying out the test runs and registering the three responses. Once the responses were obtained each factor's effect could be calculated. Factorial design such as 2^3 uses a simple statistics effect calculation to estimate the influence of factor on response.
An effect of a factor is calculated using a factor's contrast which is acquired through summing up results of each run taking signs from the factor's column. As an example a contrast of A would be: C_A = -1+a-b+c-ab+ac-bc+abc. The effect is then divided by a half of number of observations, N which is N = 2^k n.

$$Effect = \frac{Contrast}{N/2}$$

$$N = 2^3 \times 2 = 16$$

The effect shows the direction of highest influence and gives a relative magnitude of influence which was used to compare different factors in the test and study which levels of factors influence temperature rise in cells.

Test 2

Test 2 procedure was very similar to test 1 only different factors were studied. High and low levels of factors are shown in *Table 7* below:

Table 7. High and low levels of factors in test 2

	+	-
(A) SOC	50%	80%
(B) Ambient temperature	22°C	35°C
(C) Charge/Discharge	Charge	Discharge

Climate chamber was used to reach desired ambient temperatures. As the chamber has a built-in fan it was turned on prior to the test to reach the desired temperature and turned off before the test as not to induce forced convection. The test runs were two minutes long as in previous experiment which had an insignificant influence on temperature inside the chamber and did not raise the ambient temperature. As in test 1 the currents were different for all cells due to cell differences is capacity, energy and current limitations.

The responses used were also the same ones as in test 1. Test runs were designed in a similar manner and effects were calculated in the same way.

Test 3

This test was designed to get an overview of cell performance in realistic conditions running a cycle that was recorded from a hybrid vehicle. Influence from cooling was also studied in this test by making a second run for each cell with two fans blowing air onto the cell from above.

A HEV cycle is a typical example of load where cell goes through a series of short but rapid discharges and charges which corresponds to acceleration assist and braking energy regeneration respectively. Cycle included charge currents up to 45A and discharge currents up to 80A and is shown in *Figure 21*.

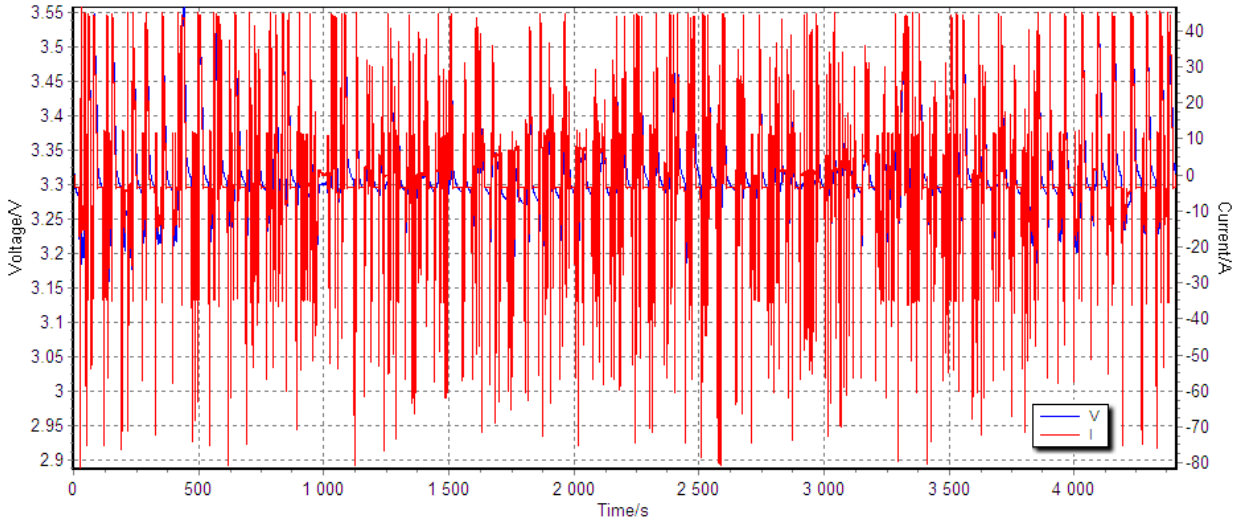

Figure 23. HEV cycle used in test 3. Current is in red and cell voltage in blue

The test was run in climate chamber at 22°C. Seeing as the chamber had a built-in fan and the cycle being 1hour 15 minutes the cell was always under a forced convection and thus had better cooling than under natural convection. The cooling setup however included two powerful fans blowing air on the cell surface which had a significant influence on convection and could be regarded as a better cooling than the built-in fan.

Six to eight thermocouples were used for temperature logging during this experiment depending on cell design and size. Thermocouples were placed to cover most areas and study variation between different points on the cell.

3.2 Thermal abuse experiment

Cells were placed in an oven on one or two bricks depending on cell size, *Figure 24*. Five thermocouples were attached to cells in different areas with reinforced tape. Sixth thermocouple was logging temperature in the oven. Cell voltage was also logged. Cells were filmed with a camera to study the behaviour. Oven was then turned up to the desired temperature.

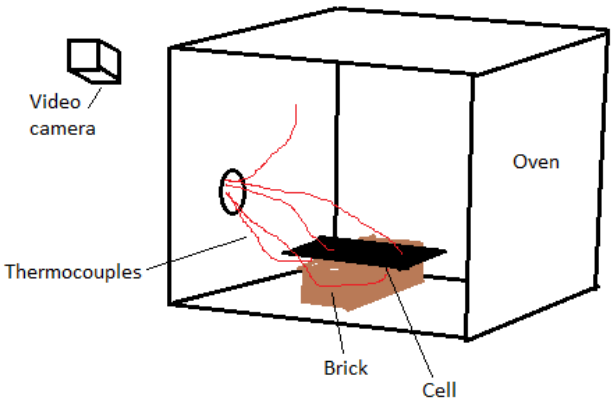

Figure 24. Thermal runaway setup

This test had a limit of six cells for testing and therefore a special procedure was needed. As a result two test procedures were designed. Procedure A involved first a fast temperature ramping up to 80°C followed by 15 minute hold at that temperature and after that a 10°C increase with a 15 minute hold up to around 300°C. Procedure B involved continuous temperature ramping from ambient temperature up to around 300°C. Temperatures were based on results of theoretical study [15] in accordance to the range of temperatures of events that account for thermal abuse. These procedures were chosen to simulate a thermal management system failure and a fire respectively and to study the results of these events.

The two procedures were then tested on three pairs of cells:

- A123 4.4Ah LFP-based positive electrode
- EiG 7Ah LFP-based positive electrode
- EiG 20Ah NMC-based positive electrode

All cells were tested fully charged to 100% SOC. Cell weight and size was noted prior to and at the end of test.

4 RESULTS

In the results chapter the results that are obtained with the methods described in the process chapter are compiled, and analyzed and compared with the existing knowledge and theory presented in the frame of reference chapter.

4.1 Test 1 results

This experiment was designed to study how continuous or pulse charge and discharge at high and low current influenced cell temperature. Test conditions were 21 to 22°C ambient temperature and 50% SOC for all cells.

An ANOVA analysis of effects for each factor was carried out to illustrate direction of influence on study factors. ANOVA results are shown below in a form of a box plot, *Figure 25*. Each factor is represented by a box that consists of four equal in size quartiles Q1-Q4. Q2 and Q3 together represent 50% of sample. Red line is a median or the middle value of a sample. If a factor median (red line) is far from another factor's medians it has a significant influence. Direction of influence (positive/negative) shows if factor has effect at high or low level.

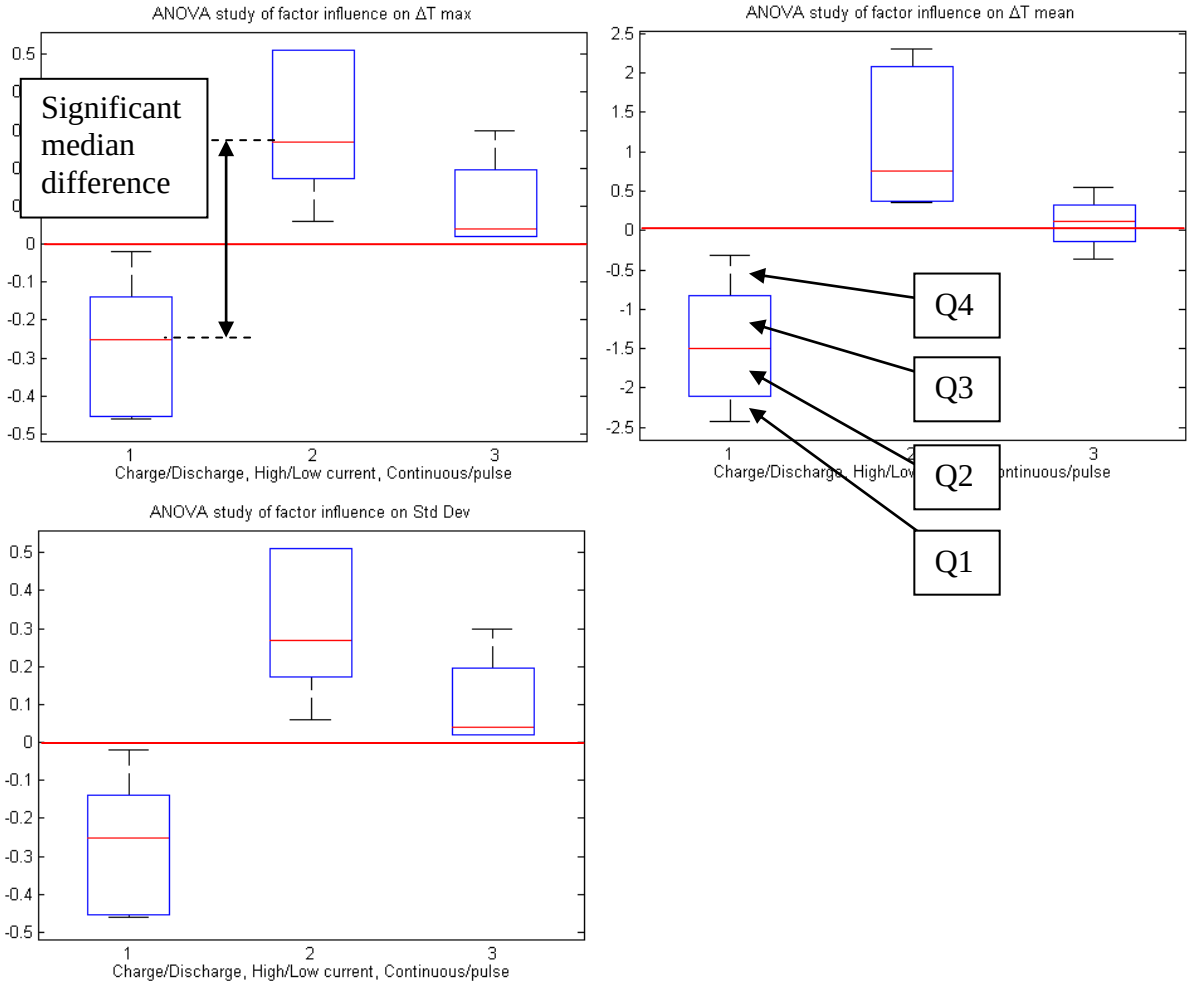

Figure 25. ANOVA analysis of general factor influence

Charge versus discharge

Discharge had a large influence on maximum and mean temperature as well as standard deviation (spread). Magnitude was cell dependent and combined with high current increased by

around 10 °C for maximum cell temperature (Max T). Discharge at low currents also showed temperature rise but on a 1 to 2°C scale.

Charge at high currents had a very similar effect on cell temperature. Currents over 1C showed a significant influence on temperature due to higher losses in the charge process. Charging at 0.2C or lower currents had a special effect on cells. Entropic heat was negative which resulted in cell temperature dropping and cell getting colder than the starting conditions. This effect however was visible only for LMO chemistries.

High and low current rate

During charging high currents generally has a large influence on Max T and spread which is why currents of 0.5 to 1C are usually employed for charging. An LTO anode however was not influenced by current to such extent and could be charged up to 10C. Low current of 0.2 - 0.5C generally had an up to 1°C effect on cells and for LMO chemistries even showed endothermic behaviour lowering the temperature by less than half-degree. Discharge at high currents increased cell maximum temperature by 7 to 3°C in average. At low currents the influence was 1 to 3°C at most.

Continuous versus pulse current

Continuous currents generally increased cell temperature more. Influence is often between 2 and 5°C. Pulse currents of the same energy amount decreased the temperature. This effect was larger for high currents. The pattern however was not followed in some few cases. Temperature spread is also affected differently in different cells and test conditions.

Details of test data are available in Appendix 1.

Supercapacitor test

Li-based supercapacitor is a different technology from Li-ion batteries. Capacitors have exceptionally high power and sustain high currents but are only able to hold very little energy.

Tested supercapacitor showed a quite linear voltage-SOC profile (Blue line, *Figure 26*) compared to Li-ion batteries (Figure 7). Temperature increased by 2°C (Magenta line, *Figure 26*) during full discharge with 10A. Charge was clearly endothermic and temperature decreased with 2°C.

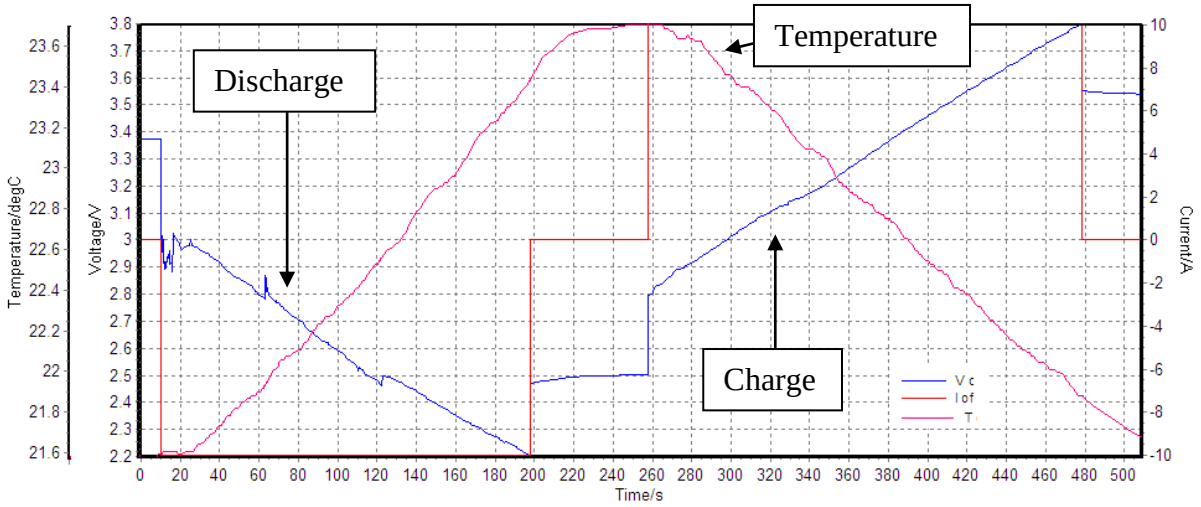

Figure 26. JSR 2000F voltage (blue), current (red) and temperature (magenta) during discharge and charge

More information about the supercapacitor and the test results is presented in Appendix 4.

4.2 Test 2 results

The aim of this experiment was to establish influence of SOC, ambient temperature and charge or discharge on cell temperature.

Similarly an ANOVA analysis of factor effects for each factor was carried out to illustrate direction of influence on study factors. The results are shown in *Figure 27* below.

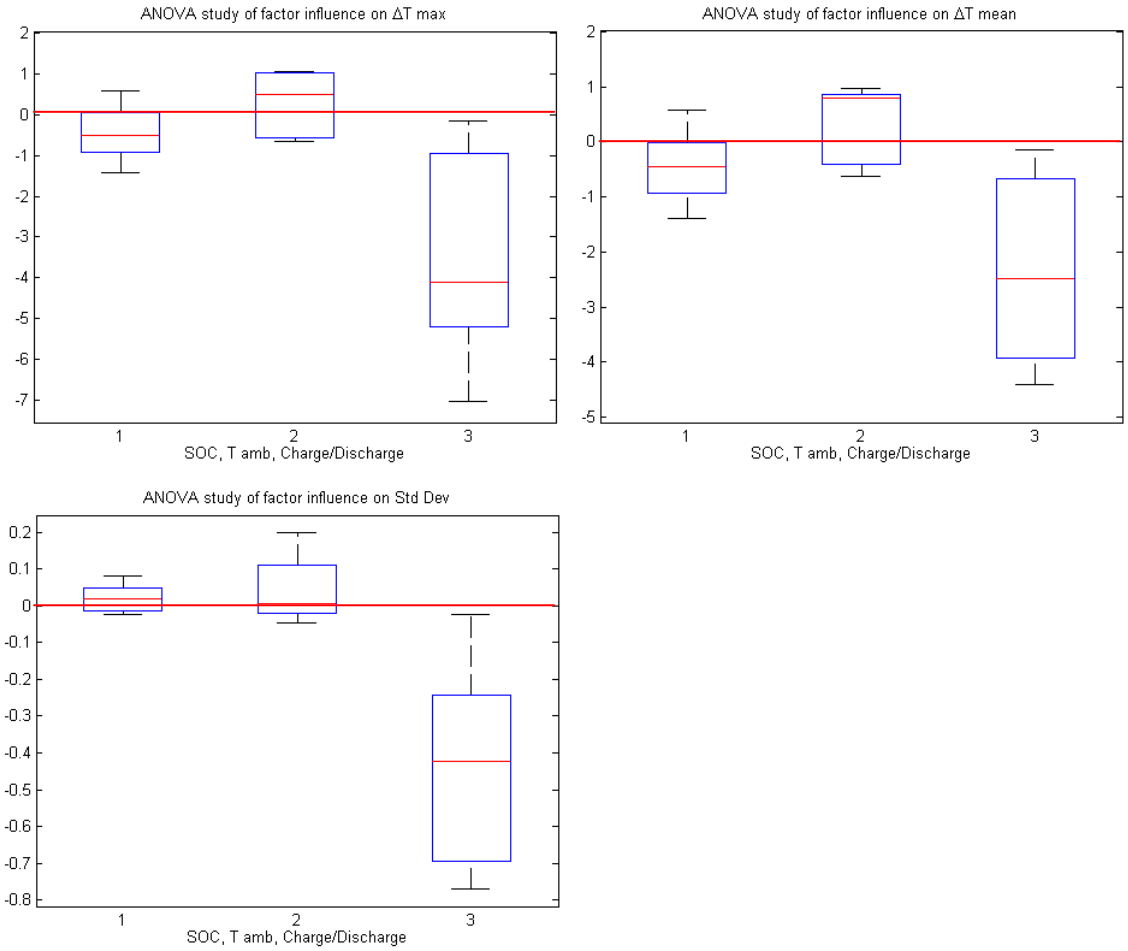

Figure 27. ANOVA analysis of general factor influence

SOC

SOC had effect on cell temperature with average magnitude of one to 4°C for both maximum and mean temperature. Each cell had a particular trend for SOC and temperature and SOC had a substantial effect. The influence was different in direction for different cells even with similar chemistries and spread could not be generalized either.

Ambient temperature

Temperature and spread increased less for higher ambient temperatures. As a result cells heated up less and more evenly at temperatures around 30-35°C. This temperature could be considered an optimal condition for cells that were made for room temperature use because higher temperatures reduced resistance in cells and speeded up cell reactions. Average magnitude of effect was 1 to 4°C.

Charge/Discharge

Discharge had a very large influence on Max and Mean T and also spread. Maximal temperature increased to at least 7°C and up to 20°C in some cells. Charge on the other hand increased temperature by 1 to 4°C in general but had some peak values for particular cells and was even endothermic in specific conditions.

Study with ANOVA showed a significant influence on cell temperature during discharge which is visible in *Figure 27*. Negative result indicated that factor was significant at its low level which was discharge.

4.3 Test 3 results

Cell temperature during HEV cycle varied within a 23 to 25°C range once the cell has heated up to that level from 21°C ambient, *Figure 28*. HEV cycle involved an overall stable energy level but during some periods more energy was discharged from the cell. Temperature was slightly higher when more energy was drawn and somewhat lower when pulses were energy and SOC neutral. Temperature on the surface was quite evenly distributed as recorded by the thermocouples.

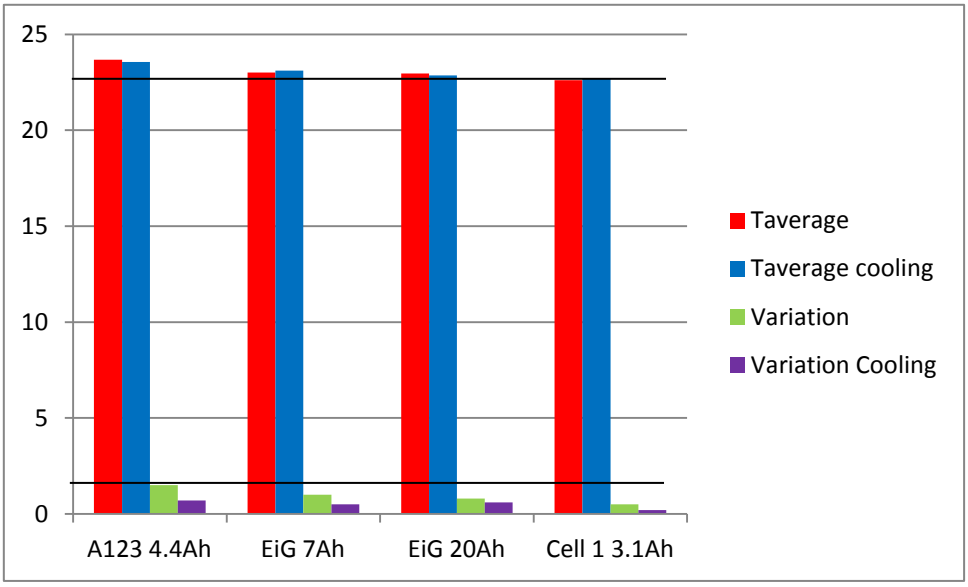

Figure 28. Cell comparison

Cells were compared in *Figure 28*. Variation is the difference between top and bottom temperatures during the cycle. Average temperatures with cooling were only lower for A123 and EiG 20Ah cells. Spread of temperature was on the other hand always lower with cooling. During tests roughly 1% less energy was taken out of the cells during HEV cycle with cooling. That indicated thermal losses.

Table 8. Temperature reduction and energy increase with cooling

Cell	Minimum temperature, °C	Maximum temperature, °C	Energy increase, %
A123 4.4Ah	23	24.5	1
EiG 7Ah	22.5	23.5	1
EiG 20Ah	22.6	23.4	1.2
Cell 1 3.1Ah	22.4	22.9	1.3

Average temperature of cells reduced in some cases and increased in some when cooling was used, *Table 8*. The effect was unstable. On the other hand as a general trend cooling reduced higher and lower levels of temperature which certainly improved cell working conditions. Thermal cycling decreased which enhanced cell life. Compared to the effects of energy that was produced by the cell cooling cycles were roughly 1% less efficient. Cooling was therefore a balance between lower thermal cycling and thus longer life or thermal efficiency. In a battery system cooling is a necessity because cells start to spread heat to each other. Ability to influence their temperature also becomes an objective.

4.4 Cell analysis based on results of tests 1-3

Cell results

All temperatures are relative to the ambient temperature at which cells were tested, 22 and 35°C depending on the experiment. More detailed results are presented in Appendix 1-3.

A123 4.4Ah

Discharging and charging at low currents (under 1C) at 22°C ambient caused temperature to increase by less than 1.5°C. At high currents (10C discharge and 5C charge) temperature increased by 7 and 4.5°C respectively.
At ambient temperature of 35°C cell temperatures during discharging and charging with high currents were 2 to 3°C less than during respective cycles at 22°C ambient. At low currents influence was similar.
During charging at 35°C ambient temperature was less at 50% SOC compared to 80% by roughly 1°C. At 22°C ambient temperature at 80% SOC was less by 1°C and at 50% 2.5°C. Discharge at 35°C ambient showed quite similar temperatures at both SOC levels. At 22°C ambient temperature at 80% SOC increased with 1.5°C compared to 50%.
Temperature pattern showed higher temperature in the core of the cell, *Figure 29*. Poles were slightly colder probably because heat was lead out through the cables.

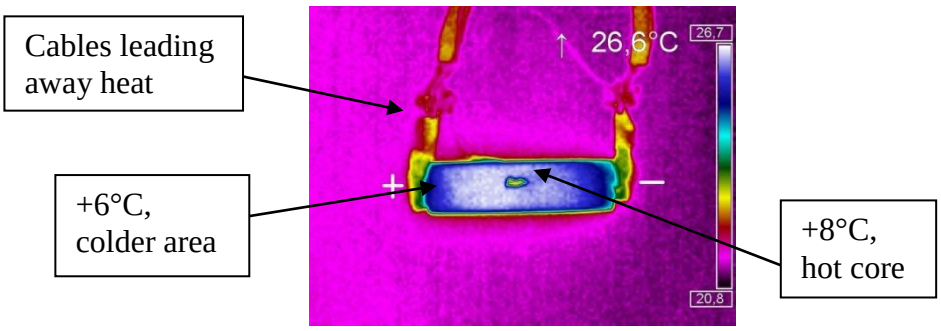

Figure 29. A123 4.4Ah temperature distribution during discharge with 10C for 2 minutes

EiG 7Ah

Discharging and charging at low currents (under 1C) caused a temperature rise of up to 3°C. Discharge at high currents and at 22°C ambient increased temperature 9 to 11°C.
Ambient temperature of 35°C decreased cell temperature by 4°C during discharge compared to 22°C. Charge was uninfluenced. During discharge temperature at 80% SOC level was continuously 1.5°C lower than 50% SOC at 35°C ambient and lower by 2.5°C at 22°C.
Area between the tabs was hottest in the cell. A temperature gradient was visible in a diagonal pattern starting with the hottest point at the positive pole. Cell temperature in the middle of electrode layers (in cell core) was higher than the measured surface temperature, *Figure 30*.

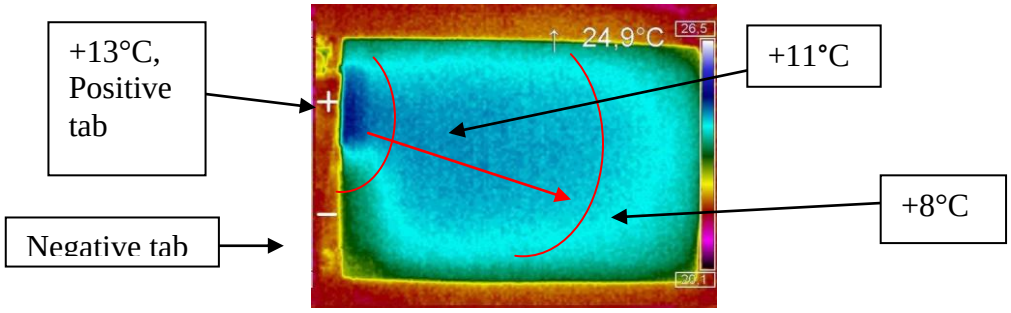

Figure 30. EiG 7Ah temperature evolution during pulse discharge with 16C for 2 minutes

EiG 20Ah

Charging at currents lower than 1C increased temperature by 1.7°C or less. Discharge had a 3 to 5°C influence. At high currents average cell temperature was 10°C and maximum 16 to 20°C. During discharge at 35°C ambient cell had a very even temperature profile at both SOC levels. Discharge at 22°C reached highest and lowest temperature of all discharge cycles at 80% and 50% SOC respectively. Charging was quite even except for a 2°C higher temperature at 22°C and 50% SOC.

Highest temperature was distributed in a diagonal gradient from the positive pole, *Figure 31*. Positive tab was emitting most heat.

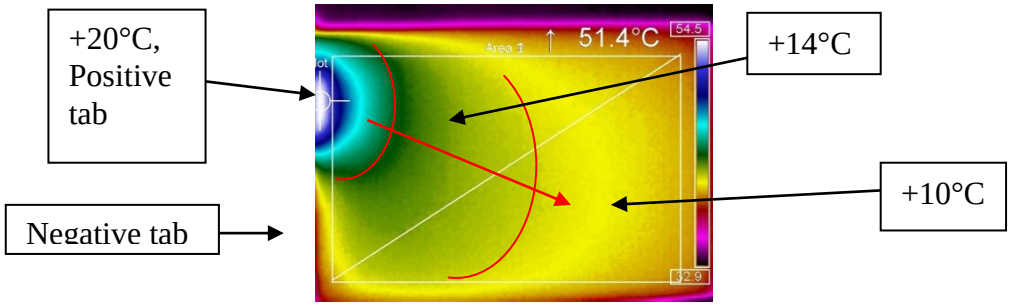

Figure 31. EiG 20Ah temperature distribution during continuous discharge with 10C for 2 minutes

LG Chem 5.3Ah

At low currents and 22°C ambient discharge influenced cell temperature by less than 2°. Charge was endothermic and decreased cell temperature with 0.1°C.

Cell temperatures at 35 and 22°C ambient were similar within 1°C. Discharge at 80% SOC increased temperature by 8°C on average and 13°C at maximum. At 50% influence was 6°C on average and 11°C at maximum. Charge at 80% SOC and 35° was 5° higher than other charge cycles.

Discharge at ambient of both 22 and 35°C was roughly 2°C colder at 50% SOC than 80%.

Cell had a very even distribution of temperature, *Figure 32*. Positive tab was very hot and high temperature was distributed as a half-circle around the tab.

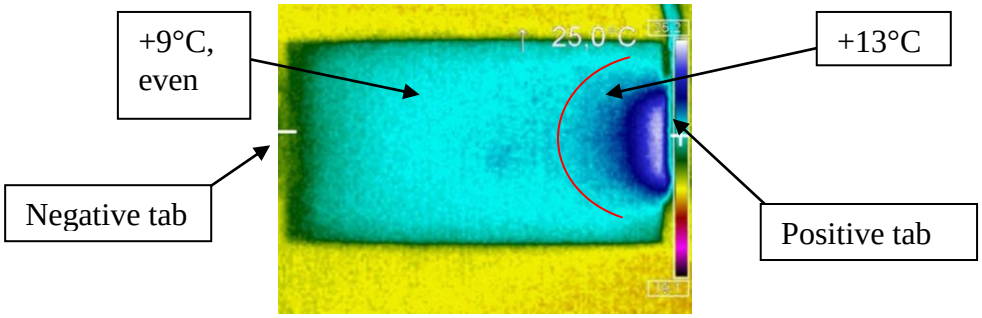

Figure 32. LG Chem 5.3 Ah temperature distribution during discharge at 10C for 2 minutes

Cell 1 3.1Ah

Charging and discharging at low currents (less than 5C) caused no influence on cell temperature. Discharge at 35°C ambient reached 1°C lower temperature than at 22°C. 50% SOC was consistently 2°C higher than 80%. Discharge at 80% SOC and 22°C ambient increased temperature by 2.75°C while at 50% temperature was higher by 4.5°C.
Charging at 50% SOC and 22°C ambient was endothermic with 0.3°C while at 35°C ambient cell temperature was 1.8°C higher. Charge at 80% SOC and 35°C ambient showed highest temperature influence through all experiments: 7.5°C.
Temperature distribution was very even on the surface of the cell, *Figure 33*. Thick prismatic packaging probably shielded the cell and temperature in the core was probably 2 to 3°C higher than the outside surface.

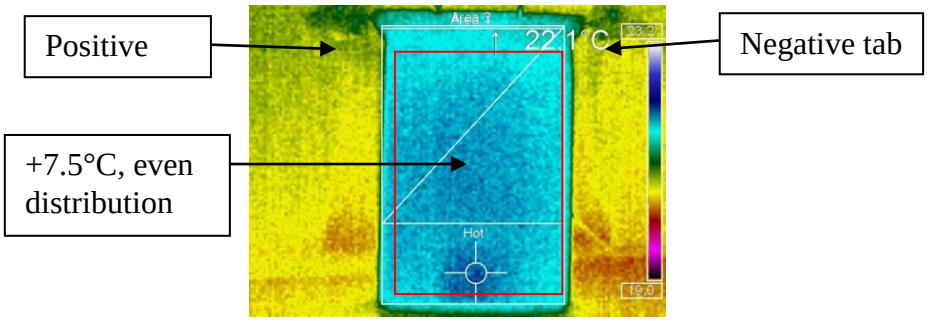

Figure 33. Cell1 3.1 Ah cell temperature distribution during charge with 1C for 2 minutes

Analysis

Results of tests 1 and 2 indicated how efficiently cells performed during controlled two-minute runs. It must be noted that all cells were tested in conditions that were set as close as possible to manufacturer specifications which infers that all cells were tested at different currents. Moreover some tested cells were made for high power while others for high energy which only does justice for comparing particular cells for a particular design objective.

Maximum cell temperature difference (Δ Max T) showed how high temperature spiked in certain parts of the cell. That indicated zones where a lot of energy was produced during redox reaction and some was converted into overflow heat. Heat was then dissipated through the cell into ambient environment and cell temperature increased. Cell energy resource was obviously limited which implicated that all energy that was wasted to the environment or used to unnecessarily heat up the cell could not be reused. Cells that produced lowest amount of excessive heat for certain conditions utilized their energy potential effectively. Cells are sorted in order of decrease in Δ Max T in *Table 9* where the top values from all the experiments were selected.

Table 9. Cells are sorted in order of decrease in Δ Max T

	Δ Max T	Std Dev	Δ Mean T
EiG 20Ah	19.6	1.84	14.04
LGChem 5.3Ah	13.3	2.63	9.22
EiG 7Ah	13.1	2.82	12.2
A123 4.4Ah	7.6	2.12	6.99
Cell 1 3.1Ah	7.5	0.29	7.33

Standard deviation reflected how evenly the temperature was distributed through the cell surface. This reflected temperature spikes on the surface. Large irregularities in cell temperature indicated a design where redox reaction flow was uneven. Some areas had a higher current density which meant that material there was utilized more than in other areas. Generally material

that is used more ages faster and its performance decreases. Temperature spread is shown in *Figure 34*.

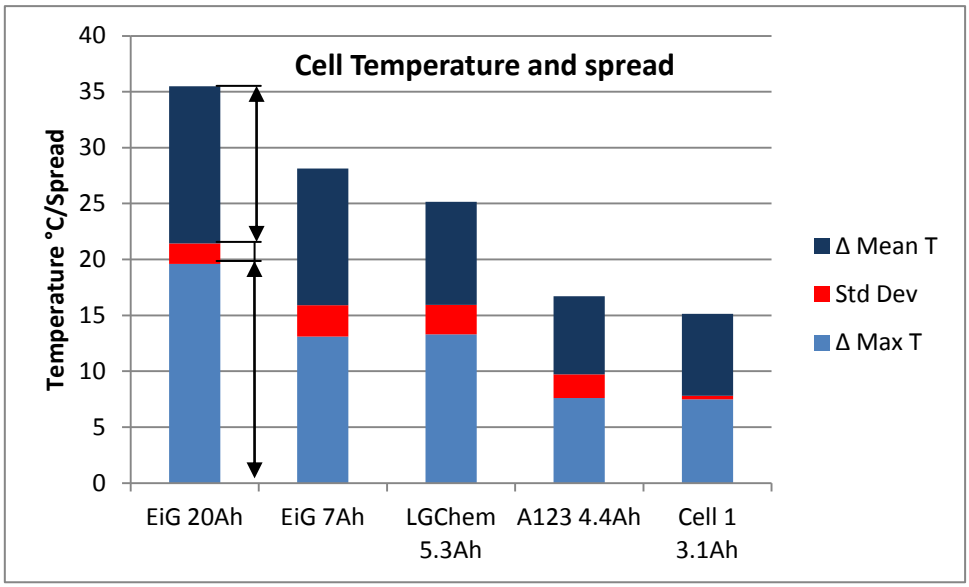

Figure 34. Cell temperatures and spread (Std Dev)

Mean cell Temperature difference (Δ Mean T) was strongly correlated with Δ Max T and spread and was both a measure of how high cell surface temperature was and how evenly the temperature spikes were distributed. A low Mean Temperature and a low spread together indicated a well-balanced cell that utilized the most out of its energy potential. Out of tested cells A123 4.4Ah and Cell 1 showed such performance. Cells are sorted in order of decrease in Mean Temperature in *Figure 34* where the top values in all the experiments were selected.

4.5 Heat evolution patterns

Difference in current density was noticeable based on cell temperature. Areas close to cell tabs were subjected to higher currents seeing as current took the shortest way through the cell. Tabs themselves proved to be a bottleneck because current from the whole current collector had to flow through the restricted size tab. Test results and a similar study [24] both indicate that tab placement on opposite sides results in a more even current and potential distribution and cell temperature. This makes a well-balanced cell which is less susceptible to uneven performance and thus shows better efficiency and health during lifetime. The same study in which cells with different tabs and electrodes are compared and concludes that neither long nor short electrodes are effective in utilizing active material and suggests that cells with tabs on opposite sides are favorable. Tabs can both be centered or placed diagonally. Test results of LG Chem 5.3Ah cell (*Figure 37*) indeed showed an even temperature distribution but the problem of bottleneck tab was very evident and material around the positive electrode tab was extensively used during cell operation

Positive electrode tabs were consistently warmer throughout all experiments (*Figure 35-39*). These results are consistent with another study [25]. Results report that positive electrode tab in aluminum dissipated heat from the battery while negative electrode tab in copper accumulated heat upon discharge. These results prove that thermal behaviour of positive electrodes tends to be exothermic and the negative – endothermic during discharge.

In pouch cells with tabs on the same side highest temperature was concentrated in an area in the middle of the cell closer to the tabs (*Figure 35-39*).

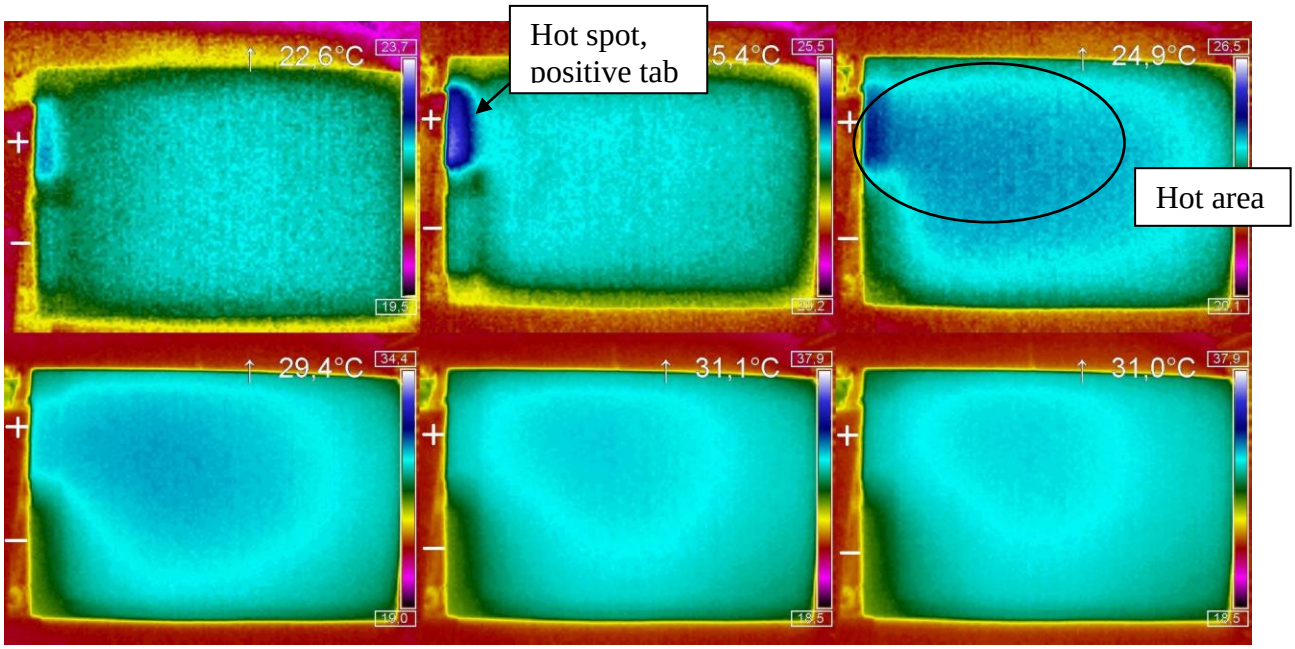

Figure 35. EiG 7Ah temperature evolution during pulse discharge with 16C for 2 minutes

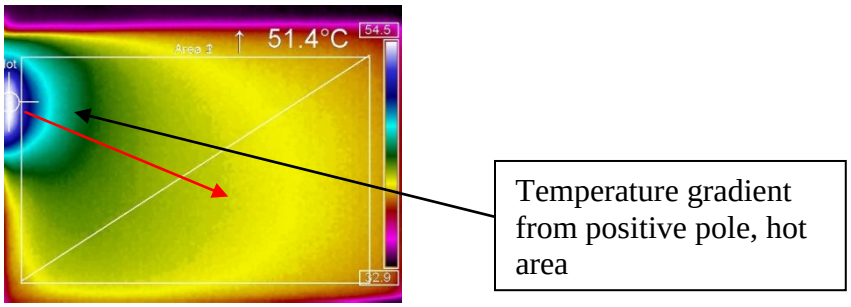

Figure 36. EiG 20Ah temperature distribution during continuous discharge with 10C for 2 minutes

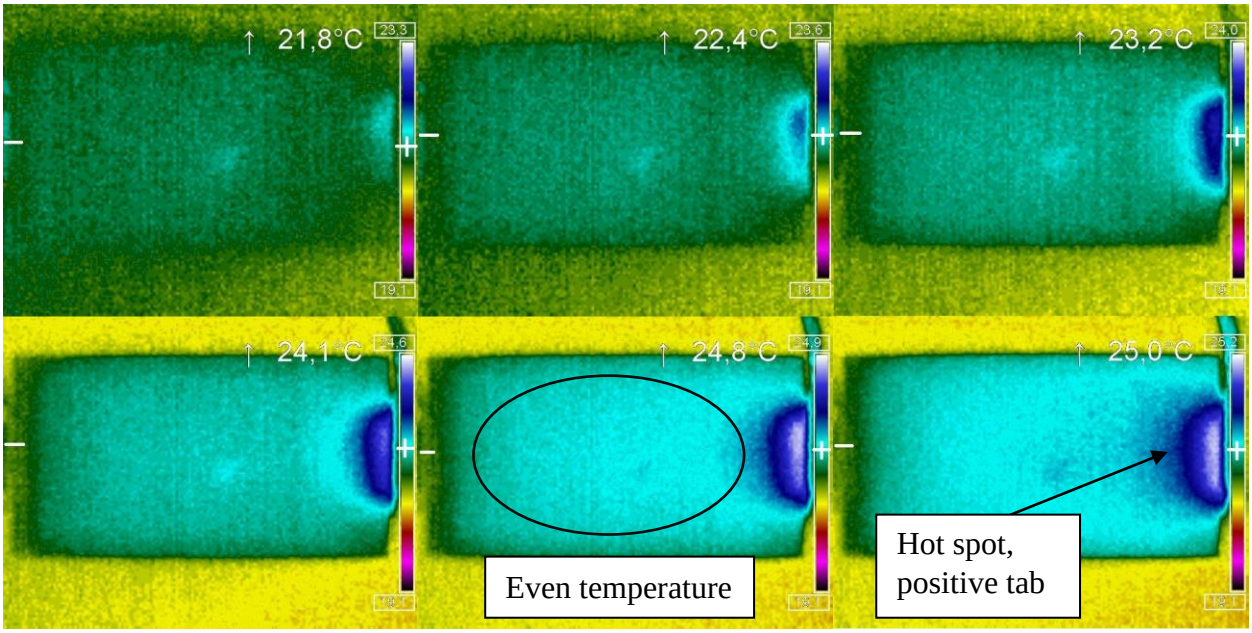

Figure 37. LG Chem 5.3 Ah temperature evolution during discharge at 16C for 2 minutes

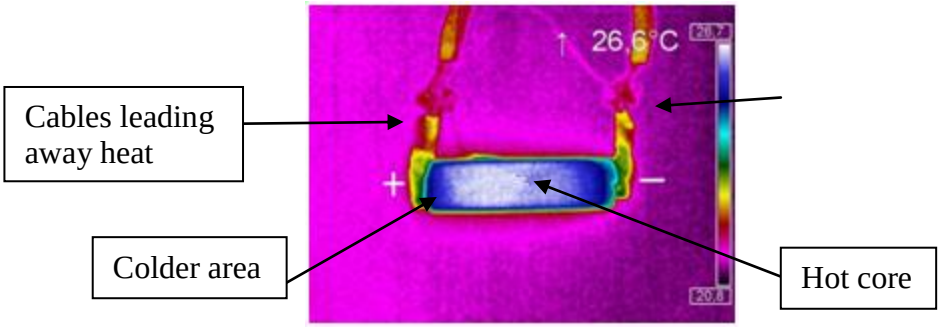

Figure 38. A123 4.4Ah temperature distribution during discharge with 10C for 2 minutes

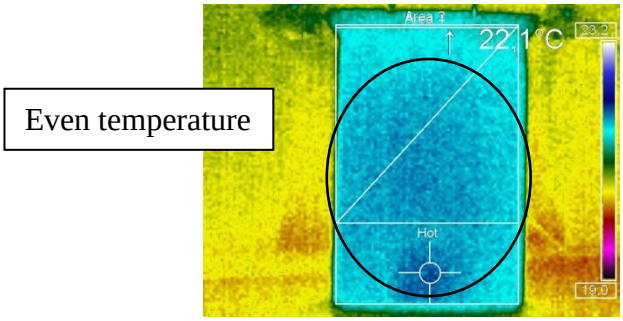

Figure 39. Cell1 3.1 Ah cell temperature distribution during charge with 1C for 2 minutes

4.6 Thermal behaviour conclusions

A thermal management system (TMS) has a large potential for improving cell performance in an ESS. Most of tested cells exhibited better efficiency at 30°C compared to ambient 20°C. Cell internal resistance decreases with higher temperature resulting in more efficient performance and longer life. Test results showed that temperatures were uneven in different cell areas. A good solution should therefore have high thermal conductivity to facilitate heat flow from cold areas on the cell to hot areas and out to TMS. Cell specifics must be taken into account when designing such system. Heat transfer inside the cell is most efficient along the layers of material as oppose to across layers. Extracting heat through short sides of package and cooling the cell through tabs would be quite effective.

Constant temperature is an ideal condition for a cell. A TMS in a vehicle will soften out cell temperature variation but thermal cycling which occurs when the system is off at night will still damage the cell. A good TMS must start heating up the cells in advance to be up at an operating temperature before vehicle starts. Moreover a required temperature profile for an ESS is dependent on driving cycle. Therefore a TMS would consume different amount of energy which must in turn be provided. A particular good TMS must be capable of both heating and cooling which hints at a large and expensive system. Nonetheless simple and cost effective systems like air cooling are quite often sufficient for specific purposes.

Entropic changes in cathodes and anodes versus SOC are a convenient indicator of cell performance and efficiency. Large change in entropy points to instability of material which determines inefficient areas of operation in the SOC domain. Entropic heat is a large contributor to cell heating which makes it possible to choose appropriate SOC with low excessive heat production.

Most effective cell performance is achieved at a state where entropic heat produced by the cell is in balance with heat that is emitted through convection and radiation. Cooling that is forced beyond a certain point will reduce cell performance by non-uniform cooling that makes outside

of the cell cold and leaves inside hot making cell temperature uneven throughout the cell [26]. These findings illustrate that cell entropy and resistance as well as heat dissipation rate needs to be determined for imaginable usage conditions in order to find a point where cell temperature is most even to achieve efficiency

High emissivity coatings will be efficient for radiating heat. As long as coating is colder than the hot material in the cell it would be effective in releasing energy.

Connecting cables lead part of the heat away from the cells. These losses were assumed to be 22% [11] and must be accounted for when designing a battery pack where cells are connected to each other. In a pack heat will flow in between the cells increasing cell temperatures.

4.7 Thermal behaviour of cells in a module

Temperature is highest in the core of the cell. Compared to the shell the core can be 2 to 5°C hotter continuously throughout cycling. When cells are connected to each other in a battery module cells closest to module poles will be colder and cells in between them hotter, *Figure 40* [11]. Due to effective heat transfer through cell connections most heat will leave the pack through the cells that are at the edges leaving them colder. Temperature distribution in cell in a pack will still be the same as single cells.

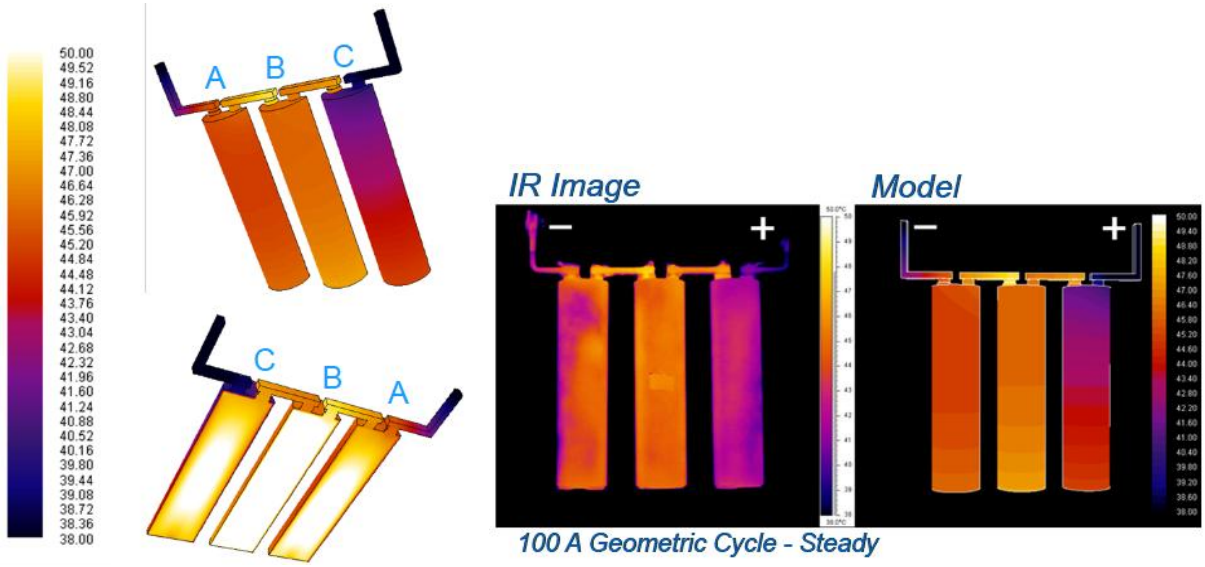

Figure 40. Temperature distribution in a module [45]

4.8 Thermal abuse test results and safety evaluation

During thermal abuse testing following cells were studied:

- EiG 20Ah NMC-based positive electrode (pouch)
- A123 4.4Ah LFP-based positive electrode (cylindrical)
- EiG 7Ah LFP-based positive electrode (pouch)

A pair of each type of cells was subjected to heating procedures A and B. Procedure A involved temperature ramping by 10°C every 15 minutes and during procedure B cell was heated straight to about 300° in an oven.

4.8.1 NMC EiG 20Ah

The cell type with NMC based positive electrode showed harsh test results during both procedures. Temperature spiked up to more than 660°C in less than a second during thermal runaway peak. Cell caught fire and burned for short period of time, *Figure 41*.

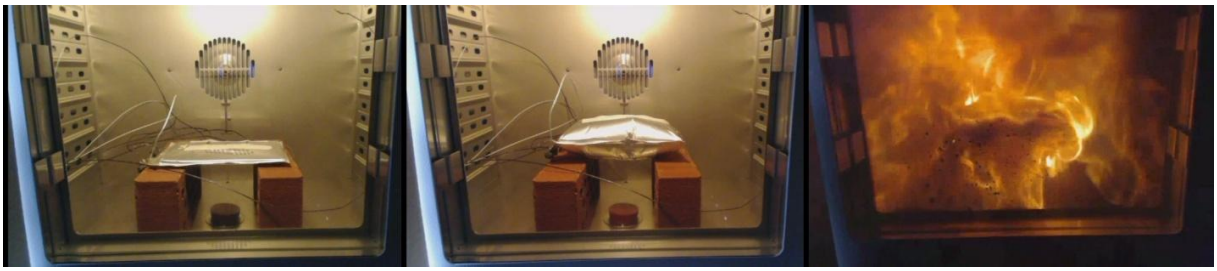

Figure 41.Thermal runaway in EiG 20Ah NMC

Procedure A

Figure 42 shows the lapse of abuse test with procedure A. Cell swelled and after that opened up and released gas. Next thermal runaway started and temperature went down quickly after the spike. Thermocouples were placed on top and bottom of the cell and legend in *Figure 42* describes respective temperatures. Temperature was quite even in different areas of the cell.

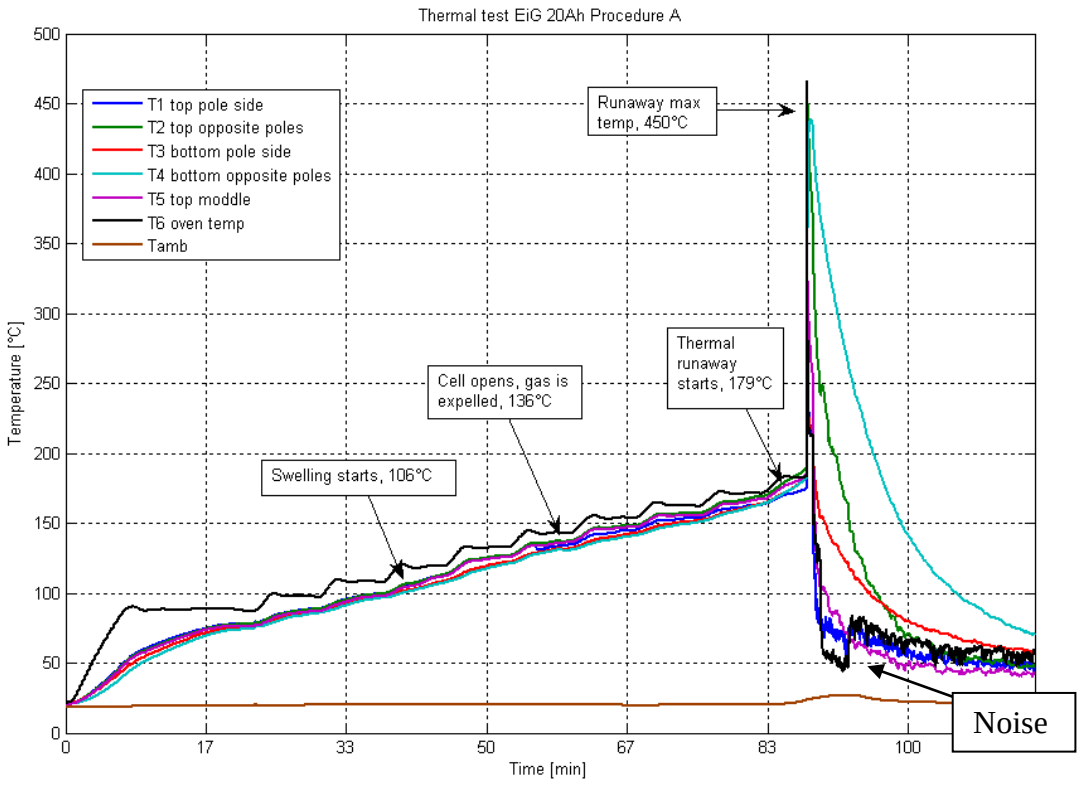

Figure 42. Temperatures during Procedure A thermal abuse test on EiG 20Ah NMC

The mechanical damage of cell surface after the runaway induced some noise on the signal from the thermocouples which resulted in temperature oscillations. Noise was present in most of test data and an example is pointed out in *Figure 42*.

Voltage started to drop at 170°C and with a large amount of oscillations reached 0V prior to thermal runaway. Given the temperature the separator was certainly melting and the electrodes coming in contact with each other in different areas caused small short circuits and voltage spikes, see *Figure 43*. Voltage behaviour was similar for all tested cells apart from the temperature to which the voltage occurred. Amount of spikes was also slightly different. *Figure 43* however gives a good picture of a typical voltage evolution.

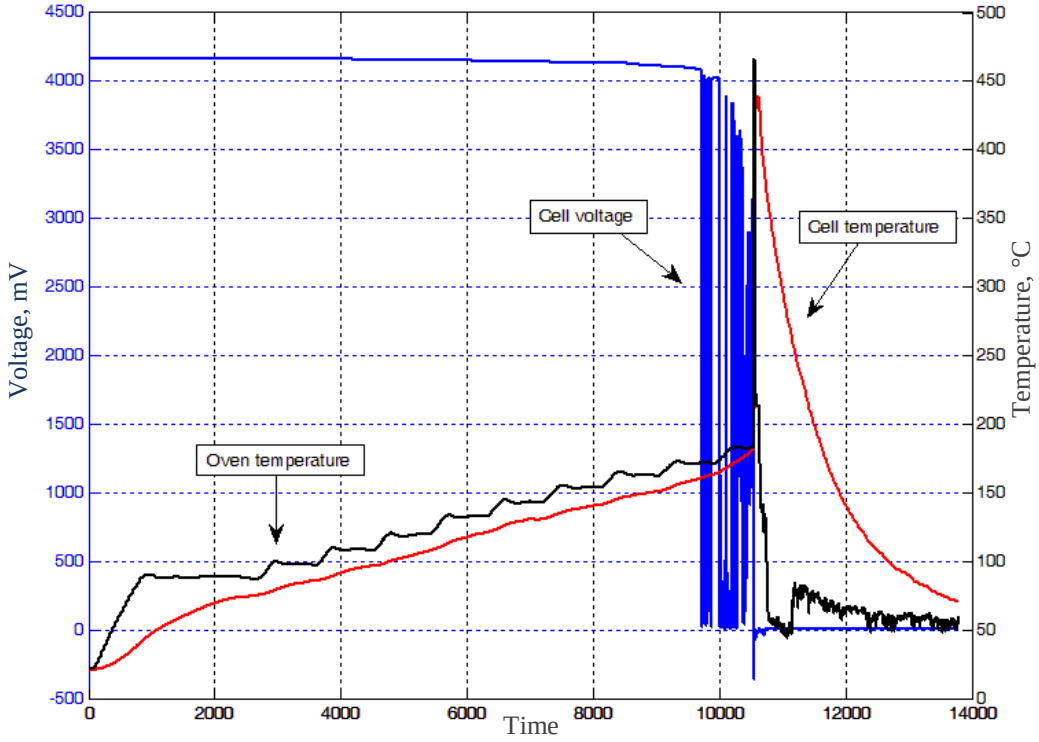

Figure 43. Cell voltage during Procedure A thermal abuse test on EiG 20Ah NMC

Procedure B

Temperatures during course of reaction are shown in *Figure 44*. During the test the cell started swelling and then ruptured and released gas. After that the cell started swelling the second time after which light smoking started. Shortly after cell temperature rapidly spiked during thermal runaway and it went back down.

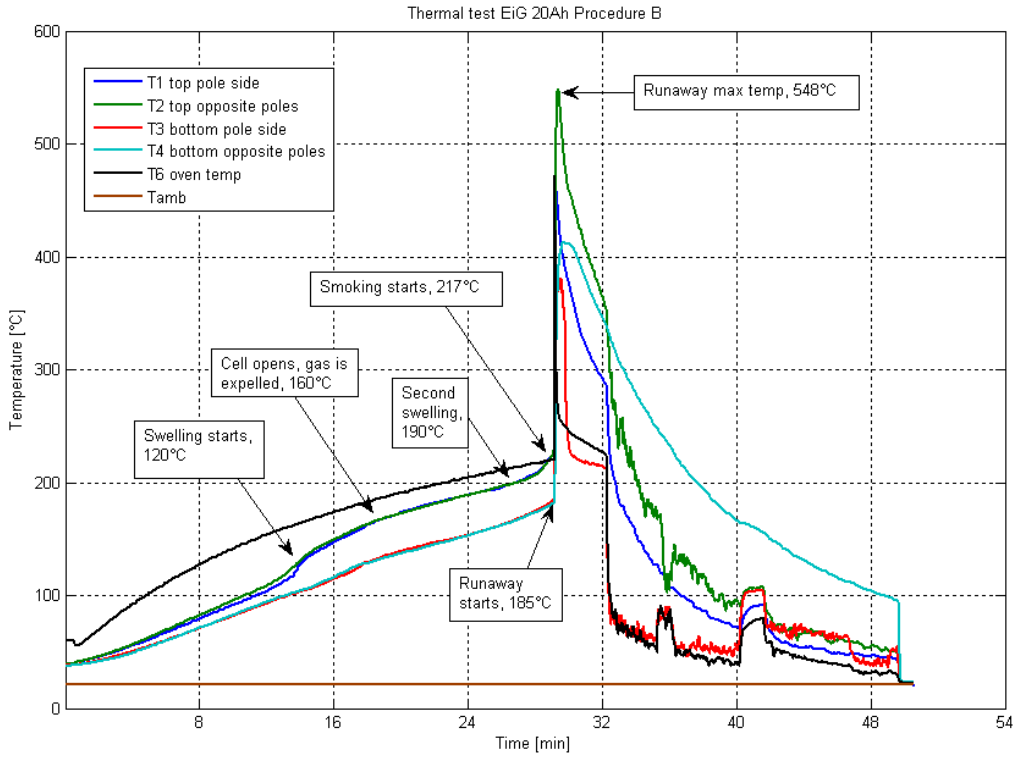

Figure 44. Temperatures during Procedure B thermal abuse test on EiG 20Ah NMC

Temperature spread between bottom and top of the cell was large during this test. Cell bottom accumulated less heat during fast heating procedure. Temperatures from different areas on the cell are shown in the legend in *Figure 44*.

Events during procedures A and B are summarized in *Table 10* and graphically in *Figure 45*. Procedure B reached a higher temperature during thermal runaway.

Table 10. Summary of events during procedures A and B on EiG 20Ah NMC

	EiG 20 Ah		
	A	**B**	**Difference**
Runaway onset temp, [°C]	179	185	6
Max runaway temp, [°C]	450	548	98
Min runaway temp, [°C]	266	381	115
Runaway end temp, [°C]	-	-	-
Runaway time to peak [sec]	0.1	0.25	0.15
Swelling, [°C]	106	120	14
Opening and gas release, [°C]	136	160	24
Smoke, [°C]		217	217
Fire	x	x	-
Explosion	x	x	-
Voltage drop temperature, [°C]	167	203	36
Mass lost [g]	149.97	150.32	0.35

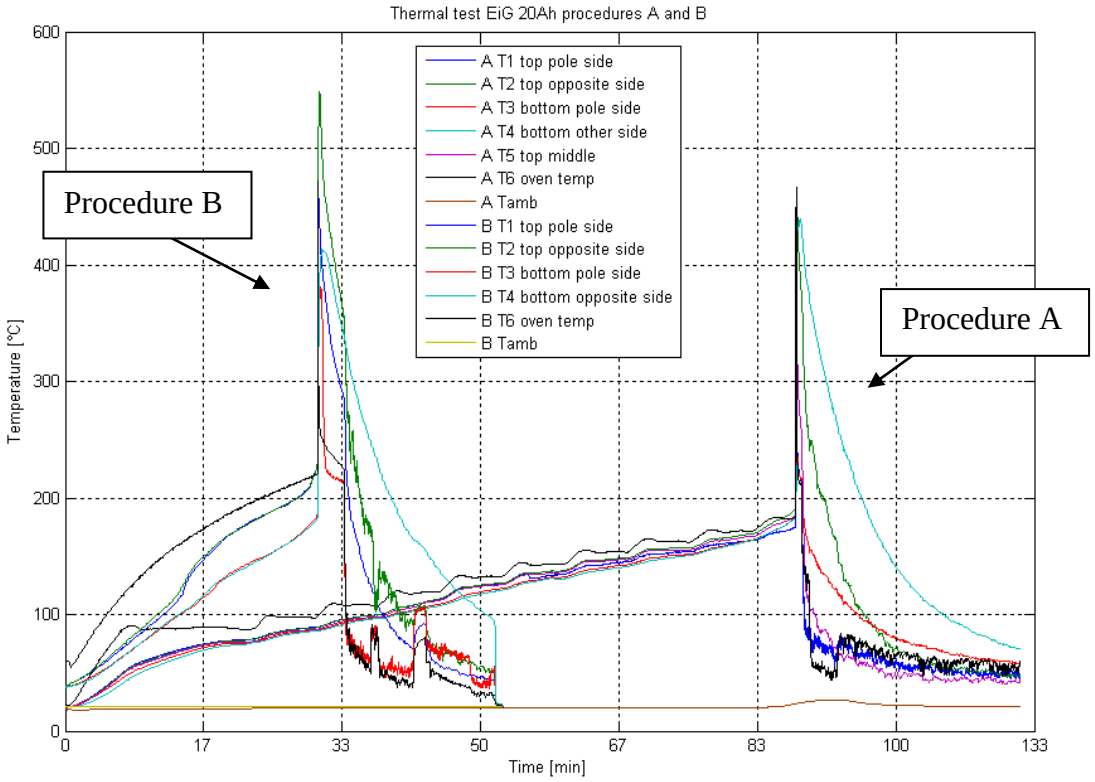

Figure 45. Procedures A and B for EiG 20Ah

4.8.2 LFP A123 4.4Ah

Procedure A

At 196°C cell's safety vents opened and gas was released. Cell packaging was made of thick aluminum which sustained pressure well and cell did not swell up. Thermal runaway started at 197°C immediately after vents opened. Temperature spiked up to 235°C during 15 seconds and dropped to 218°C. Evolution of temperatures on cell surface is shown in *Figure 46*.

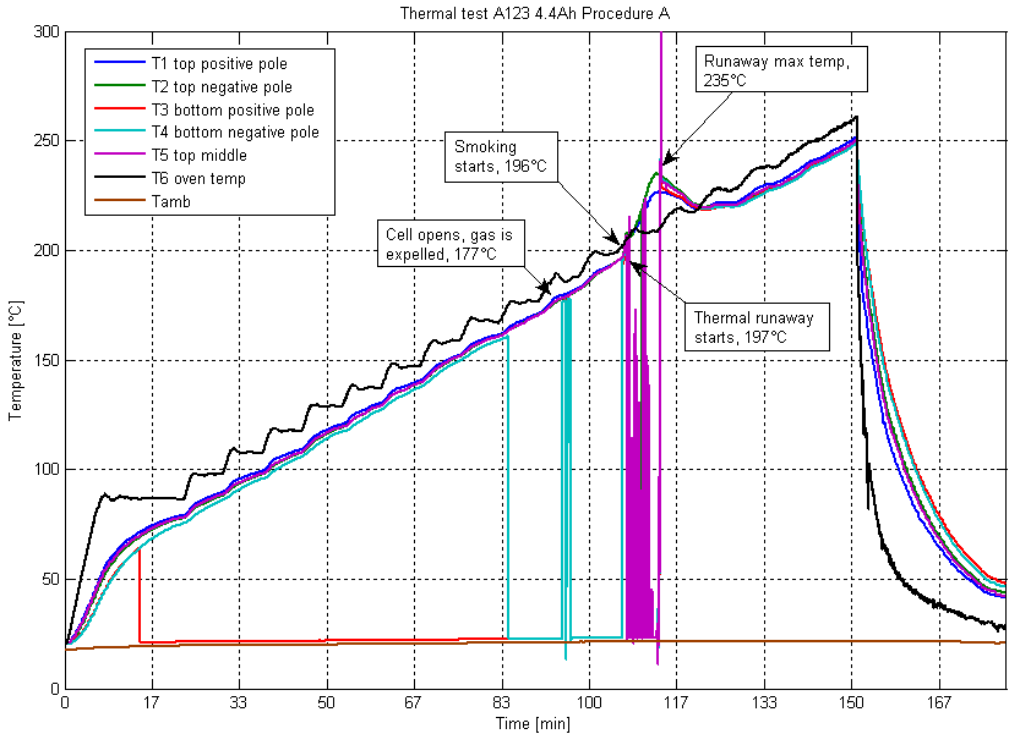

Figure 46. Temperatures during Procedure A thermal abuse test on A123 4.4Ah

Temperature increased only by 38°C during a 15 second period which is a quite mild thermal runaway compared to other cells. Runaway consisted of two peaks: a small peak in the beginning and a large peak which are shown in a thermal runaway close-up in *Figure 47*. First spike was clearly visible on top of negative pole.

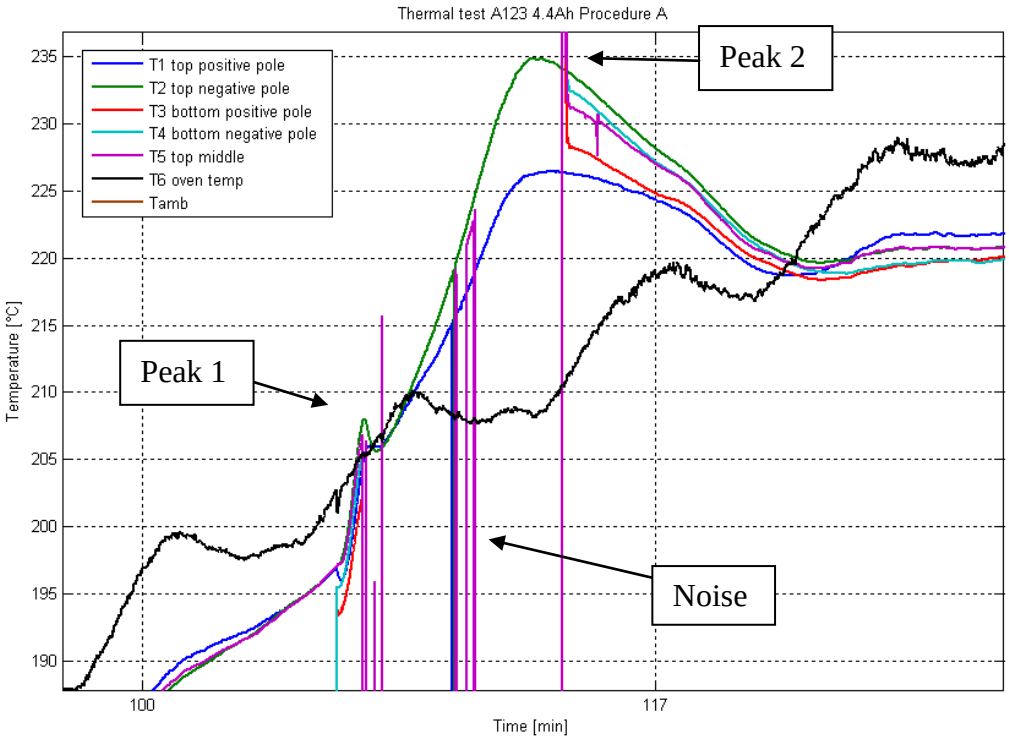

Figure 47. Thermal runaway peaks in A123 4.4Ah

Cell voltage started to fall after 138°C having only a few spikes and gradually dropped to 0V right after runaway peak. Possibly voltage was influenced by separator melt at around 130° and as it gradually melted a series of small internal short-circuits occurred visible in voltage spikes. Voltage evolution pattern was similar to that in *Figure 43*.

Procedure B

The cell was heated up until safety vents opened and gas was released. Thermal runaway followed immediately after. Temperature spiked up to 255°C during 7 seconds and dropped back. Evolution of temperatures on cell surface is shown in *Figure 48*.

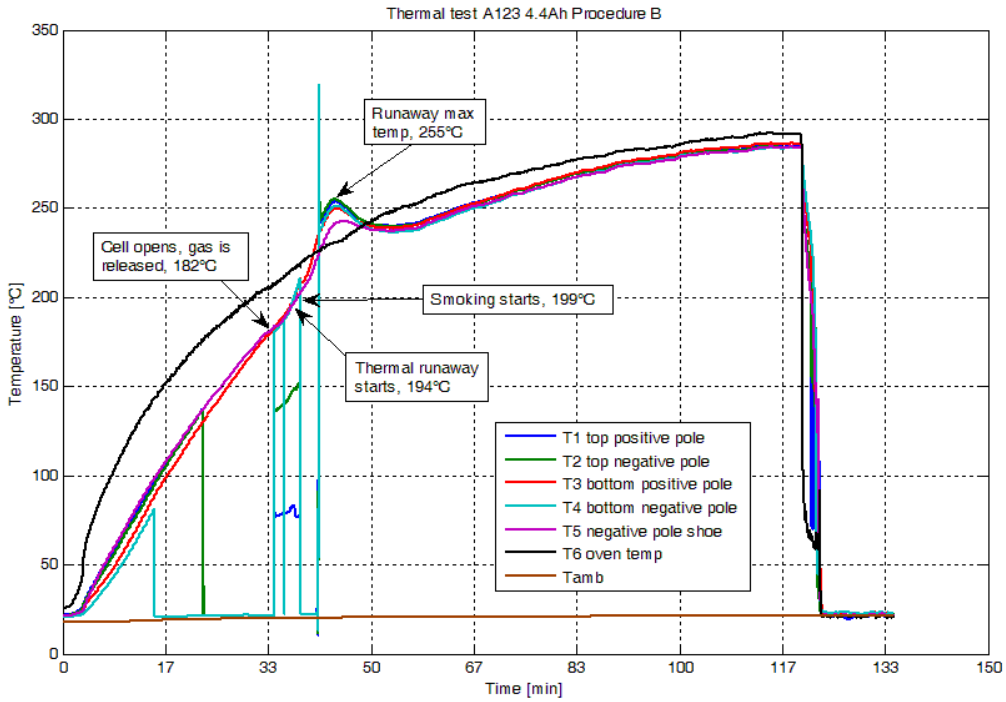

Figure 48. Temperatures during Procedure B thermal abuse test on A123 4.4Ah

Course of events during tests on A123 4.4Ah cell is presented in *Table 11* and *Figure 49*. Procedure B caused thermal runaway with higher temperature.

Table 11. Summary of events during procedures A and B on A123 4.4Ah

	A123 4.4Ah		
	A	**B**	**Difference**
Runaway onset temp, [°C]	197	194	-3
Max runaway temp, [°C]	235	255	20
Min runaway temp , [°C]	226	249	23
Runaway end temp, [°C]	218	238	20
Runaway time to peak [sec]	15	7	-8
Swelling, [°C]	-	-	-
Opening and gas release, [°C]	177	182	5
Smoke, [°C]	196	199	3
Fire	-	-	-
Explosion	-	-	-
Voltage drop temperature, [°C]	146	136	-10
Mass lost [g]	32.46	29.64	-2.82

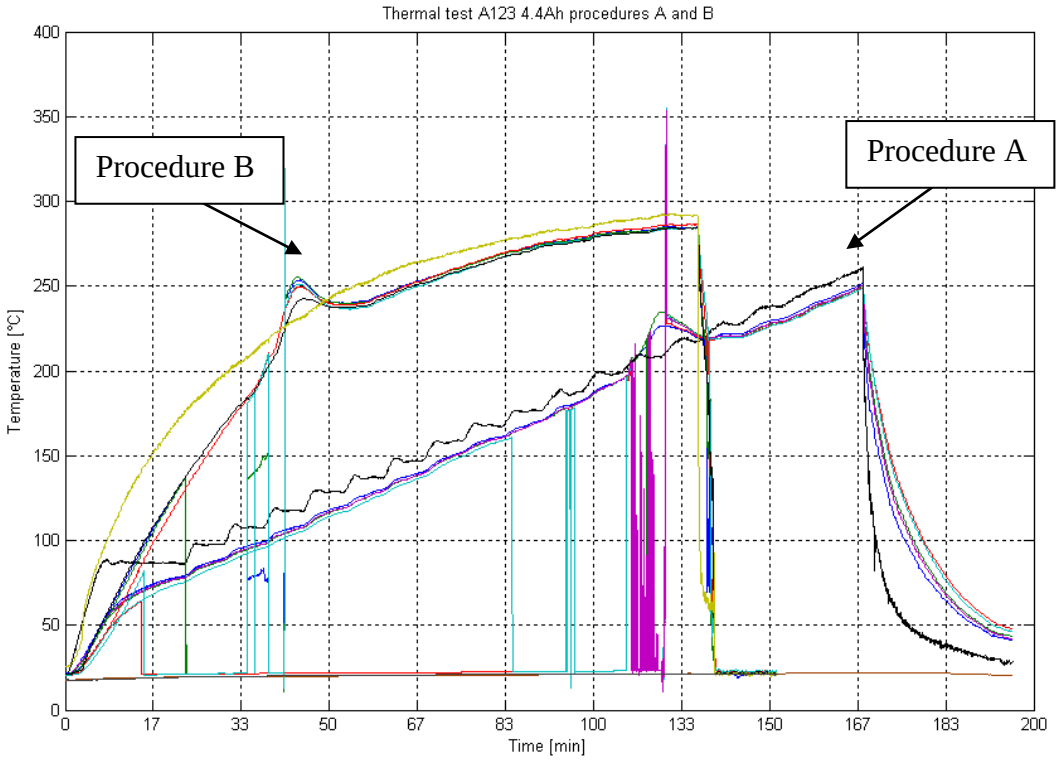

Figure 49. Procedures A and B on A123 4.4Ah. Temperatures are indicated with same colours as in procedure descriptions above

4.8.3 LFP EiG 7Ah

Procedure A

During the test cell started swelling then ruptured and released gas. Next smoking started and shortly after cell temperature rapidly spiked in a thermal runaway and went back down. Evolution of temperatures of different areas on the cell is shown in *Figure 50*.

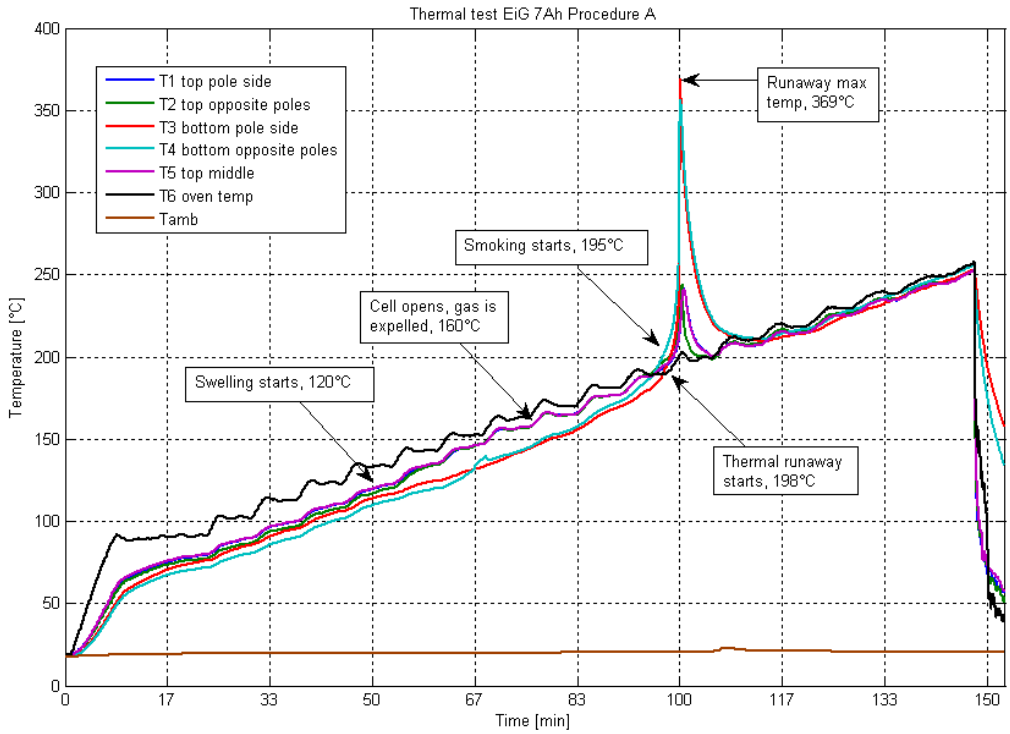

Figure 50. Temperatures during Procedure A thermal abuse test on EiG 7Ah LFP

Similarly to A123 LFP cell thermal runaway consisted of two peaks, *Figure 51*.

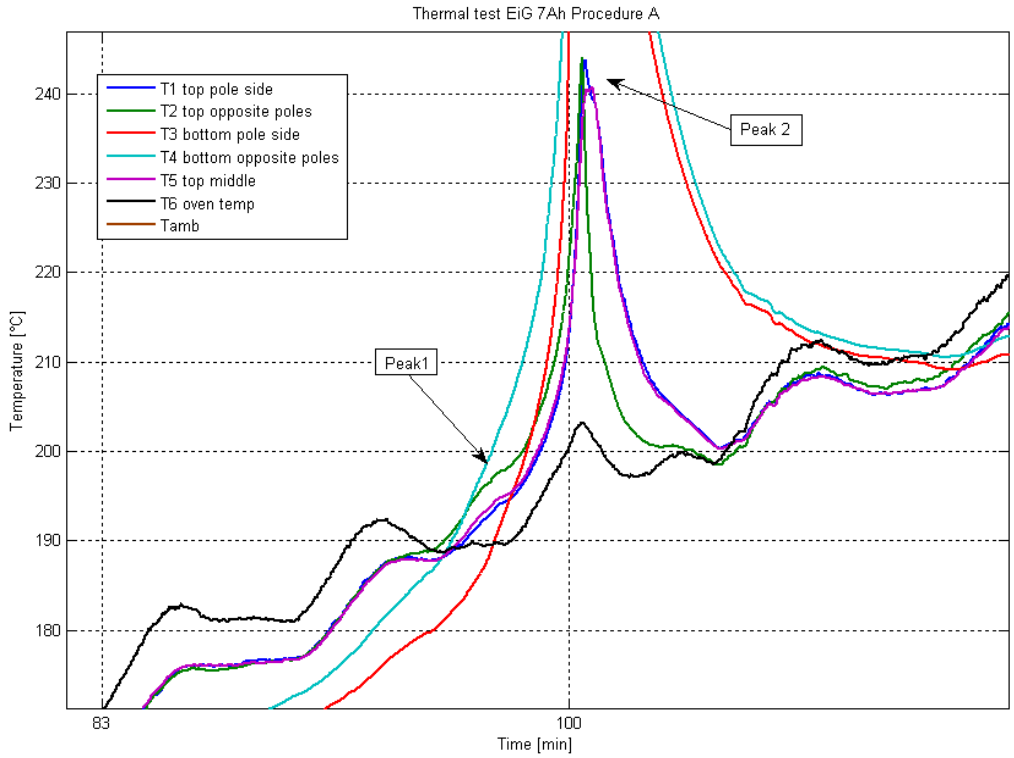

Figure 51. Two peaks in thermal runaway of EiG 7Ah

Cell voltage started to drop significantly around 160°C and showed a great amount of spiking all the way to the beginning of thermal runaway at which point it dropped to 0V. Large amount of voltage oscillations indicated a series of internal short circuits in areas where separator melted after 160°C. Short circuits however did not release a lot of energy and did not influence cell temperature. Voltage drop happened in all tested cells. Voltage evolution pattern was similar to that in *Figure 43*.

Procedure B

The cell started swelling at 137°C and opened at 168°C releasing gas. Thermal runaway started at 195°C and peaked at 265°C. Smoke came out at 226°C prior to runaway peak. Evolution of temperatures of different areas on the cell is shown in *Figure 52*.

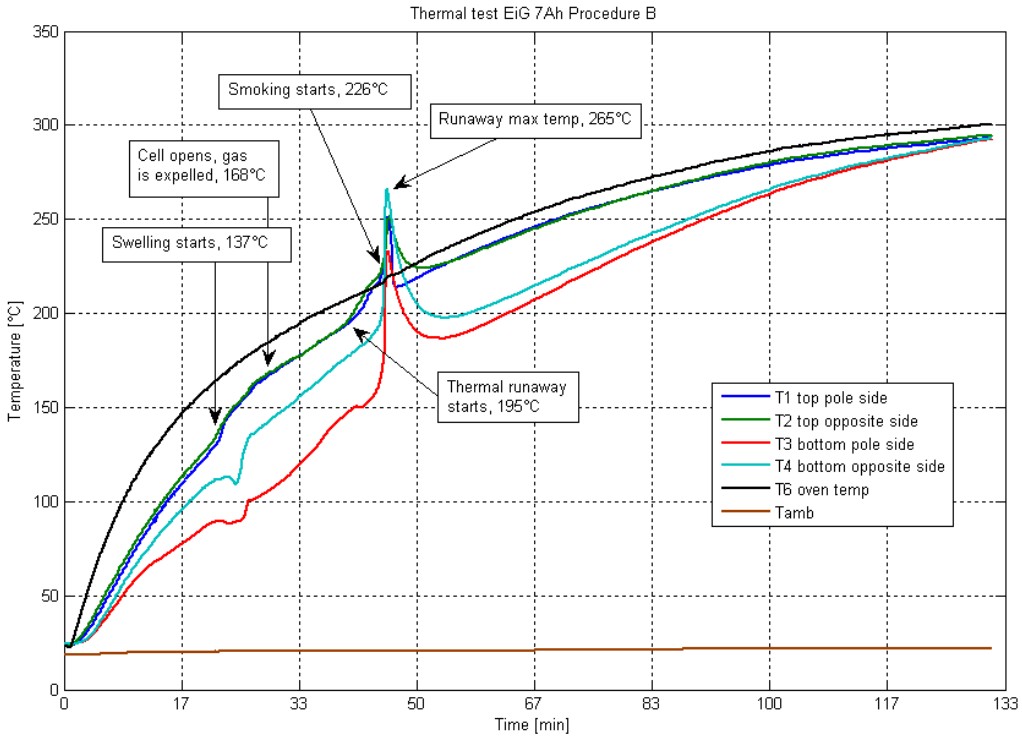

Figure 52. Temperatures during Procedure B thermal abuse test on EiG 7Ah LFP

Bottom of the cell heated up less during the experiment which is visible from *Figure 52*. Cell did not reach an even temperature due to fast heating and heat which was absorbed by the ceramic bricks the cell was resting on.

Thermocouple 1 (T1) separated from the cell right after the runaway which was visible in a fast decrease in temperature. T1 however continued to show temperature very similar to T2 which was still connected to the cell which raised a suspicion that T2 did not show a correct cell temperature after runaway.

Course of events during tests on EiG 7Ah cell is presented in *Table 12* and *Figure 53*. Procedure A caused thermal runaway with higher temperature.

Voltage spiked much more often during procedure A which indicated that separator melted in several areas. Large amount of small short-circuits did not influence cell temperature.

During procedure A swelling, opening, smoking and thermal runaway started at lower temperatures compared to fast heating. Temperatures are shown in *Table 12*. Thermal runaway however was more powerful and reached 100°C higher temperature. Fast heating showed a rapid reaction where cell was unevenly heated up and material that lied closer to the outside of the cell participated in reaction. Core material did not reach high enough temperature to take part in reactions which resulted in a milder thermal runaway. Slow heating was more dangerous because larger quantity of cell material took part in different reactions releasing more heat and hazardous substances.

Table 12. Summary of events during procedures A and B on EiG 7Ah LFP

	EiG 7Ah		
	A	**B**	**Difference**
Runaway onset temp, [°C]	189	195	6
Max runaway temp, [°C]	369	265	-104
Min runaway temp, [°C]	243	251	8
Runaway end temp, [°C]	210	225	15
Runaway time to peak [sec]	4	6	2
Swelling, [°C]	120	137	17
Opening and gas release, [°C]	160	168	8
Smoke, [°C]	195	226	31
Fire	-	-	-
Explosion	-	-	-
Voltage drop temperature, [°C]	160	170	10
Mass lost [g]	46.79	56.25	9.46

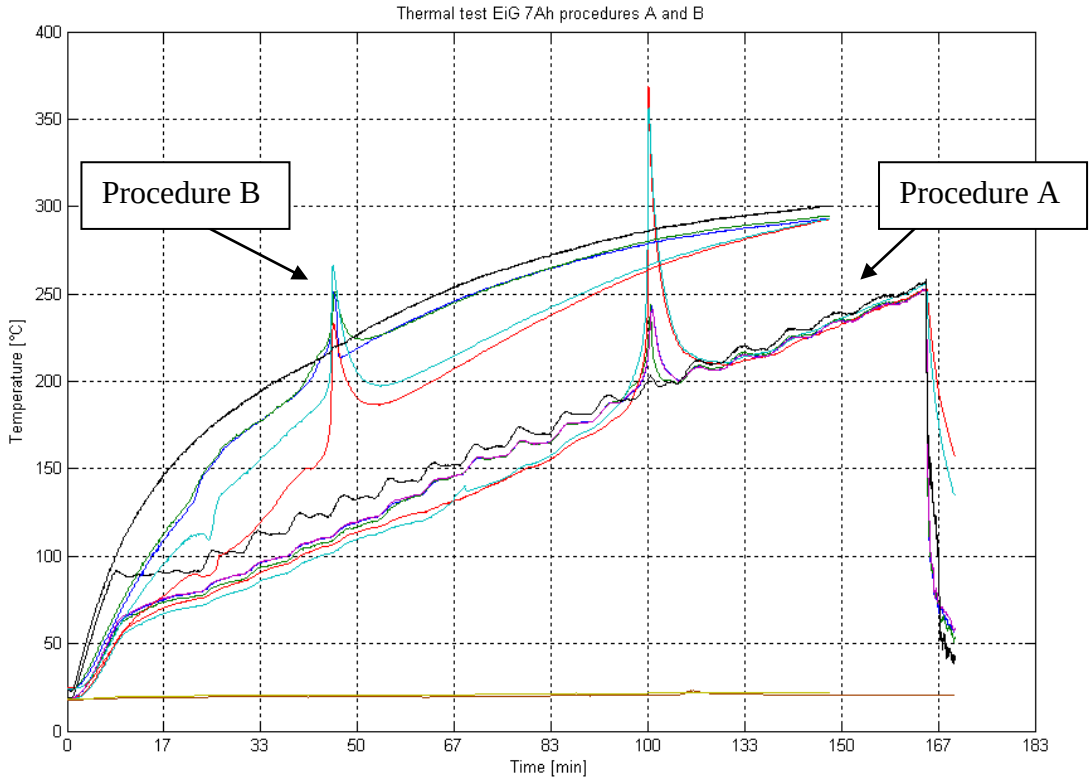

Figure 53. Procedure A and B for EiG 7Ah LFP. Temperatures are indicated with same colours as in procedure descriptions above

4.8.4 Comparison of chemistries

A graphical comparison of cell performance during procedures A and B is presented in *Figure 54* and *Figure 55*. EiG 20Ah NMC caused highest temperature during both procedures. Cells with LFP chemistries reached quite similar temperatures during procedure B but during procedure A EiG 7Ah reached a 134° higher temperature.

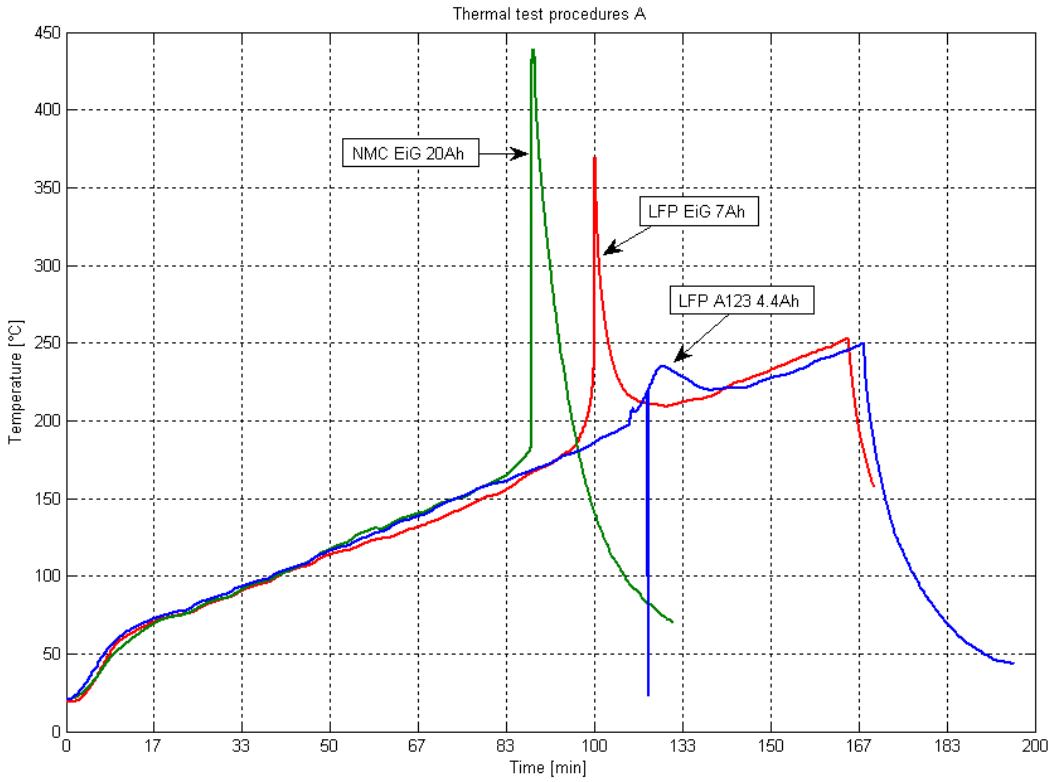

Figure 54. Thermal runaway procedures A on all 3 types of cells

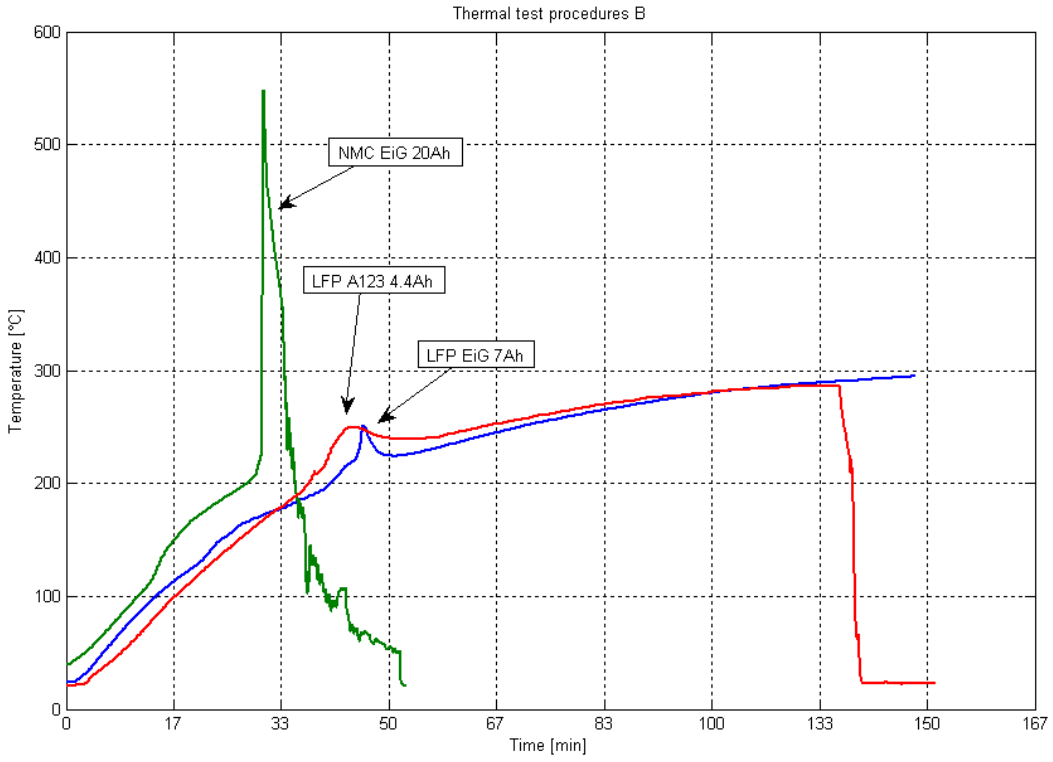

Figure 55. Thermal runaway procedures B on all 3 types of cells

A summary of results of both tests is presented in *Table 13* below.

Table 13. Summary of events and temperatures during thermal abuse tests

Temperature, [°C]	EiG 20 Ah NMC		EiG 7Ah LFP		A123 4.4Ah LFP	
	A	B	A	B	A	B
Runaway onset temp	179	185	189	195	197	194
Max runaway temp	450	548	369	265	235	255
Min runaway temp	266	381	243	251	226	249
Runaway end temp	-	-	210	225	218	238
Runaway time to peak [sec]	0.1	0.25	4	6	15	7
Swelling	106	120	120	137	-	-
Opening and gas release	136	160	160	168	177	182
Smoke		217	195	226	196	199
Fire	x	x	-	-	-	-
Explosion	x	x	-	-	-	-
Voltage drop temperature	167	203	160	170	146	136
Mass lost [g]	149.97	150.32	46.79	56.25	32.46	29.64

Results of tests on LFP chemistry showed lower temperatures, less energy release, less smoke evolution and no fire. These results are consistent with findings of P. Roth [27] (p.16) which constituted that LFP cells did not release oxygen during cathode decomposition and reaction between cathode and electrolyte had a low enthalpy. The report stated however that gases, released by LFP cells were still flammable. Runaway for LFP reaction started at around 230°C and temperature spike lower than for Cobalt-based chemistries.

Cell voltage oscillations indicated that PE separator shut off (at around 130 degrees) and started to melt causing small internal short-circuits. Internal pressure point where electrodes were in contact caused local stress on the separator leaving it more prone to melting. Nevertheless separator melt and subsequent shorting did not release more heat than the cell was producing. Cell temperature in tests kept increasing at the same rate as before the short-circuiting.

Thermal runaway reactions are self-sustaining if a cell has reached temperature higher than 80°C. Rate of reaction is however not fast enough for immediate runaway if external heat source is taken away and it will take up to two days for thermal runaway to manifest. As a result cell can catch fire much later than abuse time [28].

A calorimetric study of separator melt [28] showed two peaks at 133 and 159°C which correlates well with results of performed experiments. Cell voltage started to drop at around 160°C followed by large amount of spiking due to internal short-circuits during separator melt.

In both tests on cells with NMC chemistry aluminum current collectors melted down. Metal's melting point is at 660°C which is more than recorded cell temperature during runaway peak. A study [28] suggests that aluminum can alloy with exposed copper in current collectors causing the alloy to melt at temperature over 548°C. Pure copper however will not likely melt during runaway due to a high melt temperature of 1080°C. Packaging material did not melt during any test suggesting that its thickness was adequate.

Only NMC cells caught fire during the experiment. Cell temperatures reached more than 660°C at peak of runaway compared to 370°C and less for LFP cells. A similar study suggests that gases that are vented from the cell will ignite if in contact with a sufficiently hot material such as cell packaging. Thus gases vented by an LFP cell also were flammable but during runaway

reactions cells did not reach hot enough temperatures to ignite the gases. If a different ignition source is present LFP cell would catch fire as well. A study [27] suggests that gases do not ignite because of oxygen release from cathode. Oxygen amount released from the cell is too low.

Different studies suggest that runaway onset temperature gets lower and heat release increases with higher SOC [28]. During experiment cells were tested at 100% SOC. This effectively simulated the harshest conditions of cell performance.

Cells for home appliances are affected in the same way as cells for vehicle use which were tested. HEV cells however have much larger capacities and sizes which results in a lot more powerful effect when a cell enters thermal runaway. Moreover cells are often used in packs of around 100-300 cells on average. This means that runaway in each cell will be very powerful and other cells in an ESS may get affected multiplying consequences by the amount of cells.

Thermal runaway can have several consequences amongst which are:

- Heat from internal reactions high enough to increase cell temperature between 300 and 800℃ in 5 seconds. Heat is most likely to cause runaway in neighbouring cells or damage the surroundings and start fires by heating up ESS materials
- Release of harmful gas and smoke. Thermal runaway releases many gases that are to a harmful to humans. Particularly harmful are fluorine-based such as Hydrofluoric Acid, HF. No human should be allowed contact with gas released from cells without sufficient protection against every substance that is released
- Fire caused by material temperature rising far above flash point. Burning electrolyte or gas can be anticipated
- Explosion and thus mechanical damage to cells or other objects in proximity. Damaged neighbouring cells can also start a thermal runaway. Explosion is likely to happen due to poor design or placement in a confined space
- Pouch cells will swell which will mechanically damage components around them
- A concentrated spray of electrolyte or gas containing harmful substances might release
- Heat release, fire, gas development, swelling and explosions will mechanically damage all components inside an ESS and can end up damaging ESS shell and harming humans and environment

Some cells do not exhibit thermal runaway during external heating. In such case heating has a linear effect on the cell and does not produce a spike in temperature with a sudden heat release. Such cells are significantly safer since they do not release more heat than they absorb from the environment. These cells can however still cause all of the consequences on the thermal runaway list except for heat and explosion. Therefore the same measures of protection must be employed to shield humans against gas, fire, heat and explosion.

In a battery pack where cells are assembled close to each other thermal runaway in one cell can quickly escalate to a chain reaction. One cell with thermal runaway will likely damage most of the cells in a pack. Moreover gas and smoke are released during the reaction and they must be sustained in the pack or released without harming humans in proximity. Since oxygen is not released during the reaction fire can be sustained by limiting oxygen supply. The temperature of the pack in itself however can cause ignition of materials around the pack.

5 DISCUSSION AND CONCLUSIONS

A discussion of the results and the conclusions that were drawn during the Master of Science thesis are presented in this chapter.

5.1 Discussion

5.1.1 Literature study

Cell temperature showed to be a powerful tool for cell screening. It gave large amounts of data for statistical analysis and information about current density distribution and heat losses. However assumptions were made on 22% heat losses that could not be recorded through temperature measurement. Quantifying sources of losses would be a useful development of these results. A system to calculate cell efficiency through cell temperature can be developed and it will serve as a very powerful tool delivering a lot of useful information fast.

Analysis of sustainability was dependant on the results of two external studies. Assumptions from those studies put a limit on the analysis. However the aim of LCA was to understand the general influence from a battery which was accomplished with the help from external sources. Economic analysis was largely based on external studies as well and depends on their assumptions.

5.1.2 Test 1, 2 and 3

All tests were designed to eliminate hysteresis effect which means that cells were in a very similar state right before the test run. All cells were prepared with two formation cycles and each was in discharge state before charge run and vice versa.

Fluctuation of temperature without a trend following test cycle was discovered quite early during HEV cycle tests. Source was identified as an air-conditioning unit that turned on every half-hour and adjusted temperature in the lab. Following tests 2 and 3 were carried out in a climate chamber to eliminate the effect. Data from Test 1 was used as it was taken because ambient temperature shift had only a minor reflection on the 2-minute-long test runs.

All cells were placed on top of an insulating material during the tests. This setup made a fair comparison between cells of a similar type (pouch/prismatic/cylindrical) but cylindrical and prismatic cells had smaller contact area by far which had some effect on the heat transfer. Thus heat that was dissipated through the underlying material was not accounted for. Moreover it was discovered that part of heat was also dissipated through the connecting wires which was a necessary limitation for the experiment.

5.1.3 Thermal abuse tests

Thermocouple data was found to be inconsistent in many tests. Thermocouples at the bottom of the cell always showed lower temperature than the top. This was due to ceramic bricks that absorbed heat from the bottom. During the runaway peak itself however bottom temperature was always high indicating a more correct value. After cells started to swell the sensors on top were no longer in contact with the cell core because pouch cover lifted. Therefore sensors did not fully reflect the temperature of the cell. Post mortem examination of NMC cells showed no traces of aluminum current collectors which pointed towards cell reaching at least 660°C and not 548° which was recorded by the thermocouples.

Cells were tested at 100% SOC which is the toughest condition for runaway. No gas ignition was present

5.2 Conclusions

Li-ion battery technology was studied from a heat evolution and thermal runaway perspective.

Thermal behaviour was tested through a study of cell surface temperature. three experimental procedures were designed and carried out on five cells. A wide-scope approach was chosen for testing of factors that influence cell behavior. During thermal behavior experiments EiG 20Ah cell produced most heat when its temperature increased by 20°C. LG Chem 5.3Ah and EiG 7Ah had an increase of 13°C. A123 4.4Ah and a 3.1Ah LMO/LTO cell increased temperature by 7°C.

Pouch cells exhibited highest temperatures around positive pole. Cylindrical and prismatic cells had a slightly lower temperature around both poles. Uniform temperature distribution is a requisite for long cell life because material is used evenly during cycles. Heat was led away through convection, radiation and also through the connecting wires. Heat transfer is most efficient through the layers of materials as oppose to across the material layers and the cell. Therefore cooling cell tabs has benefits.

Thermal abuse testing was performed on three types of cells. During thermal runaway abuse tests EiG 20Ah cell with NMC chemistry reached 660°C and caught fire. LFP chemistry based cells EiG 7Ah and A123 4.4Ah reached 369 and 255°C respectively only releasing some smoke. Runaway started at roughly 190°C in all cells. Pouch EiG cells started swelling at around 106-120°C while cylindrical A123 showed first sign of runaway with release of gas. Separator melt was clearly visible through voltage drop at around 160°C.

All performed tests gave a valuable insight in cell function and secured that work results were consistent with objectives of the thesis. Test results also proved to be consistent with results of the conducted literature study. Cells performed differently throughout the tested conditions and it was evident that cells need to be chosen to fulfill specifications of a particular application. Specifics of cells behaviour were stated in the report.

It was also important to consider how cells would behave thermally when they are connected together with other cells in a pack. Work resulted in a series of practical suggestions for development of battery systems with account for efficient thermal management and performance. Thermal behaviour of cells in different conditions was explained. Economic and environmental impact of Li-ion technology was also taken into consideration.

6 RECOMMENDATIONS AND FUTURE WORK

In this chapter recommendations for future work and practical suggestions for test experiments are presented.

- Eliminate errors during testing and validate temperature trends by re-running the experiments. Running test in a different setup(change cell holders and connecting cables, test shifting cables between the poles) is crucial to confirm equipment homogeneity
- Continue testing heat evolution and relate the effects to internal factors. Test different levels of SOC and ambient temperature for an insight in cell function
- Test internal factors by comparing very similar cells
- Determine ideal operating conditions(high thermal and electric efficiency) for each cell from experimental data through the designed methodology
- Conduct a calorimetric study of cells. Study same factors as in the performed tests
- Conduct a study of thermal behaviour on module level by connecting cells together
- Develop an electrochemical model of cell heat production to study and validate internal factors
- When creating experiments, consider limitations of thermocouples, infrared camera and software. Create a fast post-processing and analysis method like an automated Matlab script
- When setting up a thermal experiment consider sources that emit and absorb heat like air-conditioning units and insulating or absorbing materials around the cell. Cells should be tested with least possible contact with surroundings to reach valid results, for example hanging up cells is a reasonable measure
- Heat that is dissipated through the connecting cables must be accounted for
- A thermal abuse experiment with heating up cell only to a point of separator melt would show if runaway reaction can power itself and lead to a peak
- Study SOC dependence of thermal runaway. Study gas flammability and content
- Deeper analysis of sustainability of Li-ion batteries and in particular cell materials is interesting for monitoring sustainability growth of the technology

7 REFERENCES

[1] R.M.Dell, D.A.J.Rand, *"Understanding batteries",* The Royal Society of Chemistry, 2001

[2] J.R. Dahn, Wenbin Luo, Fu Zhou, Xuemei Zhao, Zhonghua Lu, Junwei Jiang, Andrew van Bommel, *"Progress in high-energy-density high-safety positive electrode materials for Li-ion batteries",* Depts. of Physics and Chemistry Dalhousie University, Canada http://www.emc-mec.ca/phev/Presentations_en/S13/PHEV09-S13-5_JeffDahn.pdf

[3] John Christensen, Venkat Srinivasanb, John Newman, *"Optimization of Lithium Titanate Electrodes for High-Power Cells",* J. Electrochem. Soc. 2006 volume 153, issue 3, A560-A565

[4] From table: http://www1.eere.energy.gov/vehiclesandfuels/pdfs/merit_review_2012/energy_storage/es028_lu_2012_o.pdf 2012-09-20

[5] M. Shikano, H. Kobayashi, S. Koike, H. Sakaebe, E. Ikenaga, K. Kobayashi, K. Tatsumi, *"Investigation of positive electrodes after cycle testing of high-power Li-ion battery cells II. An approach to the power fading mechanism using hard X-ray photoemission spectroscopy"*, Journal of Power Sources 174 (2007) 795–799

[6] A.G. Ritchie, W. Howard, *"Recent developments and likely advances in lithium-ion batteries"*, Journal of Power Sources 162 (2006) 809–812

[7] Pankaj Arora, Zhengming (John) Zhang, *"Battery Separators"*, Chem. Rev. 2004, 104, 4419-4462

[8] Volvo ER-530298

[9] Hui Yang, Shabab Amiruddin, Hyun Joo Bang, Yang-Kook Sun, Jai Prakash; "*A review of Li-ioncell chemistries and their potential use in Hybrid Electric Vehicles"*; J ind Eng Chem Vol 12 no1, 2006 (12-38)

[10] Ahmad A. Pesaran, Matthew Keyser, *"Thermal Characteristics of Selected EV and HEV Batteries"*, 2001

[11] Gi-Heon Kim, Kandler Smith, *"Multi-Scale Multi-Dimensional Model for Better Cell Design and Management"*, NREL National Renewable Energy Laboratory, 2008 http://www.nrel.gov/vehiclesandfuels/energystorage/pdfs/44245.pdf 2012-09-20

[12] Kyu-Jin Lee*, Gi-HeonKim, KandlerSmith, *"3D Thermal and Electrochemical Model for Spirally Wound Large Format Lithium-ion Batteries"*, 218thECS Meeting, Las Vegas, NVOct 14, 2010 http://www.nrel.gov/vehiclesandfuels/energystorage/pdfs/49795.pdf 2012-09-20

[13] Ahmad Pesaran, Andreas Vlahinos, Desikan Bharathan, Tien Duong, *"Electrothermal Analysis of Lithium Ion Batteries"*, THE 23rd INTERNATIONAL BATTERY SEMINAR & EXHIBIT March 13 - 16, 2006 Fort Lauderdale, Florida http://www.nrel.gov/vehiclesandfuels/energystorage/pdfs/39503.pdf 2012-09-20

[14] Ahmad A. Pesaran, *"Thermal Management Studies and Modeling"*, National Renewable Energy Laboratory, Golden, Colorado, 2009 http://www.nrel.gov/vehiclesandfuels/energystorage/pdfs/45531.pdf 2012-09-20

[15] Qingsong Wang, Ping Ping, Xuejuan Zhao, Guanquan Chu, Jinhua Sun, Chunhua Chen, *"Thermal runaway caused fire and explosion of lithium ion battery"*, Journal of Power Sources Volume 208, Pages 210–224

[16] M. Gauch, R. Widmer, D. Notter, A. Stamp, H.J. Althaus, P. Wäger, "*Life Cycle Assessment LCA of Li-Ion batteries for electric vehicles"*, EMPA - Swiss Federal Laboratories for Materials Testing and Research, 2009 http://www.cars21.com/assets/link/LCApresenation.pdf 2012-09-25

[17] Mats Zackrisson, Lars Avellán, Jessica Orlenius, *"Life cycle assessment of lithium-ion batteries for plug-in hybrid electric vehicles - Critical issues"*, Journal of Cleaner Production 18 (2010) p 1519-1529

[18] PRE Consultants bv, *Eco Indicator 99*, http://www.pre-sustainability.com/download/misc/EI99_methodology_v3.pdf 2012-10-01

[19] Pike Research, *"Lithium-Ion Battery Materials: Japan Dominates in the EV Era"*, 4 feb 2011. http://www.pikeresearch.com/blog/articles/lithium-ion-battery-materials-japan-dominates-in-the-ev-era 2012-09-20

[20] McKinsey and Company , *"Battery technology charges ahead"*, july 2012, http://www.mckinseyquarterly.com/Battery_technology_charges_ahead_2997#footnote1 2012-09-20

[21] METI (2009), *"Patent Trend Report, Lithium Ion Battery"*, 2009 http://www.jpo.go.jp/shiryou/pdf/gidou-houkoku/21lithium_ion_battery.pdf 2012-09-20 via Magnus Karlström [magnus.karlstrom@chalmers.se], *"Li-jon batteri supply chains"*

[22] A123 Systems Inc http://www.a123systems.com/, EiG LTD http://www.eigbattery.com/, LG Chem Power Inc http://lgcpi.com, JSR Micro Inc http://www.jsrmicro.com/

[23] Matlab, technical computive language, The Mathworks Inc, http://www.mathworks.se/products/matlab/ 2012-10-01

[24] Ki Hyun Kwon, Chee Burm Shin, Tae Hyuk Kang, Chi-Su Kim, *"A two-dimensional modeling of a lithium-polymer battery"*, Journal of Power Sources 163 (2006) 151–157

[25] Ralph E. Williford, Vilayanur V. Viswanathan, Ji-Guang Zhang, *"Effects of entropy changes in anodes and cathodes on the thermal behaviour of lithium ion batteries"*, Journal of Power Sources 189 (2009) 101‑107

[26] S.C. Chen, C.C. Wan, Y.Y. Wang, *"Thermal analysis of lithium-ion batteries"*, Journal of Power Sources 140 (2005) 111–124

[27] P. Roth, ECS Transactions, 11 (19) 19-41 (2008)

[28] Celina Mikolajczak, Michael Kahn, Kevin White, Richard Thomas Long, *"Lithium-ion hazard and use assessment"*, The fire protection research foundation, 2011, p18,49

Figure references

Figure 1 http://etc.coedu.usf.edu/clipart/4200/4286/voltaic-pile_1_lg.gif; http://sv.wikipedia.org/wiki/Fil:Voltaic_pile.png 2012-09-25

Figure 2 http://www.a123systems.com 2012-09-25
Figure 3 www.gm.com; www.gm-volt.com 2012-09-25

Figure 4 http://www.volvobuses.com 2012-09-25

Figure 5 http://cdn.arstechnica.net/wp-content/uploads/2012/05/how_a_lithium-ion_battery_works-4fa2c98-intro.jpg 2012-09-25

Figure 8 http://www1.eere.energy.gov/vehiclesandfuels/pdfs/merit_review_2012/energy_storage/es028_lu_2012_o.pdf 2012-09-25

Figure 9 www.celgard.com 2012-09-25

Figure 11 http://www.gaia-akku.com; www.gs-yuasa.com; www.eigbattery.com 2012-09-25

Figure 12 http://www.nrel.gov/vehiclesandfuels/energystorage/pdfs/49795.pdf; http://www.nrel.gov/vehiclesandfuels/energystorage/pdfs/39503.pdf 2012-09-25

Figure 13 http://www.nrel.gov/vehiclesandfuels/energystorage/pdfs/45531.pdf 2012-09-25

Figure 15 http://www.comsol.com/stories/kobelco_lithium_ion_batteries/full/ 2012-09-25

Figure 17 http://www.cars21.com/assets/link/LCApresenation.pdf 2012-09-25

Figure 18 http://www.pikeresearch.com/blog/articles/lithium-ion-battery-materials-japan-dominates-in-the-ev-era 2012-09-25

Figure 40 http://www.nrel.gov/vehiclesandfuels/energystorage/pdfs/44245.pdf 2012-09-25

Appendix 1 Thermal behaviour Test 1

ANOVA analysis for various cells below is marked with three colors. Red marking indicates a large influence, orange a medium and yellow a slight difference, all relative to each other.

A123 4.4 Ah

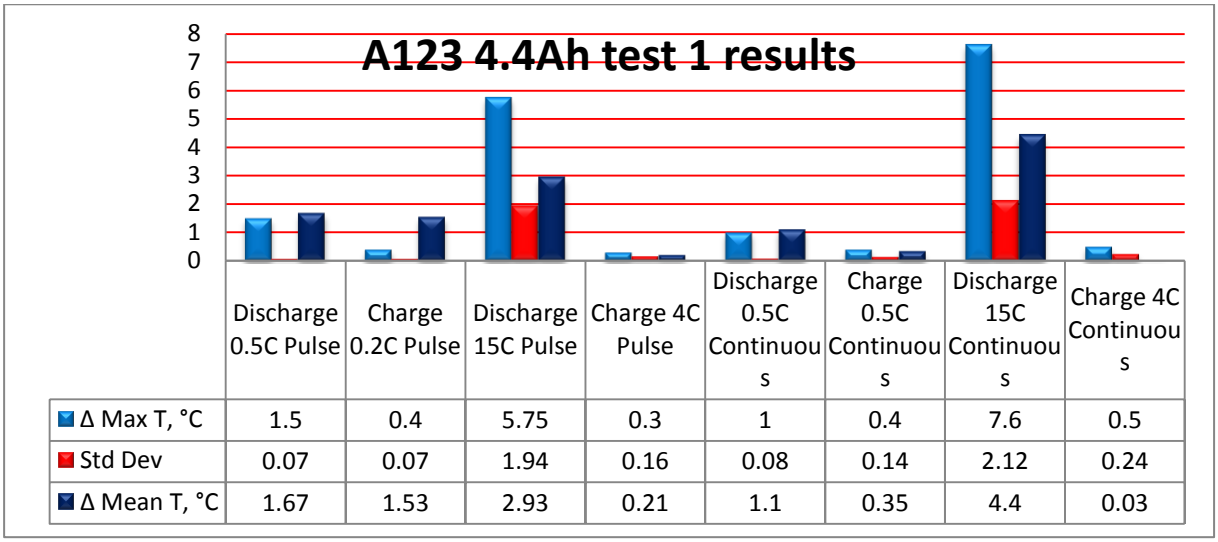

	Discharge 0.5C Pulse	Charge 0.2C Pulse	Discharge 15C Pulse	Charge 4C Pulse	Discharge 0.5C Continuous	Charge 0.5C Continuous	Discharge 15C Continuous	Charge 4C Continuous
Δ Max T, °C	1.5	0.4	5.75	0.3	1	0.4	7.6	0.5
Std Dev	0.07	0.07	1.94	0.16	0.08	0.14	2.12	0.24
Δ Mean T, °C	1.67	1.53	2.93	0.21	1.1	0.35	4.4	0.03

Figure 1-1. A123 4.4Ah results of test 1

	Δ Max T	Std Dev	Δ Mean T
Charge/Discharge	-1,78	-0,45	-1,00
Current rate	1,36	0,51	0,36
Continuous/pulse current	0,19	0,04	-0,06

Table 1-1. Study of effects of current rate and pulse versus continuous current during charge and discharge

EiG 7 Ah

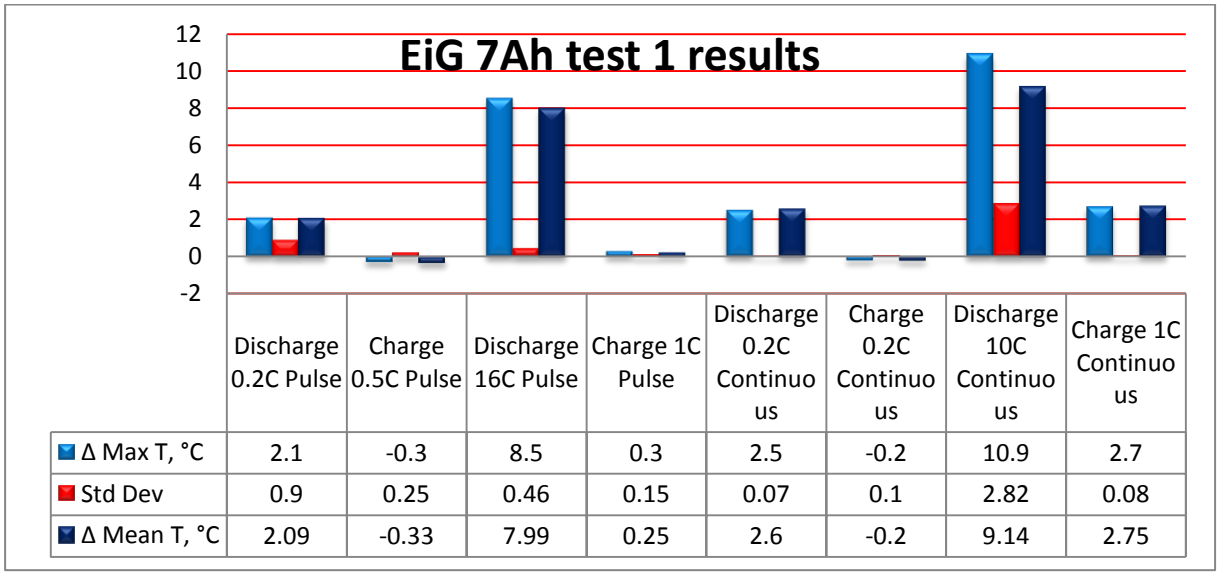

	Discharge 0.2C Pulse	Charge 0.5C Pulse	Discharge 16C Pulse	Charge 1C Pulse	Discharge 0.2C Continuous	Charge 0.2C Continuous	Discharge 10C Continuous	Charge 1C Continuous
Δ Max T, °C	2.1	-0.3	8.5	0.3	2.5	-0.2	10.9	2.7
Std Dev	0.9	0.25	0.46	0.15	0.07	0.1	2.82	0.08
Δ Mean T, °C	2.09	-0.33	7.99	0.25	2.6	-0.2	9.14	2.75

Figure 1-2. EiG 7Ah results of test 1

	Δ Max T	Std Dev	Δ Mean T
Charge/Discharge	-2,69	-0,46	-2,42
Current rate	2,29	0,27	2,00
Continuous/pulse current	0,66	0,16	0,54

Table 1-2. Study of effects of current rate and pulse versus continuous current during charge and discharge

EiG 20 Ah

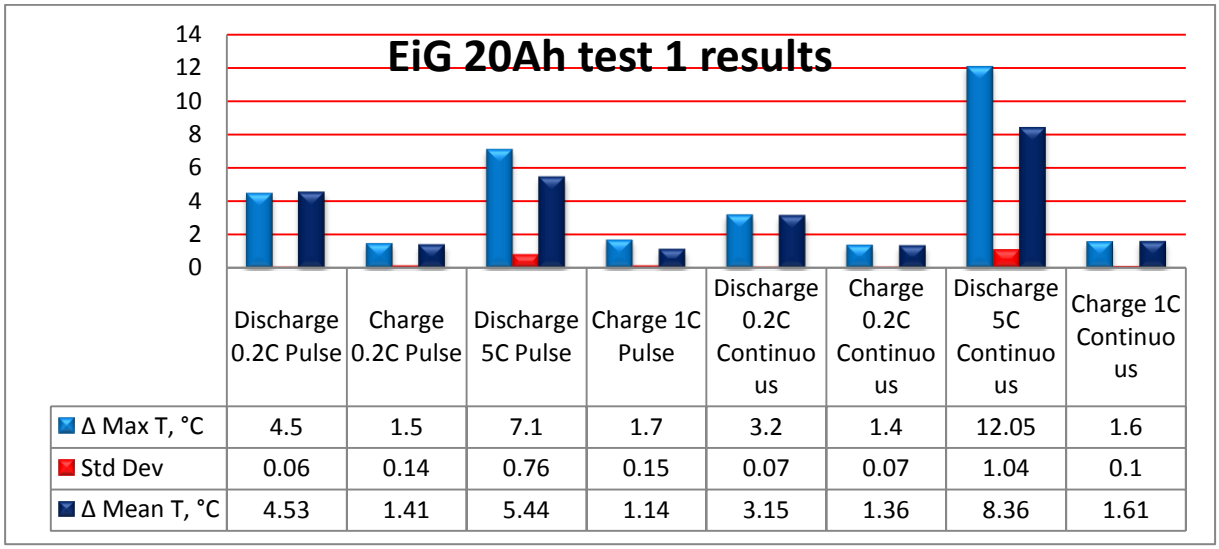

	Discharge 0.2C Pulse	Charge 0.2C Pulse	Discharge 5C Pulse	Charge 1C Pulse	Discharge 0.2C Continuous	Charge 0.2C Continuous	Discharge 5C Continuous	Charge 1C Continuous
Δ Max T, °C	4.5	1.5	7.1	1.7	3.2	1.4	12.05	1.6
Std Dev	0.06	0.14	0.76	0.15	0.07	0.07	1.04	0.1
Δ Mean T, °C	4.53	1.41	5.44	1.14	3.15	1.36	8.36	1.61

Figure 1-3. EiG 20Ah results of test 1

	Δ Max T	Std Dev	Δ Mean T
Charge/Discharge	-2,58	-0,18	-2,00
Current rate	1,48	0,21	0,76
Continuous/pulse current	0,43	0,02	0,25

Table 1-3. Study of effects of current rate and pulse versus continuous current during charge and discharge

LG Chem 5.3 Ah

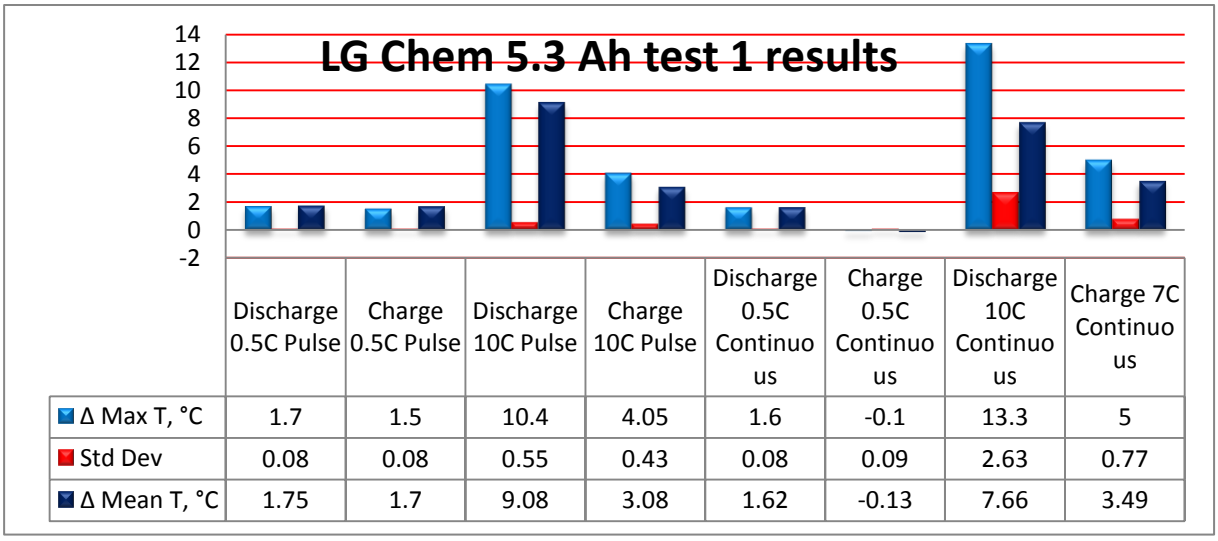

	Discharge 0.5C Pulse	Charge 0.5C Pulse	Discharge 10C Pulse	Charge 10C Pulse	Discharge 0.5C Continuous	Charge 0.5C Continuous	Discharge 10C Continuous	Charge 7C Continuous
Δ Max T, °C	1.7	1.5	10.4	4.05	1.6	-0.1	13.3	5
Std Dev	0.08	0.08	0.55	0.43	0.08	0.09	2.63	0.77
Δ Mean T, °C	1.75	1.7	9.08	3.08	1.62	-0.13	7.66	3.49

Figure 1-4. LG Chem 5.3Ah results of test 1

	Δ Max T	Std Dev	Δ Mean T
Charge/Discharge	-2,07	-0,25	-1,50
Current rate	3,51	0,51	2,30
Continuous/pulse current	0,27	0,30	-0,37

Table 1-4. Study of effects of current rate and pulse versus continuous current during charge and discharge

Cell 1 3.1 Ah

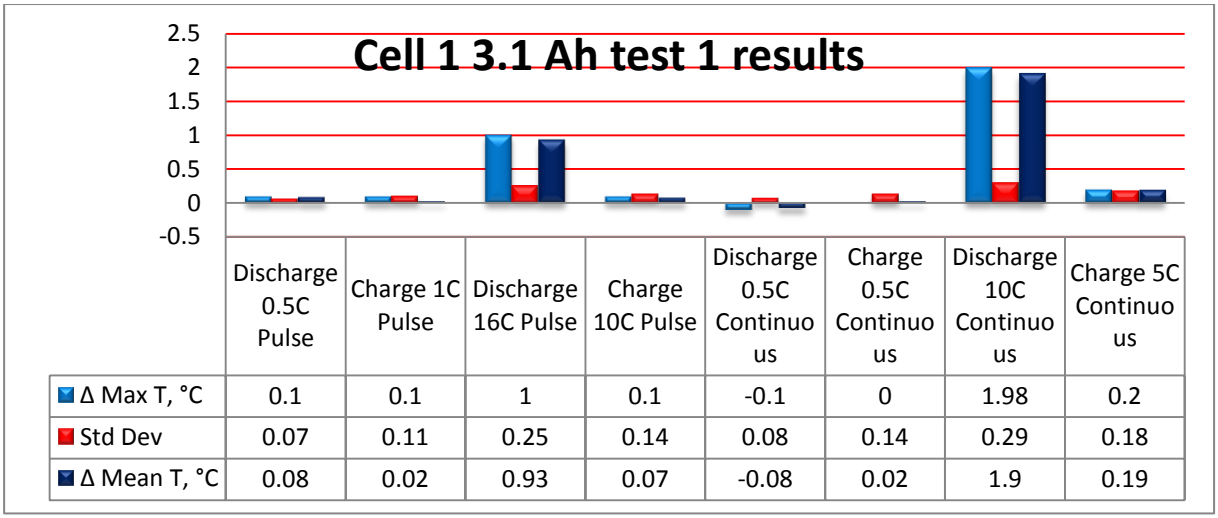

	Discharge 0.5C Pulse	Charge 1C Pulse	Discharge 16C Pulse	Charge 10C Pulse	Discharge 0.5C Continuous	Charge 0.5C Continuous	Discharge 10C Continuous	Charge 5C Continuous
Δ Max T, °C	0.1	0.1	1	0.1	-0.1	0	1.98	0.2
Std Dev	0.07	0.11	0.25	0.14	0.08	0.14	0.29	0.18
Δ Mean T, °C	0.08	0.02	0.93	0.07	-0.08	0.02	1.9	0.19

Figure 1-5. Cell 1 3.1Ah results of test 1

	Δ Max T	Std Dev	Δ Mean T
Charge/Discharge	-0,32	-0,02	-0,32
Current rate	0,40	0,06	0,38
Continuous/pulse current	0,10	0,02	0,12

Table 1-5. Study of effects of current rate and pulse versus continuous current during charge and discharge

Appendix 2 Thermal behaviour Test 2

Test run design is visible in *Table 2-1*.

		Factors and interactions							
		A	B	C	AB	AC	BC	ABC	
		SOC	T amb	Ch/Dis					
Test runs	1	-	-	-	+	+	+	-	80% 35° Discharge
	a	+	-	-	-	-	+	+	50% 35° Discharge
	b	-	+	-	-	+	-	+	80% 22° Discharge
	c	+	+	-	+	-	-	-	50% 22° Discharge
	ab	-	-	+	+	-	-	+	80% 35° Charge
	ac	+	-	+	-	+	-	-	50% 35° Charge
	bc	-	+	+	-	-	+	-	80% 22° Charge
	abc	+	+	+	+	+	+	+	50% 22° Charge

Table 2-1. Test runs in test 2

ANOVA analysis for various cells below is marked with three colors. Red marking indicates a large influence, orange a medium and yellow a slight difference, all relative to each other.

A123 4.4 Ah

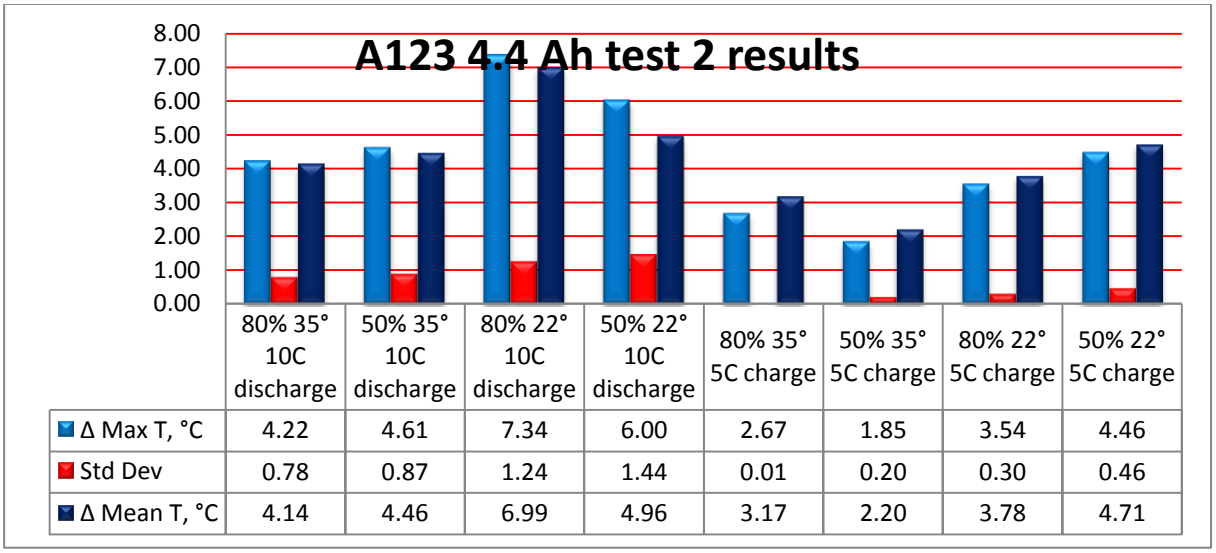

	80% 35° 10C discharge	50% 35° 10C discharge	80% 22° 10C discharge	50% 22° 10C discharge	80% 35° 5C charge	50% 35° 5C charge	80% 22° 5C charge	50% 22° 5C charge
Δ Max T, °C	4.22	4.61	7.34	6.00	2.67	1.85	3.54	4.46
Std Dev	0.78	0.87	1.24	1.44	0.01	0.20	0.30	0.46
Δ Mean T, °C	4.14	4.46	6.99	4.96	3.17	2.20	3.78	4.71

Figure 2-1. A123 4.4Ah results of test 2

	Δ Max T	Std Dev	Δ Mean T
SOC	-0,11	0,08	-0,22
Ambient T	1,00	0,20	0,81
Charge/Discharge	-1,21	-0,42	-0,84

Table 2-1. Study of factor effects on A123 4.4Ah

EiG 7Ah

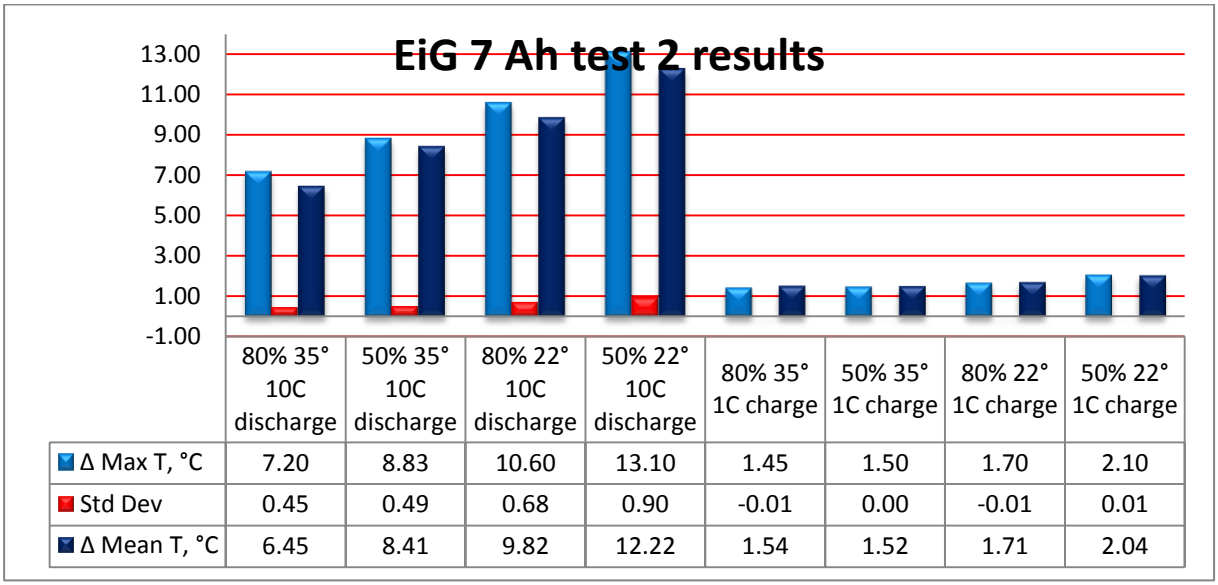

	80% 35° 10C discharge	50% 35° 10C discharge	80% 22° 10C discharge	50% 22° 10C discharge	80% 35° 1C charge	50% 35° 1C charge	80% 22° 1C charge	50% 22° 1C charge
Δ Max T, °C	7.20	8.83	10.60	13.10	1.45	1.50	1.70	2.10
Std Dev	0.45	0.49	0.68	0.90	-0.01	0.00	-0.01	0.01
Δ Mean T, °C	6.45	8.41	9.82	12.22	1.54	1.52	1.71	2.04

Figure 2-2. EiG 7Ah results of test 2

	Δ Max T	Std Dev	Δ Mean T
SOC	0,57	0,04	0,58
Ambient T	1,06	0,08	0,98
Charge/Discharge	-4,12	-0,32	-3,76

Table 2-2. Study of factor effects on EiG 7Ah

EiG 20 Ah

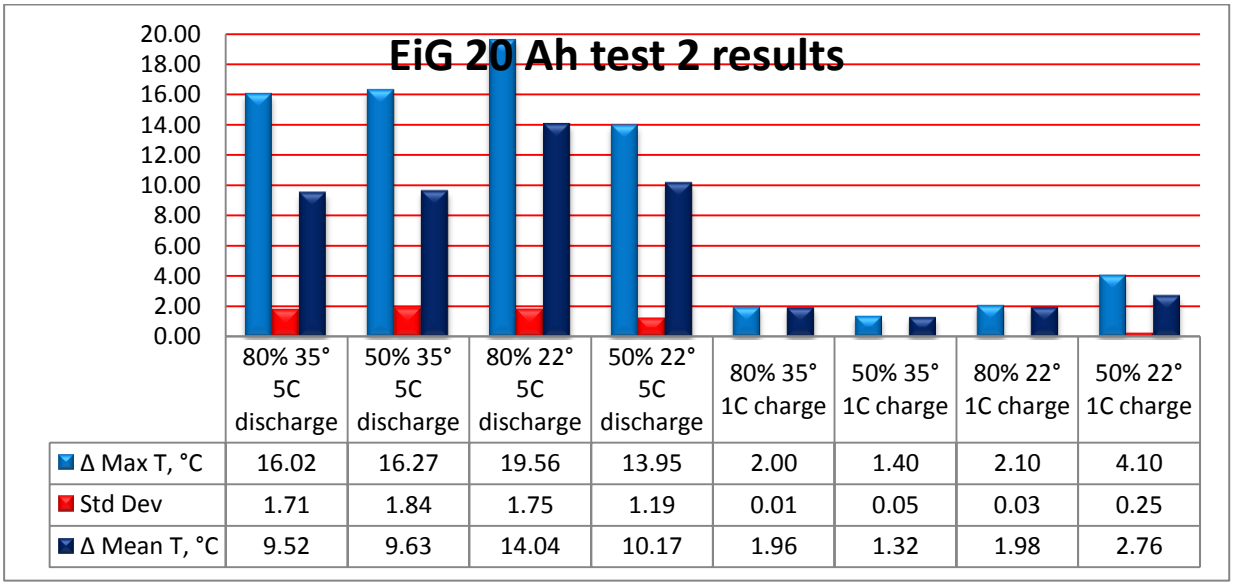

	80% 35° 5C discharge	50% 35° 5C discharge	80% 22° 5C discharge	50% 22° 5C discharge	80% 35° 1C charge	50% 35° 1C charge	80% 22° 1C charge	50% 22° 1C charge
Δ Max T, °C	16.02	16.27	19.56	13.95	2.00	1.40	2.10	4.10
Std Dev	1.71	1.84	1.75	1.19	0.01	0.05	0.03	0.25
Δ Mean T, °C	9.52	9.63	14.04	10.17	1.96	1.32	1.98	2.76

Figure 2-3. EiG 20Ah results of test 2

	Δ Max T	Std Dev	Δ Mean T
SOC	-0,49	-0,02	-0,45
Ambient T	0,50	-0,05	0,81
Charge/Discharge	-7,02	-0,77	-4,42

Table 2-3. Study of factor effects on EiG 20Ah

LG Chem 5.3 Ah

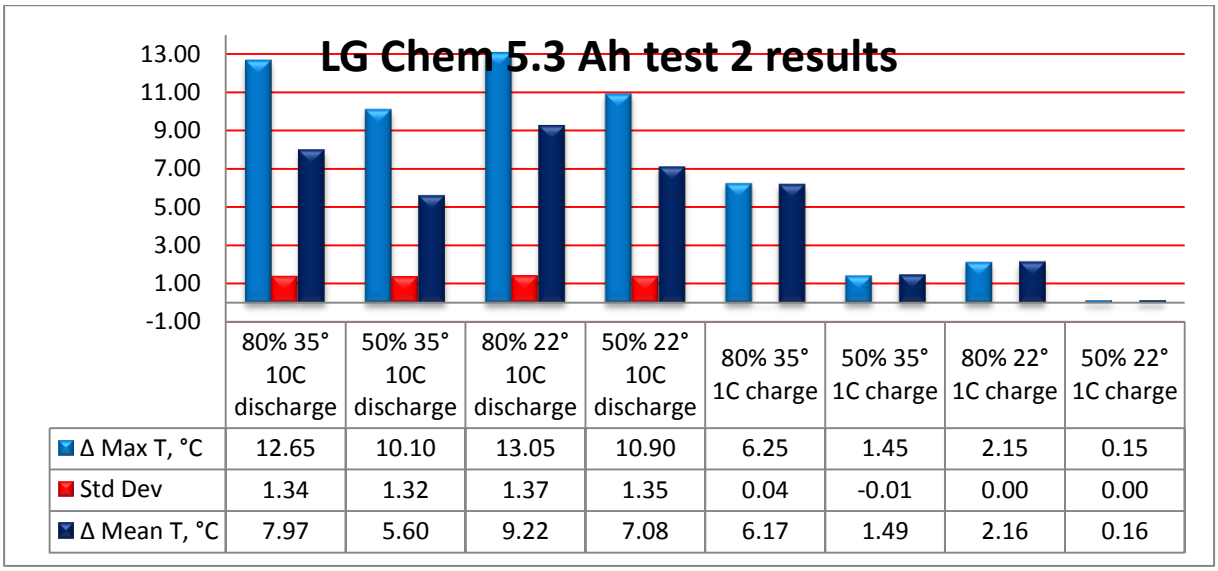

	80% 35° 10C discharge	50% 35° 10C discharge	80% 22° 10C discharge	50% 22° 10C discharge	80% 35° 1C charge	50% 35° 1C charge	80% 22° 1C charge	50% 22° 1C charge
Δ Max T, °C	12.65	10.10	13.05	10.90	6.25	1.45	2.15	0.15
Std Dev	1.34	1.32	1.37	1.35	0.04	-0.01	0.00	0.00
Δ Mean T, °C	7.97	5.60	9.22	7.08	6.17	1.49	2.16	0.16

Figure 2-4. LG Chem 5.3Ah results of test 2

	Δ Max T	Std Dev	Δ Mean T
SOC	-1,44	-0,01	-1,40
Ambient T	-0,52	0,00	-0,33
Charge/Discharge	-4,59	-0,67	-2,49

Table 2-4. Study of factor effects on LG Chem 5.3Ah

Cell 1 3.1 Ah

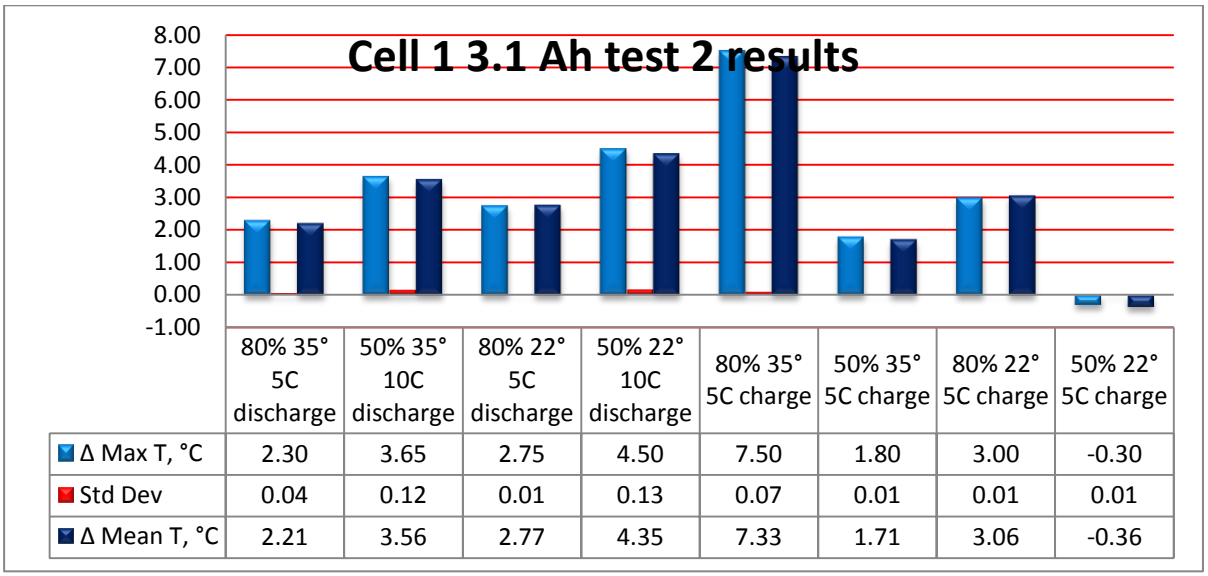

	80% 35° 5C discharge	50% 35° 10C discharge	80% 22° 5C discharge	50% 22° 10C discharge	80% 35° 5C charge	50% 35° 5C charge	80% 22° 5C charge	50% 22° 5C charge
Δ Max T, °C	2.30	3.65	2.75	4.50	7.50	1.80	3.00	-0.30
Std Dev	0.04	0.12	0.01	0.13	0.07	0.01	0.01	0.01
Δ Mean T, °C	2.21	3.56	2.77	4.35	7.33	1.71	3.06	-0.36

Figure 2-5. 3.1Ah cell results of test 2

	Δ Max T	Std Dev	Δ Mean T
SOC	-0,74	0,02	-0,76
Ambient T	-0,66	-0,01	-0,62
Charge/Discharge	-0,15	-0,02	-0,14

Table 2-5. Study of factor effects on cell 1 3.1Ah

Appendix 3 Thermal behaviour Test 3

A123 4.4Ah

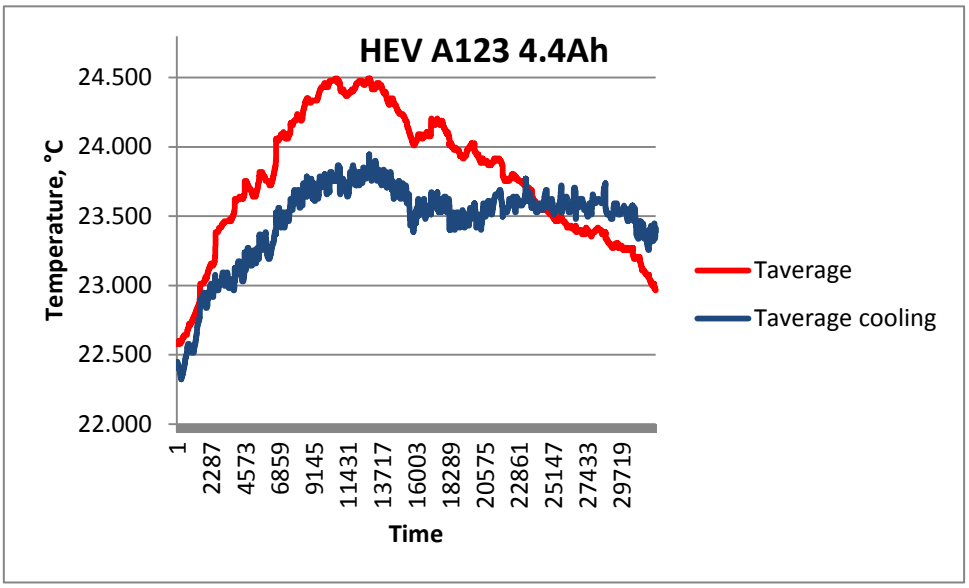

Figure 3-1. HEV cycle with and without cooling on A123 4.4Ah

The results are shown in *Figure 3-1* above. Average temperature for a HEV cycle was 23.67°C and with cooling 23.55°C. Cooling brought down thermal cycling and kept cell temperature in between 23.3 and 24°C. Regular cycle showed variation between roughly 23 and 24.5°C. Difference between cell side that was cooled and other side was not observed. Roughly 1% less energy was used by the cell during cycle with cooling.

As a result cycle without cooling had a lower average temperature than with cooling while working with a little larger amount of energy. Efficiency without cooling was therefore higher both in terms of lower temperature and higher energy from the cell. Cooling however reduced thermal cycling which is important for cell health.

EiG 7Ah

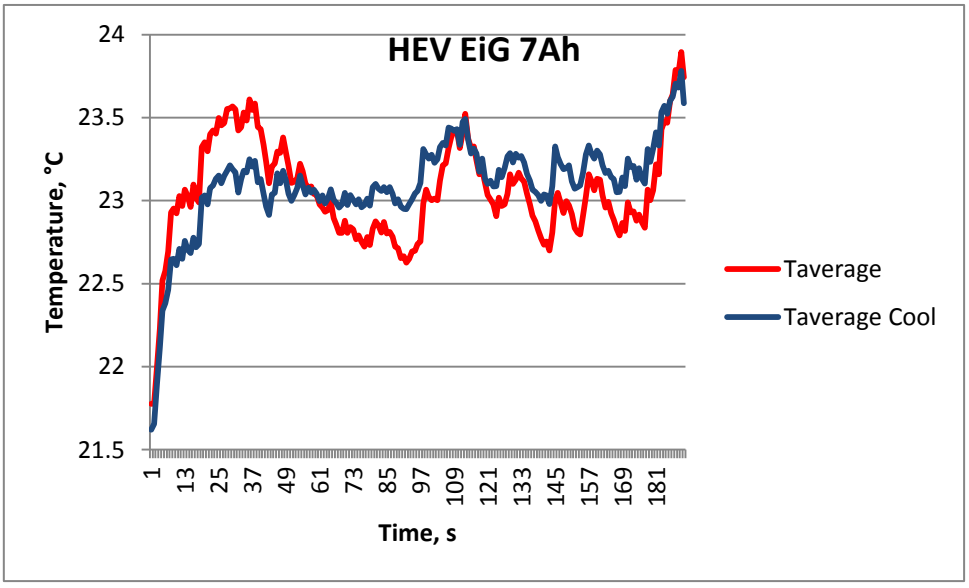

Figure 3-2. HEV cycle with and without cooling on EiG 7 Ah

The results are shown in *Figure 3-2* above. Average temperature for a HEV cycle was 23°C and with cooling 23.1°C. Cooling brought down thermal cycling and kept cell temperature in between 23 and 23.5°C. Regular cycle showed variation between roughly 22.5 and 23.5°C. Difference between cell side that was cooled and other side was not observed. Roughly 1% less energy was used by the cell during cycle with cooling.

As a result cycle without cooling had a lower average temperature than with cooling while working with a little larger amount of energy. Efficiency without cooling was therefore higher both in terms of lower temperature and higher energy from the cell. Cooling however reduced thermal cycling which is important for cell health.

EiG 20Ah

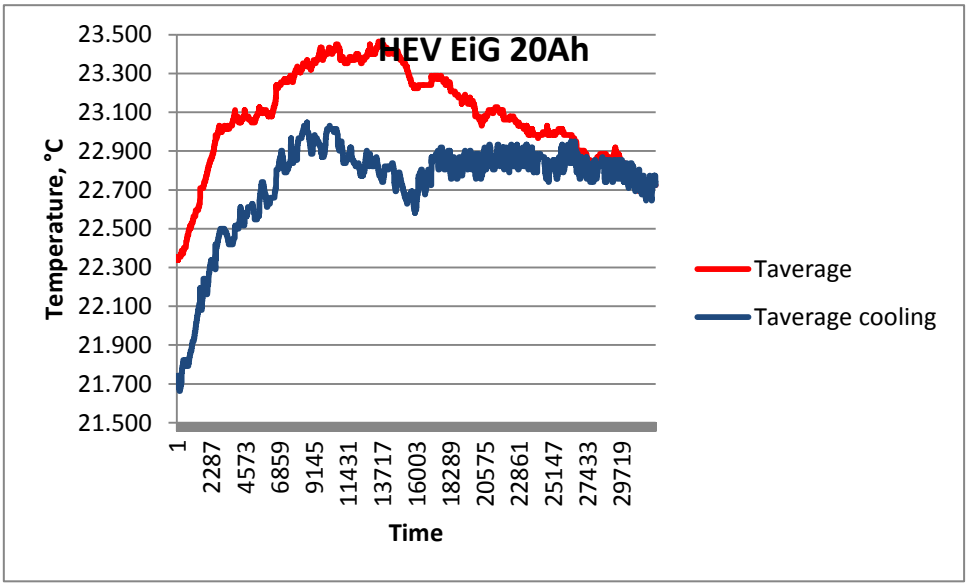

Figure 3-3. HEV cycle with and without cooling on EiG 20Ah

The results are shown in *Figure 3-3* above. Average temperature during regular hybrid cycle was changing between 22.6 and 23.4°C while cooling cycle showed a spread between 22.6 and 23.2°C. Cooling evened out temperature and brought down thermal cycling. Average cell temperature decreased from 22.95 to 22.86°C with cooling. Cooling cycle used around 1.2% less electrical energy. Fan was installed on one side of the cell but no visible effect on temperatures of the two sides was recorded.

Cell had lower average temperature with cooling. Thermal cycling was slightly lower. Regular HEV cycle however showed higher thermal efficiency.

Cell1 3.1Ah

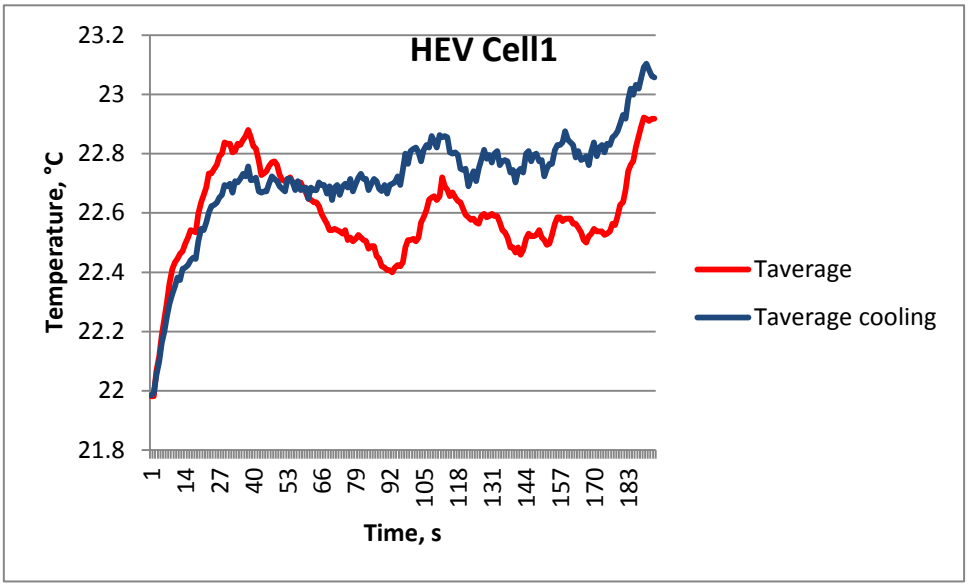

Figure 3-4. HEV cycle with and without cooling on Cell1 3.1Ah

The results are shown in *Figure 3-4* above. Average temperature during regular hybrid cycle was changing between 22.4 and 22.9°C while cooling cycle showed a spread between 22.7 and 22.9°C. Cooling evened out temperature and brought down thermal cycling. At the same time average cell temperature increased from 22.6 to 22.7°C for cooling cycle. Amount of electrical energy was the same in both tests. Fan was installed on one side of the cell but no visible effect on temperatures of the two sides was recorded.

As a result cycle without cooling had a lower average temperature than with cooling while working with exactly the same amount of energy. Efficiency without cooling was therefore higher. Cooling however reduced thermal cycling. An even cell temperature is important for cell health and in these circumstances cooling benefits outweighed efficiency.

Appendix 4 Supercapacitor test

JSR 2000F supercapacitor

Supercapacitors are a different technology compared to Li-ion cells. In a JSR 2000F one electrode is activated carbon and the other is Li-doped carbon, *Figure 4-1*. Capacitors operate based on electrostatic induction. An electric field is created when there is a potential difference on the electrodes. Negatively charged particles are collected on one electrode and positively charged are pushed to the other electrode by the electric field.

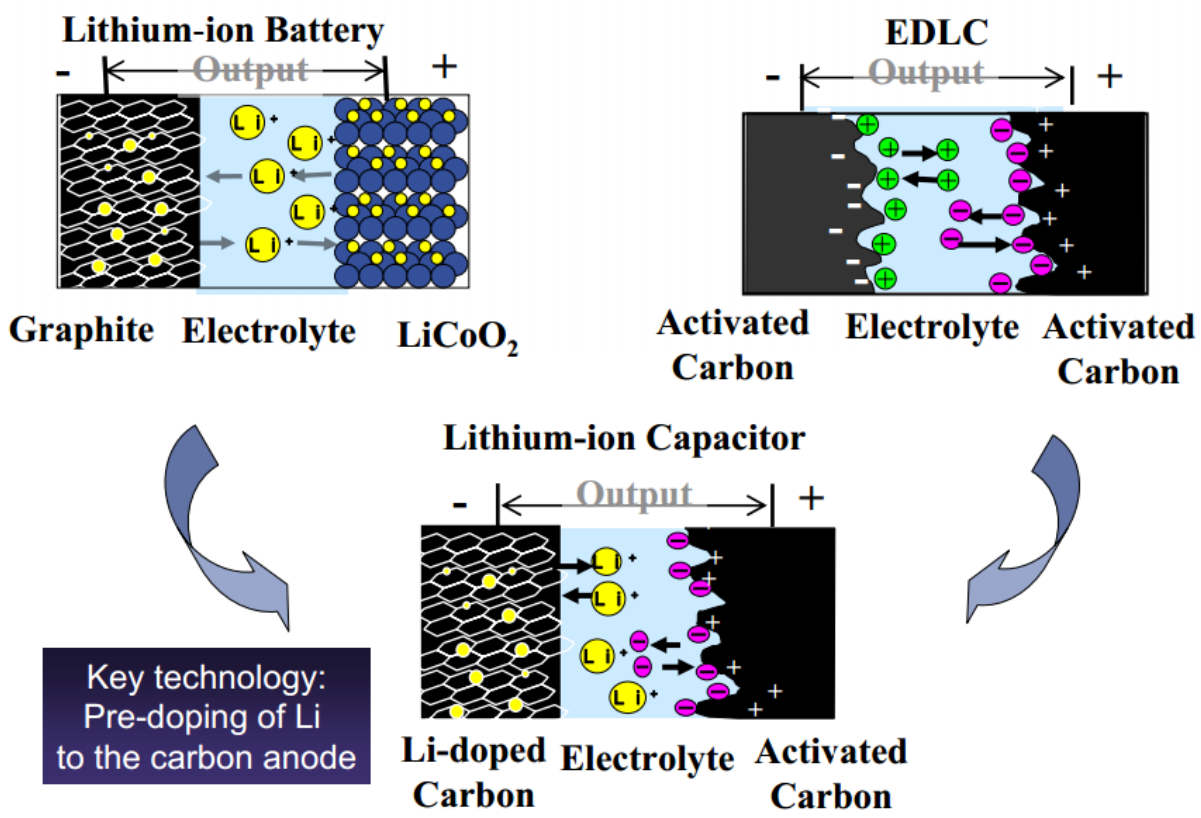

Figure 4-1. Materials in Li-ion batteries and capacitors

Capacitors cannot store large amounts of energy. Their benefit is fast charges and discharges. Seeing as their voltage is proportional to quantity of electricity they hold voltage profile is quite linear compared to Li-ion cells, *Figure 4-2*.

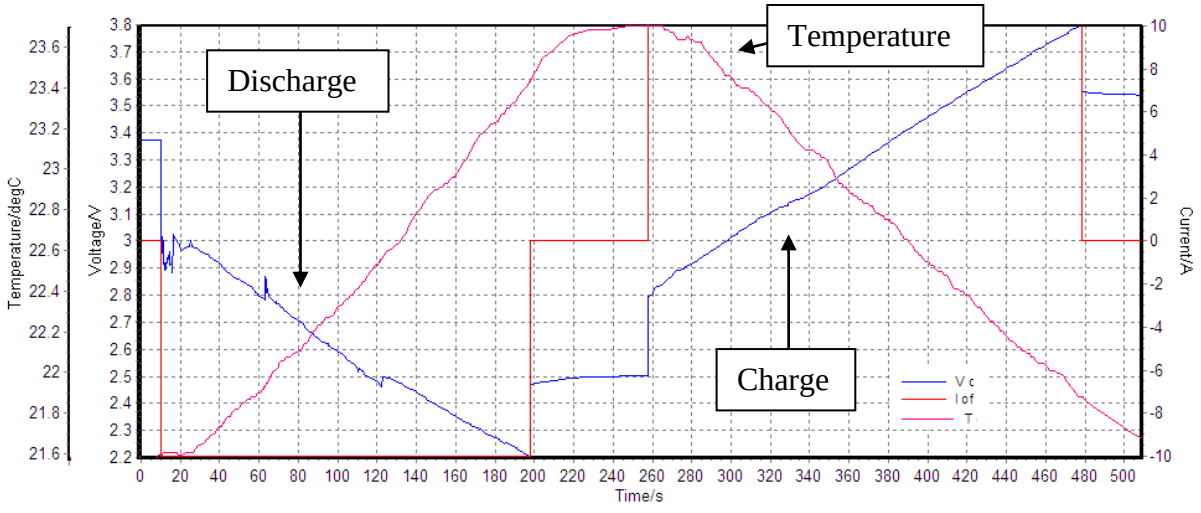

Figure 4-2. JSR 2000F voltage, current and temperature during discharge and charge

Other benefits of lithium capacitors (LiC) are shown below, *Figure 4-3*.

- Hybrid construction summary:
  - The activated carbon cathode is a capacitor cathode.
    - ✓ In a Lithium Ion Battery thermal runaway occurs at the cathode when the Li spinel decomposes and reacts with the electrolyte.
  - Since LIC has an activated carbon cathode, thermal runaway will not occur.
  - The Li-doped carbon anode is a battery anode, undergoing Li doping during charge and de-doping during discharge
  - The electrolyte contains a Li salt and is a battery electrolyte.

- Hybrid construction creates a capacitor which yields the best performance features of batteries and capacitors

- **Battery-Like Advantages**
  - High Energy Density
    - ✓ 14-15 Wh/kg
  - High Voltage
    - ✓ 3.8v to 2.2v discharge range
    - ✓ When connected in series, 1/3 fewer LIC cells are needed compared to a conventional EDLC supercapacitor
  - Low Self-Discharge Rate
    - ✓ Will hold 95% of its charge after 3 months

- **Capacitor-Like Advantages**
  - **Safety: No Thermal Runaway**
    - ✓ Since the cathode does not contain Li spinel, thermal runaway cannot occur
  - High Power Density
    - ✓ >1000 W/kg
  - Can be charged/discharged quickly.
  - High Reliability
    - ✓ Estimated life is 1 million charge/discharge cycles
  - Wide Temperature Range
    - ✓ -20°C to 70°C

Figure 4-3. Benefits of lithium capacitors

Temperature of supercapacitor showed quite linear relationship with time of procedure (*Figure 4-2*). Discharge was exothermic (temperature increased) while charge was an endothermic reaction (temperature decreased). A similar endothermic charge was visible in LMO chemistries but not to the same extent (only 0.5°C).

Temperature distribution on the surface was even. Tabs were emitting heat. Areas around the tabs did not heat up like they did in batteries which indicated a more even current density. During discharge edges of the supercapacitor were slightly colder than its center which showed that temperature inside the core was higher. Charge procedure showed temperature gradient from the tab. It indicated that heat produced by the tab was greater than the heat absorbed by the cell. Cell temperature was at that point evenly distributed underneath the packaging. Charge and discharge are shown in *Figure 4-4*.

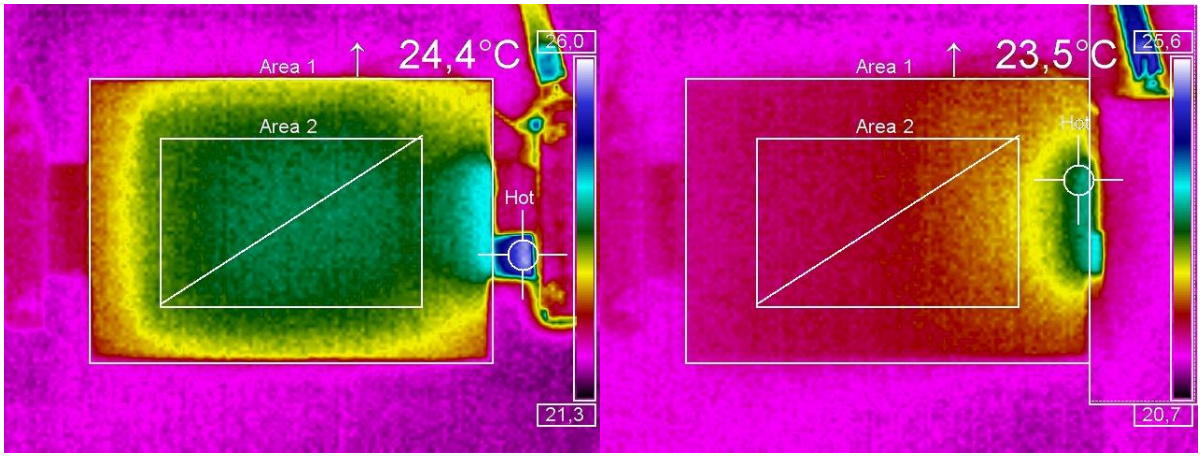

Figure 4-4. JSR F2000 Supercapacitor's discharge and charge temperature patterns

A set of tests were run charging and discharging the capacitor at different currents. Results showed average temperature of the capacitor, *Table 4-1*.

Table 4-1. Study of factors effects on JSR 2000F

Procedure	ΔT,°C
Charge, 1A	-0.14
Charge, 10A	-0.9
Discharge, 1A	1.2
Discharge, 10A	1.2

Source: JSR Micro http://www.avsusergroups.org/tfug_pdfs/2009_2banas.pdf 2012-09-30

Appendix 5 Basis for battery system design

Heat and efficiency calculation through temperature

Sources that contribute to heat production on a cell level are [9]:

- Q_{joule} Joule heat (Ohmic heat) & Q_P potential deviation heat $Q_P = I(V - V_0) = I^2R$
- Q_S entropy change heat $Q_S = I\Delta S = IT\frac{\partial E_{emf}}{\partial T}$

1. Specific heat capacity *C* is 800 J/kg/°C [10]. Heat can be calculated through $Q = C \cdot m \cdot T$ where *m* is cell mass in kg and *T* is difference in average cell temperature
2. Heat losses can on average account for 22% of total heat [11]. Thus $Q_{tot} = 1.28 \cdot Q$
3. Thermal efficiency of a cell can then be calculated by dividing overall heat by the sum of energy that was put in and taken out of the cell during the studied cycle:$Efficiency = 1 - (Q_{tot} \div E_{in/out})$ [10]
4. Dividing total heat by cycle time gives heat generation rate ΔQ which is measured in W and is important for dimensioning thermal management system. $\Delta Q = Q \div t$

Heat

Cells with LFP, NMC, LMO and LTO chemistries in cylindrical, prismatic and pouch design were tested. Thermal behaviour of cells is described in the report (Chapter 4, Appendix 1-3).

Difference in current density was noticeable based on cell temperature. Areas close to cell tabs were subjected to higher currents seeing as current took the shortest way through the cell. Tabs themselves proved to be a bottleneck because current from the whole current collector had to flow through the restricted size tab. Tab placement on opposite sides results in a more even current and potential distribution and cell temperature[20]. This makes a well-balanced cell which is less susceptible to uneven performance and thus shows better efficiency and health during lifetime. Positive electrode tabs were consistently warmer throughout all experiments.

A thermal management system has a large potential for improving cell performance in an ESS. Most of tested cells exhibited better efficiency at 30°C compared to ambient 20°C.

Heat transfer inside the cell is most efficient along the layers of material as oppose to across layers. Extracting heat through short sides of package and cooling the cell through tabs would be quite effective.

A good TMS must start heating up the cells in advance to be up at an operating temperature before vehicle starts. Nonetheless simple and cost effective systems like air cooling are quite often sufficient for specific purposes.

Entropic changes in cathodes and anodes versus SOC is a convenient indicator of cell performance and efficiency. Large change in entropy points to instability of material which determines inefficient areas of operation in the SOC domain.

Most effective cell performance is achieved at a state where entropic heat produced by the cell is in balance with heat that is emitted through convection and radiation. Cooling that is forced beyond a certain point will reduce cell performance by non-uniform cooling that makes outside of the cell cold and leaves inside hot making cell temperature uneven throughout the cell.

Temperature is highest in the center of the cell. Compared to the shell center can be 2 to 5°C hotter continuously throughout cycling.

Connecting cables lead away part of the heat from cells. When cells are connected to each other in a battery module cells closest to module poles will be colder and cells in between them hotter

Safety

Only NMC cells caught fire during the experiment. Cell temperatures reached more than 660°C at peak of runaway compared to 370°C and less for LFP cells. A study [23] suggests that gases that are vented from the cell will ignite if in contact with a sufficiently hot material such as cell packaging. Thus gases vented by an LFP cell also were flammable but during runaway reactions cells did not reach hot enough temperatures to ignite the gases. If a different ignition source is present LFP cell would catch fire as well. Gases do not ignite because of oxygen release from cathode. Oxygen amount released from the cell is too low.

In both tests on cells with NMC chemistry aluminum current collectors melted down. Metal's melting point is at 660°C. Pure copper however will not likely melt during runaway due to a high melt temperature of 1080°C. Packaging material did not melt during any test suggesting that its thickness was adequate.

Cell voltage oscillations indicated that PE separator already shut off (at around 160 degrees) and started to melt causing small internal short-circuits. Nevertheless shorting did not cause a specific temperature increase.

Thermal runaway reactions are self-sustaining if a cell has reached temperature higher than 80°C. If external heat source is taken away it can take up to 2 days for thermal runaway to manifest [24].

In a battery pack where cells are assembled close to each other thermal runaway in one cell can quickly escalate to a chain reaction. One cell with thermal runaway will likely damage most of the cells in a pack. Moreover gas and smoke are released during the reaction and they must be sustained in the pack or released without harming humans in proximity. Since oxygen is not released during the reaction fire can be sustained by limiting oxygen supply. The temperature of the pack in itself however can cause ignition of materials around the pack.

Sustainability

Metals in the cell showed the highest influence. Aluminum caused highest CO_2 emissions while copper highest environmental damage [16]. Sustainability and/or emissions of electricity sources in different areas of the world influences usage phase of battery [17].

Optimizing usage conditions for best cell performance will cut the losses and less electricity would be needed for charging. Also inverter efficiency can be added to these losses. These losses were found to be dominating throughout battery usage (roughly 75%) and not the weight that it adds to a car [17].

Easy connections between the cells can save material. Pack electronic equipment can also be designed more efficiently material-wise and in terms of performance.

Battery thermal management system is a large and energy consuming unit. It must be optimized to achieve best vehicle performance. Re-using the thermal energy is a potential approach to dealing with this problem. More advanced insulating and heat transfer materials can also be used for that matter.

Better understanding of cell health is crucial for designing a system that will utilize cell power to the maximum within reasonable limits. A support for battery service or upgrade will prolong the life of the vehicle which will have a positive influence on sustainability.

Cost of components of a cell is distributed in the following way [19]: Anode: 5% to 15%, Cathode: 5% to 11%, Electrolyte: 10% to 14%, Separator: 40% to 60%

Reduction of components prices can potentially lower cell cost by 25%. Manufacturing improvements stand for another 30% reduction. Improvement of capacity of cell materials has a 40-45% price reduction opportunity [20].